earthquake occurrence frequency. Given the occurrence frequency of earthquakes, the probability that slip will occur in a given event, P_t(slip|event on j), was assessed using the logistic regression model shown on Figure H-13c.

The conditional probability of exceeding a specified displacement, $P(D>d)$, was evaluated using an assessment of the expected maximum slip in the maximum event, MD^{max}, and the exponential distribution for D/MD^{max} discussed above. Two alternative approaches for estimating MD^{max} were considered, one based on the length of the feature and one based on the cumulative offset. If only one of these types of data were known for a feature, the assessment of MD^{max} was based on a single approach.

Displacement Approach. The displacement approach for sites of only distributed faulting hazard parallels that discussed above for principal faulting hazard. The first assessment in the logic tree (Figure 4-79) is an evaluation of the probability the feature can slip, $P(C)$, which is the same as the assessment of $P(C)$ in the earthquake approach.

The frequency of displacement events again is obtained using Equation (4-13). Three alternative approaches are used to estimate slip rate on the feature: (1) one based on assuming uniform slip for the past 11.6 Ma, (2) one assuming uniform slip for the past 3.7 Ma, and (3) one based on a empirical regression model developed by the AAR team relating Quaternary slip rate to cumulative bedrock offset. For the uniform slip approaches, the AAR team assessed the fraction of the cumulative offset that occurred prior to the period of uniform slip and used only the remaining portion of the cumulative slip to compute the slip rate. For example, one assessment is that 84% of the cumulative slip occurred prior to 3.7 Ma. The fault slip rate then is obtained by the expression: $SR = 0.16 \times D_{cum}/3.7$ Ma. The assessment of the average displacement per event, $\bar{D}_E$, likewise is based on the expression $\bar{D}_E = 0.83\ MD^{max}$, with MD^{max} estimated using either fault length or cumulative displacement in the same way as is done for the earthquake approach. The exponential distribution for D/MD^{max} is used to assess $P(D>d)$. Uncertainty in the cumulative displacement was included in the assessment.

Summary of Application of Model to Nine Demonstration Points. The AAR team interprets Points 1, 2, 4, and 6 to lie on faults that are potentially seismogenic and utilizes the logic tree shown on Figure 4-78 to characterize the hazard at these sites. Point 6 is interpreted to lie on a seismic source that they designated as west Dune Wash fault 1 (WD1 on Figure 4-18). The remaining points are interpreted to be subject to distributed faulting hazard only and the logic tree shown on Figure 4-79 is used to characterize hazard at these sites. Considering the hypothetical features at points 7 and 8, they utilize the assumed cumulative displacements of 2 m and 10 cm to Characterize the hazard for conditions (a) and (b), respectively; provide a distribution for the length of a fracture to characterize the hazard at point (c); and make the assessment that the potential fault displacement hazard for a point in intact rock is essentially zero.

Ake, Slemmons, McCalpin Team. The ASM team utilizes the earthquake approach to assess the hazard at all locations within the Controlled Area. Their hazard characterization is developed in terms of principal faulting hazard and distributed faulting hazard.

Principal Faulting Hazard Model. Figure 4-80 presents the logic tree that defines the ASM team's characterization of principal faulting hazard. The first assessment is whether the fault can experience principal faulting. This assessment is equal to the probability that the fault is seismogenic, as defined by the ASM team's seismic source characterization for the ground motion hazard assessment.

Conditional on the fault being seismogenic, the frequency of occurrence of earthquakes of various magnitudes on each of the seismic sources is assessed using the characterization of earthquake recurrence developed by the ASM team for the ground motion hazard assessment. Given the occurrence frequency of earthquakes, the next assessment is the probability that surface displacement will occur in a given event. The ASM team assessed P_t(slip|event on i) [Equation (4-16)] using the empirical logistic regression model for the probability of surface rupture, Equation (4-15). Two alternative empirical relationships were considered for the probability of surface rupture: one based on post-1930 Great Basin earthquakes and one based on earthquakes from the extensional Cordillera (see Figure 4-11).

The conditional probability of exceeding a specified displacement, $P(D>d)$, was evaluated using the two-part method defined by Equation (4-19). The distribution for the maximum displacement in an earthquake, *MD*, was defined using a published empirical model based on earthquake magnitude. The location of the point of interest within the rupture was assessed for each rupture to define the parameter x/L, and the distribution for D/MD was based on the analysis of historical ruptures shown on Figure 4-13.

Distributed Faulting Hazard Model. Figure 4-81 presents the logic tree that defines the ASM team's characterization of distributed faulting hazard. The first assessment is whether the fault can experience slip. This is composed of two assessments. The ASM team categorized the features in the site vicinity into six classes based on their cumulative slip (see Table ASM-9 in Appendix E). For each class of features, an assessment was made of the probability that the feature could undergo slip. The probability the feature can slip was further modified by a factor equal to the cosine of the strike azimuth of the feature, thus reducing the probability that the feature can slip with increasing deviation of its orientation from north-south. The resulting relationship is $P(C) = P(\text{slip}|\text{class})\times\cos(\phi)$, where ϕ is the strike azimuth of the feature of interest.

The frequency of earthquakes on each of the seismic sources that could cause distributed rupture on the feature of interest was assessed using the seismic source characterization developed by the ASM team for the ground motion hazard characterization. The probability that a specific earthquake on source j induces slip on feature i was assessed using a two-part approach:

$$P_i(\text{slip}|\text{earthquake on } j) = P(\text{surface rupture on } j) \times P_i(\text{distributed slip}|r,h) \qquad (4\text{-}20)$$

The first term to the right of the equal sign is the probability that a earthquake on source i will produce surface rupture. This probability is given by the logistic regression model used in the principal faulting hazard characterization, Equation (4-15). The second term is the probability that a surface-rupturing earthquake on source j produces distributed slip on the feature of interest at point i. This probability is assessed using a form of the logistic regression model defined by Equation (4-17). The ASM team developed two alternative relationships that define the likelihood of the occurrence of distributed slip at a point as

functions of distance from the principal rupture and location in the hanging wall (h=1) or footwall (h=0) of the rupture (Figure 4-82). While these relationships are independent of earthquake magnitude, the combined assessment defined by Equation (4-20) depends on the magnitude of the earthquake on source i through the probability of principal surface rupture.

The probability defined by Equation (4-20) represents aleatory probability in that it defines the likelihood of distributed slip in an individual earthquake. Epistemic uncertainty in the assessment is represented by the two alternative relationships for the probability of surface rupture and the two alternative relationships for the probability of distributed slip.

The ASM team assesses the distributed faulting displacement as a reduction factor, *RF*, times the principal faulting displacement that occurs on the seismic source at its closest approach to the point of interest. Two approaches are used to define the reduction factor, one based on a displacement potential defined on the basis of an observed ground displacement profile and one based on the relative cumulative slip between the principal fault and the feature of interest.

The displacement potential approach assumes the amount of displacement that can occur decreases with distance from the principal rupture in the same manner as the ground surface displacement decays. The ASM team utilizes the fault-normal geodetic displacement profile for the 1983 Borah Peak earthquake normalized by the displacement at the fault (Figure 4-83) as the basis for defining the net ground surface movement resulting from an earthquake. The normalized displacement profile was fit with the following algebraic expression to provide a relationship for the reduction factor, RF:

$$\begin{aligned} RF &= \varepsilon \times \exp(-0.045 r_n^{1.5}) \text{ for hanging wall} \\ RF &= \varepsilon \times 0.21 \exp(-0.14 r_n) \text{ for footwall} \end{aligned} \qquad (4\text{-}21)$$

where ε is a factor that defines what portion of the displacement potential is realized in an event. The distance term r_n is the distance from the principal rupture normalized to the conditions for the Borah Peak earthquake. The normalizing factor is the crustal depth of the rupture compared to that for the Borah Peak earthquake, such that a decrease in the crustal depth of the rupture decreases the distance extent of the displacement potential. The

resulting relationship is $r_n = r \times 16\text{km}/[w \times \sin(\text{dip})]$, where w is the rupture width of the earthquake.

Parameter ε defines how the displacement potential is distributed among the available structures that could slip in the vicinity of the site of interest. Four alternatives are proposed that are considered to be event-to-event variability in how the displacement potential is distributed. The possibilities include full realization ($\varepsilon = 1.0$), distribution equally among the possible classes of features ($\varepsilon = 0.2$), distribution equally among the estimated number of features of a specific class available ($\varepsilon = 1/N$), or distribution equally among the possible classes of features and the estimated number of features of a specific class ($\varepsilon = 0.2/N$). The expected number of features present, N, is evaluated assuming a power law for feature density, with the relative number of features in two classes proportional to the ratio of their cumulative slip raised to a power of -0.7. The resulting values of N are listed in Table ASM-9 in Appendix E.

The second approach for assessing RF involves identification of the portion of the cumulative displacement on the feature of interest at point i that resulted from earthquakes occurring on source j and using the ratio of this cumulative displacement to the cumulative displacement on earthquake source j to estimate the relative amplitude of displacements in individual events. The term within the summation in Equation (4-14), $\lambda_j \times P_i(\text{slip}|\text{event on } j)$, defines the frequency of earthquakes on source j producing distributed slip on the feature at point i. If all events produce comparable amounts of displacement, then the portion of the cumulative displacement at i that is contributed by source j is given by $\lambda_j \times P_i(\text{slip}|\text{event on } j) / \sum \lambda_j \times P_i(\text{slip}|\text{event on } j)$. However, the displacements induced by various magnitude earthquakes on the various earthquake sources are not equal. To address this, the ASM team makes the assumption that the relative contribution of each source to the cumulative displacement at point i can be estimated from the results of the displacement potential approach. Using Equation (4-12), the displacement hazard curve from each source j is used to obtain an effective slip rate from source j, ESR_j. The ratio of this effective slip rate to the effective slip rate obtained from the total displacement hazard curve from all sources provides a estimate of the contribution of source j to the cumulative slip at point i. Thus, the interpretation developed by the ASM team is that the reduction factor to scale, on average,

the principal rupture displacement occurring on source j to the distributed rupture displacement at point i is given by the expression:

$$RF = \frac{ESR_j}{\sum ESR_j} \times \frac{(D_{cum})_i}{(D_{cum})_j \times P_i(\text{slip}|\text{event on } j)} \qquad (4\text{-}22)$$

In Equation (4-22), the cumulative slip on source j is multiplied by P_i(slip|event on j) to account for the fact that not every principal faulting earthquake on source j that contributed to its cumulative slip also produced distributed slip at point i.

Summary of Application of Model to Nine Demonstration Points. The ASM team interprets Points 1 and 2 to lie on faults that are potentially seismogenic and utilizes the logic tree shown on Figure 4-80 to characterize the hazard at these sites. The remaining points are interpreted to be subject to distributed faulting hazard only and the logic tree shown on Figure 4-81 is used to characterize hazard at these sites. Considering the hypothetical features at Points 7 and 8, they utilize the assumed cumulative displacements of 2 m and 10 cm to characterize the hazard for conditions (a) and (b), respectively; provide an assumed maximum cumulative displacement of 1 cm for a fracture with no measurable offset to characterize the hazard at condition (c); and make the assessment that the potential fault displacement hazard for a point in intact rock is essentially zero.

Doser, Fridrich, Swan Team. The DFS team uses the displacement approach for assessing the hazard at all locations.

Principal and Distributed Faulting Hazard Model. Figure 4-84 shows the logic tree used by the DFS team to characterize fault displacement hazard. The first assessment addresses the probability that the feature of interest can slip in a displacement event, $P(C)$. Features that display evidence of Quaternary movement (typically the block-bounding faults) are assigned a probability of 1.0. North-south-striking intrablock faults are assigned a probability of activity of 0.4 and northwest-southeast-trending faults are assigned a probability of activity of 0.01. Minor faults and shears are assigned a probability of activity of 0.05 to 0.01, depending on proximity to block-bounding faults.

The next two assessments are the approaches for estimating the frequency of slip events and the average displacement per event. The DFS team uses the relationship given in Equation (4-13) in two ways. In one approach, a direct estimate of the frequency of slip events is used together with the slip rate on the feature to calculate the average displacement per event. In the second approach, a direct estimate of the average slip per event together with the slip rate is used to evaluate the frequency of slip events.

Both approaches for estimating slip event frequency and average slip per event require an estimate of the slip rate on the feature. The DFS team considers four alternative approaches for estimating the Quaternary slip rate. The favored approach is the use of paleoseismic data from trenching studies on the feature. The other three approaches estimate the Quaternary slip rate utilizing the cumulative offset of the top of the Tiva Canyon tuff and alternative assumptions for the history of deformation. The first interpretation is that the slip rate has been uniform post-Tiva Canyon and the fault slip rate is $SR=D_{cum(\text{Tiva Canyon})}/12.7\pm1.3$ Ma. The second interpretation is that 80 percent of the post-Tiva Canyon slip occurred prior to deposition of the 11.6±1 Ma Rainier Mesa member of the Timber Mountain tuff and the slip rate has been uniform post-Rainier Mesa, resulting in $SR=0.2D_{cum(\text{Tiva Canyon})}/11.6\pm1$ Ma. The third interpretation is that slip rates have been decreasing through time such that the Quaternary slip rate is in the range of 0.3 to 3.9 percent of the late Miocene slip rate. The late Miocene slip is defined to be the deformation that occurred post-Tiva Canyon and pre-Rainier Mesa and is interpreted to be 80 percent of the post-Tiva Canyon cumulative slip. The resulting relationship for Quaternary slip rate is $SR=RF\times0.8D_{cum(\text{Tiva Canyon})}/1.1\pm0.6$ Ma, where RF is the reduction factor from late Miocene to Quaternary slip rates and ranges from 0.3 to 3.9 percent. If no paleoseismic data are available for a feature, then the DFS team utilizes the three estimates based on the alternative slip history interpretations, giving each equal weight. Uncertainty in the cumulative displacement and age of the units was included in the assessment.

For fractures and unbroken rock, the frequency of displacement events and the average displacement per event are assessed directly. The frequency of events is assessed to lie within a broad range of uncertainty defined from alternative assumptions for the deformation history of Yucca Mountain. The average displacement per event for fractures with no offset

and unbroken rock was assessed on the basis of the level of detection for deformation. The assessments for these features are considered to be upperbound values by the DFS team.

The final part of the displacement hazard model is the evaluation of the conditional probability of exceedance. The DFS team developed a triangular probability distribution for *D/AD* from the trenching data in the Yucca Mountain region (see Appendix E) As described in Section H.2.1, a gamma distribution provides a better fit to the data and the DFS team actually adopted this distribution for hazard computation. The selected distribution is shown on the left-hand side of Figure 4-14. The probability of exceeding a specified value of d is computed using this distribution together with the estimate of the average displacement per event given for the feature ($\overline{D}_E = AD$).

Summary of Application of Model to Nine Demonstration Points. The DFS team interprets Points 1, 2, 4, and 9 to lie on features that have paleoseismic data for slip rate. Slip rates for the remaining points are evaluated solely from the cumulative slip and alternative interpretations of the deformation history. Considering the hypothetical features at Points 7 and 8, they utilize the assumed cumulative displacements of 2 m and 10 cm to characterize the hazard for conditions (a) and (b), respectively, and estimate the average displacement per event and displacement event frequency for fractures and intact rock, conditions (c) and (d).

Rogers, Yount, Anderson Team. The RYA team uses the displacement approach to characterize the hazard at all locations. Their displacement hazard characterization differs depending on whether or not Quaternary paleoseismic data are available for the location of interest.

Displacement Hazard Characterization for Sites with Quaternary Data. Figure 4-85 shows the logic tree used by the RYA team to characterize the displacement data at locations for which Quaternary paleoseismic data are available. The first assessment is the likelihood that the feature of interest can slip in a displacement event, $P(C)$. This probability is assessed based on evidence for recency of slip and the relationship of the feature to the structural elements of Yucca Mountain. Block-bounding faults with evidence of Quaternary movement are assigned $P(C)=1.0$.

The next assessment is the approach used to assess the frequency of displacement events. The RYA team considers two alternatives: the use of direct estimates of the frequency of displacement events from paleoseismic data, and the use of slip rate and Equation (4-13). The distributions for the average displacement per event, the Quaternary slip rate, and direct estimates of the frequency of displacement events are all based on paleoseismic data.

The final assessment is the approach for estimating the conditional probability of exceedance. Two alternatives are considered. The first is the use of the empirical distribution for D/AD developed by the DFS team from Yucca Mountain data. These data were fit with a gamma distribution (see Section H.2.1). The second approach is the distribution for D/MD^{max} developed by the AAR team from Yucca Mountain data. These data were fit by an exponential distribution (see Section H.2.5). The appropriate value of MD^{max} was assessed from paleoseismic data for the feature.

Displacement Hazard Characterization for Sites Without Quaternary Data. Figure 4-86 shows the logic tree used by the RYA team to characterize the displacement data at locations for which no Quaternary paleoseismic data are available. The overall approach parallels are shown on Figure 4-85, except that scaling relationships based on fault length and cumulative displacement are used in place of Quaternary data. The first assessment is the likelihood that the feature of interest can slip in a displacement event, $P(C)$. Intrablock faults with north-south trends are assigned $P(C)=0.4$, and those with northwest-southeast trends are assigned $P(C)=0.1$. Small faults and shears are assigned $P(C)=0.5$ to 0.3.

The frequency of displacement events is assessed using only slip rate and Equation (4-13). The slip rate is assessed based on the cumulative offset of a feature, which is considered to be an uncertain parameter. Three alternative interpretations of the slip history of the faults are considered. The first is that the slip rate has been uniform post deposition of the Tiva Canyon Tuff and the slip rate is given by $SR=D_{cum(\text{Tiva Canyon})}/12.7$ Ma. The second interpretation is that 20 percent of the cumulative deformation on the Yucca Mountain faults occurred after the onset of volcanism in Crater Flat about 3.7 Ma, yielding an estimate of $SR=0.2D_{cum(\text{Tiva Canyon})}/3.7$ Ma. The favored interpretation is that 98 percent of the deformation occurred prior to the Quaternary. The resulting slip-rate estimate is

SR=0.02$D_{cum(\text{Tiva Canyon})}$/1.6 Ma. Uncertainty in the cumulative displacement was included in the assessment.

The next assessment is the average displacement per event. The RYA team considers two alternative scaling relationships developed by the AAR team to be appropriate, one based on the length of the feature and one based on the cumulative offset of the feature. These relationships provide estimates of MD^{max}. The data for D/MD^{max} have a mean value of 0.83 and the RYA team interpreted $\bar{D}_E$ to be equal to 0.83 MD^{max}. If length information is not available for a feature (such as is the case for the hypothetical features at Points 7 and 8), then the assessments are made using only the cumulative offset of the feature.

The final assessment is the approach for estimating the conditional probability of exceedance. The same two alternatives are considered for these sites as were used for sites with Quaternary data (Figure 4-85).

Summary of Application of Model to Nine Demonstration Points. The RYA team interprets Points 1 and 2 to lie on features that have paleoseismic data. Slip rates for the remaining points are evaluated solely from the cumulative slip and alternative interpretations of the deformation history. Considering the hypothetical features at Points 7 and 8, they utilize the assumed cumulative displacements of 2 m and 10 cm to characterize the hazard for conditions (a) and (b), respectively, and interpret the probability of fault slip on a fracture with no measurable offset (c) or in intact rock (d) to be essentially zero.

Smith, Bruhn, Knuepfer Team. The SBK team's characterization of fault displacement hazard differentiates between those sites that are subject to potential principal faulting hazard and those sites that are subject to only distributed faulting hazard.

Characterization for Sites of Potential Principal Faulting Hazard. Figure 4-87 presents the SBK team's logic tree for characterization of sites subject to principal faulting hazard. The SBK team considers both the earthquake and displacement approaches.

Earthquake Approach. In the earthquake approach, two contributions to hazard are included (indicated by the vertical line on the logic tree under sources of hazard): hazard from

principal faulting due to the occurrence of earthquakes on the fault and distributed faulting hazard from earthquakes occurring on other seismic sources. The first assessment in the earthquake approach is an evaluation of whether or not the feature can experience principal faulting, $P(C)$. This is interpreted to be equal to the probability that the fault is seismogenic, $P(S)$, which was assessed as part of the SBK team's seismic source characterization (see Section 4.3.1.1). The SBK team's assessment is that all faults can experience distributed slip.

The next assessment in the earthquake approach is an evaluation of the frequency of occurrence of earthquakes of various magnitudes on each of the seismic sources. The characterization of earthquake recurrence developed by the SBK team for the ground motion hazard assessment was used directly to define the distributions for earthquake occurrence frequency.

Given the occurrence frequency of earthquakes, the next assessment is the approach for assessing the probability that slip will occur in a given event. For principal faulting, the SBK team assessed P_i(slip|event on i) using the logistic regression model, Equation (4-15), to assess the probability that surface rupture occurs, selecting the parameters of the model developed from the data base of 32 post-1930 Great Basin earthquakes (Figure 4-11). The probability of intersection with the site was computed by randomization of the rupture length along the fault.

For distributed faulting, the SBK team developed a two-part approach for assessing P_i(slip|event on j):

$$P_i(\text{Slip} \mid \text{event on } j) = P(\theta) \times F(event) \qquad (4\text{-}23)$$

where $P(\theta)$ is a function of the orientation of the feature of interest at point i and $F(event)$ is a function of the earthquake occurring on source j. Two alternatives were used to evaluate the probability $P(\theta)$. The first utilizes an assessment of the slip tendency of the feature with respect to the present stress regime. The slip tendency analysis indicates that features with a north-south orientation are favorably oriented for slip in the present stress regime. Thus, the SBK team considered $P(\theta)$ for these features to be at or near 1.0, if there was evidence of

Quaternary displacement. Alternative values of $P(\theta)$ were assessed to account for uncertainty in the interpretation. For features oriented in a northwest-southeast direction, the assessed values for $P(\theta)$ were about 0.5. The second approach for assessing $P(\theta)$ utilized the analysis of the distribution for the angle between the strike azimuths of the principal fault rupture and the associated distributed ruptures presented in Section H.4.3. An evaluation of the focal mechanisms for earthquakes in the immediate Yucca Mountain vicinity (see Chapter 7, USGS, written communication, 1996) indicates that the distribution of nodal plane strike azimuths is approximately uniform and an average value of $P(\theta)$ was computed assuming random strike to apply to earthquakes occurring in the areal source zones.

The second term of Equation (4-23) expresses the probability of slip as a function of the earthquake on the seismic source. The SBK used two alternative approaches for assessing this probability. The first approach is the logistic regression model developed from the analysis of the density of distributed faulting in historical ruptures defined by Equation (4-17) and shown on Figure 4-12. The second approach defines the probability of slip as a function of the peak velocity (PV in cm/sec) induced by the earthquake at the site. The relationship developed by the SBK team (see Figure SBK-19 in Appendix E) was fit with the logistic regression model:

$$F(event) = \frac{e^{-7.0+0.14PV}}{1+e^{-7.0+0.14PV}} \qquad (4\text{-}24)$$

The peak velocity induced by the earthquake is estimated using the ground motion models developed for the Yucca Mountain site. The SBK team considers this approach to be valid for underground openings.

The final assessment is the approach for evaluating the conditional probability of exceeding a specified displacement, $P(D>d)$. For principal faulting, this probability was evaluated using the two-part method defined by Equation (4-19). The distribution for MD was defined by a published empirical model based on earthquake magnitude. The location of the point of interest was assessed for each rupture to define the parameter x/L. Two alternatives are considered for the distribution for D/MD. The first is the analysis of data from historical ruptures shown on Figure 4-13. The second is a model developed from numerical

simulations of fault displacements (see Section H.3.2). For distributed faulting, an empirical distribution for D/D_{cum} (see Section H.2.6) is used to evaluate the probability of exceeding a specified displacement.

Displacement Approach. The displacement approach does not distinguish between principal and distributed ruptures (Figure 4-87). The first assessment in the logic tree is an evaluation of the probability the feature can slip, $P(C)$. This assessment is the same as the assessment of $P(C)$ for distributed faulting in the earthquake approach.

The SBK team uses two approaches for estimating the frequency of displacement events. The first method uses a direct estimate of the frequency from paleoseismic data. The second approach uses estimates of fault slip rate and average displacement per event to obtain the frequency of displacement events [Equation (4-13)]. The recurrence rate (inverse of recurrence interval) and slip-rate estimates are given by the seismic source characterization model developed by the SBK team.

The SBK team uses three alternative methods to assess the average displacement per event, $\bar{D}_E$, and the conditional probability of exceedance, $P(D>d)$ that are based on evaluations of the data from Yucca Mountain trenching studies. The first method utilizes the average displacement estimated for paleoearthquakes, designated as AD_{paleo}, to specify $\bar{D}_E$ and uses a distribution for D/AD_{paleo} to compute $P(D>d)$. This distribution is discussed in Appendix H, Section H.2.2. For the second approach, the SBK team used an empirical model between rupture length and average displacement, designated $AD_{F(RL)}$ to develop a distribution for $D/AD_{F(RL)}$ (see Section H.2.3). The mean of this distribution is 1.46 and $\bar{D}_E$ is set equal to $1.46 \times AD_{F(RL)}$. The distribution for $D/AD_{F(RL)}$ is used to compute $P(D>d)$. For the third approach, the SBK team used an empirical model between rupture length and maximum displacement, designated $MD_{F(RL)}$ to develop a distribution for $D/MD_{F(RL)}$ (see Section H.2.4). The mean of this distribution is 0.72 and $\bar{D}_E$ is set equal to $0.72 \times MD_{F(RL)}$. The distribution for $D/MD_{F(RL)}$ is used to compute $P(D>d)$.

Characterization for Sites of Only Potential Distributed Faulting Hazard. Figure 4-88 presents the SBK team's logic tree for characterization of sites subject to only distributed faulting hazard. The SBK team considers both the earthquake and displacement approaches, and the hazard characterization model is similar to that for sites of principal faulting hazard (Figure 4-87). The differences between the approaches for hazard characterization at the two types of sites primarily reflect the different types of data available.

Earthquake Approach. The earthquake approach for sites subject to distributed faulting hazard is identical to that shown on Figure 4-87.

Displacement Approach. The displacement approach for sites of only distributed faulting hazard parallels that discussed above for principal faulting hazard, except that slip rates and average displacements estimated from paleoseismic data are not available and are replaced by scaling relationships utilizing cumulative displacement.

The frequency of displacement events is again obtained using Equation (4-13). Two alternative approaches are used to estimate slip rate on the feature. The first approach is based on the cumulative slip and three alternative interpretations of the history of slip. The first interpretation is uniform slip post-Tiva Canyon. The second interpretation is uniform slip post-Rainier Mesa 11.6 Ma tuff deposition, in which 20 percent of the post-Tiva Canyon deformation has occurred. The third interpretation is that the Quaternary slip rates are 2.1±1.8 percent of the late Miocene slip rates, with the late Miocene rates computed by dividing 80 percent of the post-Tiva Canyon displacement by 0.9 Ma. The second approach for estimating slip rate used by the SBK team involves using the ratio of cumulative slip between the feature of interest and the cumulative slip on those faults with Quaternary slip rate estimates to scale the measured Quaternary slip rates to an estimate for the feature of interest. Uncertainty in the cumulative displacement was included in the assessment.

The SBK team again uses three alternative methods to assess the average displacement per event, $\overline{D}_E$, and the conditional probability of exceedance, $P(D>d)$ that are based on evaluations of the data from Yucca Mountain trenching studies. Two of these are the estimates based on $AD_{F(RL)}$ and $MD_{F(RL)}$ discussed above. For the third approach, the SBK team developed a distribution from the Yucca Mountain data for D/D_{cum} (see Section H.2.6).

The mean of this distribution is 0.00176 and $\bar{D}_E$ is set equal to $0.00176 \times D_{cum}$. The distribution for D/D_{cum} is used to compute $P(D>d)$. If the length of the feature is not known, the SBK team uses only the estimate based on cumulative displacement.

Summary of Application of Model to Nine Demonstration Points. The SBK team interprets Points 1 and 2 to lie on faults that are subject to both principal and distributed faulting hazard and utilizes the logic tree shown on Figure 4-87 to characterize the hazard at these sites. The remaining points are interpreted to be subject to distributed faulting hazard only and the logic tree shown on Figure 4-88 is used to characterize hazard at these sites. Considering the hypothetical features at Points 7 and 8, they utilize the assumed cumulative displacements of 2 m and 10 cm to characterize the hazard for conditions (a) and (b), respectively; provide a distribution for the relative hazard between a fracture, condition (c), and a minor shear, condition (b); and make an estimate of the frequency and amplitude for displacement in intact rock, condition (d).

Smith, de Polo, O'Leary Team. The SDO team's characterization of fault displacement hazard differentiates between those sites that are subject to potential principal faulting hazard and those sites that are subject to only distributed faulting hazard.

Principal Faulting Hazard Model. The SDO team uses the earthquake approach for characterizing the hazard due to principal faulting. Figure 4-89 shows the logic tree that defines their characterization. The frequency of occurrence of earthquakes of various magnitudes on each seismic source are defined by the seismic source characterization model (Section 4.3.1.1). The probability of slip at or near the surface given the occurrence of a magnitude m earthquake is computed using the logistic regression model defined by Equation (4-15). The SDO team uses two alternative data sets to develop the parameters for Equation (4-15): one based on 32 post-1930 Great Basin earthquakes and one based on 47 post-1930 northern Basin and Range earthquakes (Figure 4-11). The probability of intersection of the point of interest is computed by randomizing the location of the rupture length for an earthquake of magnitude m along the fault trace.

The conditional probability of exceeding a specified displacement, $P(D>d)$ for principal faulting was evaluated using two alternative approaches: one based on average displacement,

AD, and one based on maximum displacement, *MD*. The assessment of *AD* and *MD* depended upon the size of the earthquake. For earthquakes of magnitude smaller than the characteristic magnitude (defined as $m \leq m^U$-½), the values of *AD* and *MD* are assessed using an empirical relationship between displacement per event and earthquake magnitude. For the characteristic magnitude earthquakes (m^U-½ $\leq m \leq m^U$) assessments of *AD* and *MD* also are made using the maximum rupture length of the fault and paleoseismic data. Two scaling relationships are used between *AD* and rupture length: a published empirical model and a scaling model developed by the AAR team. In addition, the SDO team utilized the displacement profile for the Solitario Canyon fault presented by Alan Ramelli in Workshop #6 to characterize the average displacement at Point 2. Given an assessment of *AD*, the distribution for *D/AD* developed by the DFS team (Section H.2.1) was used to compute $P(D>d)$. Given an assessment of *MD*, the two-part method defined by Equation (4-19) was used to compute $P(D>d)$. The distribution for *MD* was defined as lognormal using the standard deviation associated with the empirical model. Two alternatives are considered for the distribution for *D/MD*. The first is the analysis of historical ruptures shown on Figure 4-13. The second is a model developed from numerical simulations of fault displacements (see Section H.3.2).

The SDO team also considered the potential for distributed faulting hazard at sites subject to principal faulting hazard. Their earthquake approach for characterizing distributed faulting hazard, discussed below, was used for these sites.

Distributed Faulting Hazard Model. Figure 4-90 presents the SDO team's logic tree for characterization of distributed faulting hazard. The SDO team considers both the earthquake and displacement approaches for sites subject to only distributed faulting hazard and only the earthquake approach for sites subject to both principal and distributed faulting hazard.

Earthquake Approach. The first assessment is the probability that the feature can slip in the present stress regime, $P(C)$. The SDO team's interpretation is that features oriented in a north-south direction (or are interpreted to be seismogenic) are assigned $P(C) = 1.0$. Features oriented in a northwest-southeast direction are assigned $P(C) = 0.8$.

The frequency of earthquakes occurring on each of the seismic sources is defined as part of the SDO team's seismic source characterization for the ground motion hazard assessment. The probability that slip occurs in an individual earthquake was assessed using the two-part approach defined by Equation (4-23) discussed above for the SBK team. The probability $P(\theta)$, was assessed using the analysis of the distribution of angles between the strikes of principal and distributed ruptures presented in Section H.4.3. An evaluation of the focal mechanisms for earthquakes in the immediate Yucca Mountain vicinity (see Chapter 7 of USGS, written communication, 1996) indicates that the distribution of nodal plane strike azimuths is approximately uniform and an average value of $P(\theta)$ was computed assuming random strike to apply to earthquakes occurring in the areal source zones. The probability $F(event)$ was assessed using the logistic regression model developed from the analysis of the density of distributed faulting in historical ruptures defined by Equation (4-17) and shown on Figure H-13c.

The conditional probability of exceedance, $P(D>d)$, was assessed using two approaches. The first approach defined a reduction factor, RF, equal to the ratio of the cumulative displacements on the feature of interest to the cumulative displacement on the earthquake source. The procedures described above for principal faulting were used to assess the distribution for displacement on the earthquake source at its closest approach to the point of interest. The distribution for displacement at the point of interest then is set equal to RF times the distribution on the earthquake source. The second approach utilized empirical observations of the displacement on distributed ruptures normalized to the maximum displacement on the principal rupture. A curve was defined that approximately enveloped these data (see Figure 4-91). This curve is considered to represent the 95th percentile of the distribution of possible displacements on a distributed rupture. For earthquakes occurring in the areal source zones, the conditional probability of exceedance was computed using only the second approach and the assumption that the point of interest was equally likely to lie in the hanging wall or footwall of the rupture.

Displacement Approach. The first assessment in the displacement approach for characterization of distributed faulting hazard is an assessment of whether or not slip can occur, $P(C)$. This assessment is the same as that for the earthquake approach.
The frequency of displacement events is obtained using Equation (4-13). The slip rate on the feature is estimated from the interpretation that from 0.2 to 2.0 percent of the cumulative

post-Tiva Canyon slip has occurred in the Quaternary. The average displacement per event, $\overline{D}_e$, is estimated from the cumulative displacement using two approaches. The first is the scaling relationship developed by the AAR team in which $D_E = 0.83 \times 1.32 \times \beta \times D_{cum}$, where β varies from 1.40×10^{-3} to 1.85×10^{-2}. The second approach is the empirical distribution for D/D_{cum} (see Section H.2.6). The mean of this distribution is 0.00176 and $\overline{D}_e$ is set equal to $0.00176 \times D_{cum}$.

The conditional probability of exceedance, $P(D>d)$, is assessed using two approaches that correlate with those used to assess D_E. If the scaling relationship developed by the AAR team is used, then $P(D>d)$ is assessed using the distribution for D/MD^{max} (see Section H.2.5) with $MD^{max} = D_E/0.83$. If the mean of the empirical distribution for D/D_{cum} presented in Section H.2.6 is used, then the same distribution is used to assess $P(D>d)$.

Summary of Application of Model to Nine Demonstration Points. The SDO team interprets Points 1 and 2 to lie on faults that are subject to both principal and distributed faulting hazard and utilizes the logic tree shown on Figure 4-89 plus the earthquake approach on the logic tree shown on Figure 4-90 to characterize the hazard at these sites. The remaining points are interpreted to be subject to distributed faulting hazard only and the logic tree shown on Figure 4-90 is used to characterize hazard at these sites. Considering the hypothetical features at Points 7 and 8, they utilize the assumed cumulative displacements of 2 m and 10 cm to characterize the hazard for conditions (a) and (b), respectively, and interpret the probability of fault slip on a fracture with no measurable offset, condition (c), or in intact rock, condition (d), to be essentially zero.

4.3.2.2 Summary of Fault Displacement Hazard Characterization Approaches. In this section we summarize the range of interpretations made by the SSFD expert teams regarding their characterization of fault displacement hazard. A summary of the key components of their models is provided in Table 4-3.

Overall Approach for Characterizing Faulting Hazard. In aggregate, the six SSFD expert teams slightly prefer the displacement approach (aggregate weight ~ 0.6) over the earthquake approach for characterizing fault displacement hazard at sites subject to principal faulting and at sites subject to only distributed faulting. For characterizing principal faulting hazard, four

of the teams (ASM, DFS, RYA, and SDO) considered only one approach for characterizing the hazard. Three of the teams (ASM, DFS, and RYA) considered only one approach for characterizing distributed faulting hazard.

Displacement Approach for Principal Faulting Hazard. Principal faulting hazard was assessed for sites located on faults that the SSFD expert teams identified as being seismogenic. The preferred approach for estimating the frequency of displacement events is the use of slip rate divided by the average displacement per event [Equation (4-13)]. The slip rates were primarily based on the teams' seismic source characterization for the ground motion hazard assessment. One team (DFS) included slip-rate estimates based on cumulative displacement and slip history. The alternative approach used was a direct assessment of the frequency of events from the paleoseismic data applied in the seismic source characterization. The average displacement per event was primarily assessed from paleoseismic data for the sources of principal faulting hazard.

The teams used a variety of approaches to evaluate the conditional probability of exceedance. These are based on empirical distributions derived from Yucca Mountain trenching data normalized by various parameters, including the expected maximum displacement in the maximum event, MD^{max}, the average displacement estimated from displacement data, and the average and maximum displacements estimated from the length of the feature.

Earthquake Approach for Principal Faulting Hazard. The approach used for assessing the frequency of displacement events used by all of the teams was to use the frequency of earthquakes developed for the ground motion hazard assessment multiplied by a probability that each event produces rupture at the site of interest. This probability is the product of the probability of surface rupture times the probability of intersection of the rupture along the strike of the fault. The along-strike intersection probability was computed using the rupture length estimated from the magnitude of the event randomly located along the fault length. Most teams used the empirical model based on historical ruptures (Figure 4-11) to compute the probability of surface rupture. The AAR team used randomization of the rupture location over the down-dip width of the fault to compute the probability of surface rupture.

The approach used by most of the teams to assess the conditional probability of exceedance was to define a distribution for the maximum displacement, *MD*, based either on the magnitude or the rupture length of the earthquake. This distribution is then convolved with a distribution for *D/MD* to compute $P(D>d)$. The preferred distribution of *D/MD* is the empirical model developed by the ASM team from data compiled by Wheeler (1989) on historical ruptures. Some weight was given to a model developed by the SBK team from fractal simulations of fault ruptures. The SDO team also gave some weight to using the average displacement per event, *AD*, estimated from magnitude, rupture dimensions, and paleoseismic data together with an empirical distribution for *D/AD*.

Displacement Approach for Distributed Faulting Hazard. The majority of the SSFD expert teams specified that the frequency of displacement events on features subject to only distributed faulting be estimated by slip rate divided by the average displacement per event [Equation (4-13)]. The slip rates were primarily based on the cumulative displacement and slip history, though the AAR team developed a correlation between cumulative displacement and Quaternary slip rate from Yucca Mountain data. The interpretations of the slip histories were similar across all teams. The preferred model is that slip has been decreasing with time and the present-day rate is a small percentage of the late Miocene rate. Low weight was given to a uniform slip history for deformation post-12.7 Ma Tiva Canyon tuff deposition. Somewhat higher weight was given to an intermediate model of uniform slip for a time period that ranged from 3.7 to 11.6 Ma. The average displacement per event for features subject to only distributed faulting hazard was estimated using scaling relationships based on either the length of the feature or the cumulative displacement of the feature. If both length and cumulative displacement are known, then the teams gave nearly equal weights to these two approaches.

The teams used similar approaches for evaluating the conditional probability of exceedance to those used in the displacement approach for characterizing principal faulting hazard. The empirical distributions used are typically correlated with the scaling relationship used to estimate the average displacement per event. For example, if the average displacement per event is to be estimated from the cumulative displacement, then the associated distribution for displacement in a single event is based on D/D_{cum}.

Earthquake Approach for Distributed Faulting Hazard. The SSFD expert teams displayed the most variability in characterizing distributed faulting hazard using the earthquake approach. The basic assessment of the frequency of earthquakes was derived from the seismic source characterization for the ground motion hazard assessment defined by each team. The probability that an earthquake causes slip at the point of interest was assessed in a variety of ways. Most teams utilized the logistic regression model based on analyses of the pattern of historical ruptures (e.g., Figure 4-12). Two of the teams (SBK and SDO) introduced an additional factor based on either the orientation of the feature in the present stress field (slip tendency) or on the angle between the strikes of the feature and the principal rupture. The ASM team introduced a factor that depends on the probability of the earthquake producing principal faulting surface rupture. The SBK team also introduced an approach that is based on the peak velocity induced by the earthquake at the point of interest.

The widest variations in approaches were those for assessing the distribution for displacement per event on the distributed ruptures. Two of the teams (ASM and SDO) used methods defined as a reduction factor, *RF*, times the displacement distribution on the principal rupture. The methods used to assess *RF* were based on (1) the relative cumulative displacement of the feature of interest compared to that of the earthquake source, (2) a scaling relationship defined from the observed ground displacement profile in the 1983 Borah Peak earthquake, and (3) empirical data for the amount of cumulative displacement normalized by the maximum principal faulting displacement. Two other teams (AAR and SBK) used distributions defined by the characteristics of the feature at the point of interest, either length or cumulative displacement. These distributions were the same as those used in the displacement approach.

Application of Models to Nine Demonstration Points. All of the teams considered that Points 1 and 2 are subject to principal faulting hazard. Two of the teams (AAR and DFS) also considered some potential for principal faulting hazard at Point 4 because they had interpreted some probability that the Ghost Dance fault is seismogenic. The AAR team also made the interpretation that Point 6 in Dune Wash lies on their West Dune Wash Number 2 seismic source and may also be subject to principal faulting hazard.

The teams widely varied in their assessments of the probability that distributed faulting could occur in future earthquakes at Points 3 through 9, which are located off of the block bounding faults. These assessment were based on fault orientation, cumulative slip, and structural relationship. The SBK team's interpretation is that all features with some evidence of cumulative displacement are capable of displacement in future earthquakes. The DFS team's interpretation is that for most of these features, the probability that they are capable of displacement in future earthquakes is low. Four of the teams (AAR, ASM, RYA, and SDO) consider that the probability of displacement at a point in intact rock due to the occurrence of a future earthquake is essentially zero.

TABLE 4-1
SUMMARY OF SEISMIC SOURCE CHARACTERIZATION MODELS
Page 1 of 9

Issue	AAR Team	ASM Team	DFS Team	RYA Team	SBK Team	SDO Team
TECTONIC MODELS						
Overall Approach	Viable models based on observations and inferred processes for the Crater Flat structural domain, with simple shear model given full weight (1.0). Superposed NW-SE dextral shear manifested as specific structures (tectonic models A, B, & C) (0.5) or not (tectonic model D) (0.5).	The source model incorporates various aspects of planar block fault (preferred), detachment, lateral shear, and volcanic-tectonic models.	Alternative tectonic and structural models are considered primarily in the characterization of local faults: domino model (0.8) (planar fault); detachment (0.2) (includes hypothetical hidden strike-slip fault of either local or regional extent).	None of the tectonic models presented provides a unified explanation for all the seismic, geologic, and geophysical data. Alternative tectonic and structural models are considered primarily in the characterization of local faults. A coalescing fault model best fits the Yucca Mountain area.	Preferred model: oblique rift-planar faults. 3D strain accommodated on planar, strike-slip, normal, and oblique-slip faults. Rock Valley and Highway 95 faults act as accommodation zones in the rift.	Alternative tectonic and structural models are considered in the characterization of local faults. Preferred model for Crater Flat – Yucca Mountain is a half-graben formed within a larger rift that opens and deepens to the north. Deformation history and structure are associated with carapace effect, clockwise vertical axis rotation, basaltic volcanism, age and behavior of Bare Mountain fault.
Planar Block-Faulting Models	Regional faults are modeled as independent and linked (for selected faults) planar faults to maximum seismogenic depth. Local faults include linked and coalesced models; planar faults to maximum seismogenic depth, to depth of local detachment, or in some cases to a depth constrained by allowable aspect ratio or by intersection with a higher-order fault.	Regional faults are modeled as independent planar faults to maximum seismogenic depth. Local faults—the preferred model is that the faults are planar to a depth controlled by the brittle-ductile transition and the Bare Mountain fault; treated as independent and coalescing faults that merge at depth.	Regional faults are modeled as independent planar faults to maximum seismogenic depth. Local faults—include models of independent (0.95) and distributed (0.05) fault behavior; alternative structural models (domino-planar and detachment-listric) used to constrain downdip geometry and extent.	Bare Mountain and regional faults are modeled as independent planar faults to maximum seismogenic depth. Local faults—planar to listric (1 to 3 coalescing systems).	Regional faults are modeled as independent planar faults to maximum seismogenic depth. Local faults—Yucca Mountain faults are part of a half-graben, with Bare Mountain as the master fault, predominantly normal slip with a left-lateral component.	Regional faults are modeled as independent planar faults to maximum seismogenic depth. Local faults: half-graben model (1) end member—all Yucca Mountain faults are seismogenic, continuous planar faults to maximum seismogenic depth. (2) carapace effect—only major block-bounding faults are through-the-crust seismogenic faults; other intrablock faults are confined to the carapace (i.e., are aseismic) or link to faults having different attitudes and aspect ratios below the unconformity.

TABLE 4-1
SUMMARY OF SEISMIC SOURCE CHARACTERIZATION MODELS

Issue	AAR Team	ASM Team	DFS Team	RYA Team	SBK Team	SDO Team
Shear Models (buried strike-slip faults or fault systems)	Included three alternatives: Model A – Throughgoing regional dextral shear zone (0.05); Model B - right-stepping dextral shear zone that produces a pull-apart basin WITHOUT an underlying cross-basin fault (0.6); and Model C - right-stepping dextral shear zone that produces a pull-apart basin WITH an underlying cross-basin fault (0.35).	Model 1 – Continuous, long (240-km) strike-slip fault zone as proposed by Schweikert considered. Regional (60-km-long) strike-slip fault given low weight. Model 2 – Shorter (25-km), more complex or segmented zone. Assessment of existence of buried strike-slip fault conditional (yes–0.2; no–0.05) on whether or not detachment exists; assessment of the seismogenic potential of the buried strike-slip fault is conditional on the depth of the detachment (shallow–0.8, moderate–0.6, deep–0.0).	Model allows for component of northwest-directed right-lateral strike-slip strain. Hypothetical hidden strike-slip fault source (P_A = 0.05) is included in detachment model. Two postulated strike-slip fault sources are included: regional strike-slip fault (0.5) local strike-slip fault (0.5)	None (possibility of local buried source covered by background source).	A buried regional shear zone model is given low weight (0.01); no evidence for a buried strike-slip fault trending northwest across Crater Flat that would result in a earthquake larger than the maximum assigned to the host source zone.	Three sources of dextral shear were evaluated to account for vertical axis rotation at Yucca Mountain: (1) distributed shear (restricted to Crater Flat basin; basin is a discrete domain controlled by local bounding faults); (2) external transcurrent strike-slip fault (passes through the basin, totally hidden); and (3) external strike-slip fault enters basin from southeast (manifested at Yucca Mountain by the N25°W striking "hingeline") and terminates in Crater Flat. Only (1) and (3) are credible modifications to the basic model.
Detachment Models	Regional detachment not viable (0.0), but hypothesized local detachments included, with weights dependent on the type of dextral shear structures assumed to be present. Local detachments not included as specific seismic sources; detachments affect only down-dip fault extent for local fault sources. Depths included for local detachments range from 3 km to the maximum thickness of the seismogenic crust, with 3 to 10 km preferred.	Detachment Model (0.15): Hypothesized detachment affects down-dip geometry and extent of local fault sources; seismogenic detachment is included as possible fault source with very low probability (see below).	Detachment Model (0.2): Hypothesized detachment chiefly affects down-dip geometry and extent of local fault sources; seismogenic detachment is included as possible fault source with very low probability (see below).	Detachments are not explicitly modeled. Possibility that local faults truncate down dip in a detachment or zone of decoupling is included in coalescing fault model.	Hypothesized detachment affects only the down-dip extent of local fault sources.	A seismogenic detachment (modeled as an independent source) was thoroughly considered but could not be substantiated by the available evidence.

TABLE 4-1
SUMMARY OF SEISMIC SOURCE CHARACTERIZATION MODELS
Page 3 of 9

Issue	AAR Team	ASM Team	DFS Team	RYA Team	SBK Team	SDO Team
Volcanic-Tectonic Models ("ash event")	The possibility of simultaneous rupture on subparallel Yucca Mountain faults as postulated for the "ash event" is included in coalesced fault models for local faults.	The possibility that some surface rupturing earthquakes in Crater Flat are accompanied by dike injection (e.g., the 70-ka "ash event") is included in simultaneous rupture models for local faults.	The possibility of simultaneous rupture on subparallel Yucca Mountain faults as postulated for the "ash event" is included in the distributed faulting model for local faults.	The coalescing fault model used to model local faults (see below) would explain the apparent sychroneity of faulting on Yucca Mountain faults (i.e., the 70 ka "ash event").	Explicitly models a simultaneous rupture event (triggered by volcanic event; see Local Fault Model)	Distributed fault models involve simultaneous rupture of local faults that are parallel to each other. Such models would account for volcanism and tectonic faulting as a coupled process.
Thickness of Seismogenic Crust	Dmax1 11 km (0.185) 15 km (0.63) 17 km (0.185) Dmax2 14 km (0.185) 18 km (0.63) 22 km (0.185)	12 (0.1) 15 (0.6) 17 (0.3)	12 (0.6) 14 (0.3) 16 (0.1)	12 km (0.2) 15 km (0.7) 20 km (0.1)	12 (0.3) 15 (0.6) 17 (0.1)	14 km (0.2) 17 km (0.7) 19 km (0.1)
SEISMIC SOURCES						
Seismic Source Zones	Four scenarios: Scenario I w/3 zones (0.3), Scenario II w/2 zones (0.3), Scenario III w/3 zones (0.3), and Scenario IV w/1 zone (0.1). For all scenarios, a host zone (within 20-km radius) is defined only for assigning a lower M_{max}—not for separate recurrence estimate.	Two source zones within 100-km radius of site. A local zone (within 50-km radius) is included that is defined solely for assigning a lower M_{max}.	Model A (0.2) One zone Model B (0.8) Three zones Both models include a local zone that is defined for constraining M_{max} in the area of the detailed site characterization studies.	Three primary source zones within 100 km of site; two alternative configurations to model Zone A (local Yucca Mountain region) and Zone B (the zone surrounding Zone A).	Model A (0.7) 3 zones Model B (0.3) 4 zones Both models include a local zone that is defined solely for assigning a lower M_{max}.	Eight source zones within a 300-km radius of the site were considered initially, but only 3 remained given a filter of radius <100 km.
Seismic Source Zones—Recurrence	Truncated exponential recurrence model (1.0)	Truncated exponential recurrence model (1.0)	Truncated exponential recurrence model (1.0)	Truncated exponential recurrence model (1.0)	Truncated exponential recurrence model (1.0)	Truncated exponential recurrence model (1.0)

TABLE 4-1
SUMMARY OF SEISMIC SOURCE CHARACTERIZATION MODELS

Issue	AAR Team	ASM Team	DFS Team	RYA Team	SBK Team	SDO Team
Seismicity Catalog	300-km radius catalog Version 7 (1.0) Adjustment made for UNEs in relevant source zones.	300-km radius catalog Version 7 (0.7) Version 5 (0.3) Adjustment made for UNEs.	300-km radius catalog Version 7 (0.5) Version 5 (0.5)	100-km radius catalog Version 5 (0.5) Version 7 (0.5)	100-km radius catalog Version 7 (0.3 -0.6) Version 5 (0.4 -0.7) Weights vary depending on source zone. In relevant zones, adjustments made for UNEs weighted (0.4) versus no adjustment (0.6).	300-km radius catalog Version 5 (0.6) Version 7 (0.2) Version 8 (0.2)
Spatial Smoothing Model	For Scenarios I - III: Uniform (1.0). For Scenario IV: h = 5 km (0.25) h = 10 km (0.5) h = 20 km (0.25)	Uniform (1.0)	Model A: h = 10 km (0.25) h = 25 km (0.6) Uniform (0.15) Model B: h = 10 km (0.22) h = 25 km (0.53) Uniform (0.25)	Uniform (0.4); h = 5 km (0.4) h = 15 km (0.2)	Uniform (1.0)	Uniform (0.5) h = 10 km (0.25) h = 20 km (0.25)
Seismic Source Zones—M_{max}	Excluding Host Zone 6.6 (0.3) 6.9 (0.4) 7.3 (0.3) Host Zone (within 20 km) 6.0 (0.3) 6.3 (0.4) 6.6 (0.3)	Walker Lane 6.5 (0.185) 6.8 (0.63) 7.1 (0.185) Basin and Range 6.9 (0.185) 7.2 (0.63) 7.5 (0.185) Site Region (within 50 km) 6.0 (0.185) 6.3 (0.63) 6.6 (0.185)	Model A (not including site vicinity) 7.0 (0.2) 7.3 (0.6) 7.7 (0.2) Model B (not including site vicinity) SW Walker Lane 7.0 (0.2) 7.3 (0.6) 7.7 (0.2) NE Walker Lane and Basin and Range 7.0 (0.2) 7.25 (0.6) 7.5 (0.2) Site Vicinity 5.6 (0.2) 5.8 (0.6) 6.0 (0.2)	6.0 (0.185) 6.3 (0.63) 6.6 (0.185)	Excluding Local Zone: 6.2 (0.2) 6.3 (0.5) 6.4 (0.2) 6.6 (0.1) Local Zone 5.6 (0.2) 6.0 (0.6) 6.2 (0.2)	Within 100 km 6.4 ± 0.2 cumulative lognormal distribution 6.2 (0.03) 6.4 (0.5) 6.6 (0.97 Beyond 100 km: estimated from a correlation of fault length with magnitude for longest fault: in Zones 2 and 3 Ms 7.4 ± 0.2

TABLE 4-1
SUMMARY OF SEISMIC SOURCE CHARACTERIZATION MODELS
Page 5 of 9

Issue	AAR Team	ASM Team	DFS Team	RYA Team	SBK Team	SDO Team
Regional Fault Sources	19 regional fault sources; includes faults with Pa of <1.0; includes two possibly linked fault systems: Death Valley with Furnace Creek (0.8), and Amargosa River with Pahrump (0.1); also includes five faults considered as segmented (max. rupture length < total fault length); included range of rupture lengths for each source. Preferred dips: normal 65° strike-slip 90°	24 regional faults (within 15 to 100 km of site); all fault sources active (1.0); considers alternative total lengths, generalized down-dip geometry (strike-slip 90°, normal 60°).	18 regional fault sources (within 100 km of site vicinity); all fault sources active (1.0); considered alternative total lengths, generalized down-dip geometry (strike-slip 90°, normal-60°).	11 regional fault sources (within 100 km of site); all fault sources active (1.0); includes possibility (0.1) of simultaneous rupture of Death Valley and Furnace Creek faults; includes alternative rupture lengths for 9 faults, generalized down-dip geometry (strike-slip 90°, normal 60°).	16 regional fault sources (within 100 km radius); includes faults with Pa < 1.0; includes range of rupture lengths for each source—for long faults ranges reflect probable rupture segment lengths, assigned dips based on fault type, with preferred values of: strike-slip 90°, normal 60°, and oblique 70°.	36 regional fault sources (24 faults (Pa 1.0), 12 faults (Pa < 1.0); two faults generally outside 100 km (Panamint Valley and Ash Hill fault zone) included; alternative total lengths, generalized down-dip geometry (strike-slip 90°, normal 60°).
Regional Faults—M_{max}	SRL (0.4) RA (0.2) SRL and S (0.4) $M_{max} \pm ¼$ unit, $M_{max} + ¼ = m^u$	SRL (1.0) $M_{max} \pm ¼$ unit, $M_{max} + ¼ = m^u$	SRL (1.0) Alternative rupture segments (SRL) are considered resulting in a range of M_{max} for each fault. $M_{max} \pm ¼$ unit (with some exceptions)	SRL (0.35) RA (0.35) MD (0.3) Or RL (0.5) RA (0.5) depending on available data $M_{max} \pm 0.5$ unit	SRL, RA, MD, AD, and moment approaches; weighted on a fault basis depending on available data. $M_{max} \pm ¼$ unit, $M_{max} + ¼ = m^u$	RL, MD, RL x MD, Slip rate +RL; weighted on a fault basis depending on available data. $M_{max} \pm ¼$ unit, $M_{max} + ¼ = m^u$
Regional Faults—Recurrence Approach	Slip Rate Approach (0.6); Recurrence Interval Approach (0.4) - where data are available. Characteristic (0.7) Modified exponential (0.3) DV -FC Characteristic (1.0) $M_{max} + ¼ = m^u$ b-value 0.80 (0.3), 1.00 (0.4), 1.20 (0.3)	Slip Rate Approach (0.5) Recurrence Interval (0.5) or Slip Rate (1.0) depending on available data. Characteristic (0.2) Maximum moment (0.8) b-value varies from fault to fault.	Slip Rate Approach (1.0) Characteristic (0.6) Maximum moment (0.3) Truncated exponential (0.1) b-value varies from fault to fault.	Slip Rate Approach (1.0) Characteristic (0.9) Truncated exponential(0.1) b-value 1.07 (0.185) 1.12 (0.63) 1.2 (0.185) $M_{min} = 6.3$	Slip Rate and Recurrence Interval Approaches; weights vary from fault to fault depending on available data. Characteristic and truncated exponential models used. Weights vary from fault to fault, with characteristic behavior favored for range-bounding faults, and exponential for zones with multiple distributed traces. b-value varies from fault to fault.	Moment rates (slip rates) Characteristic (0.7) Truncated exponential (0.3) b-value varies from fault to fault. $M_{min} = 6.2$

TABLE 4-1
SUMMARY OF SEISMIC SOURCE CHARACTERIZATION MODELS

Issue	AAR Team	ASM Team	DFS Team	RYA Team	SBK Team	SDO Team
Local Fault Sources	20 individual faults included w/ P[s] 0.1 to 1.0 Synchronous Behavior Approach: (1) Faults rupture independently or are grouped in distributed systems by linkages along strike or coalescence down dip. (2) Likelihood of coalesced behavior is dependent on tectonic model (in general, coalesced behavior strongly favored over independent behavior). (3) Four coalesced models defined with from one to four fault systems. Assigned weights depend on tectonic models, but models having three to four systems are strongly favored. (4) For independent fault behavior, two cases of possibly linked faults are generally favored. Preferred dip 60°. Dominantly normal slip w/ left-lateral component.	Planar Fault Block Model- 5 faults modeled as major block-bounding faults (seismogenic–1.0) 5 faults modeled as minor or secondary faults (probability of being seismogenic—fault, P_A ranges from 0.5 to 0.9). Simultaneous rupture models are based on the probability of linkage at depth (geometric constraints) and temporal overlap inferred from paleoseismic data.	Two Fault Behavioral Models: Distributed (0.05) 9 scenarios Independent (0.95) Two Structural Models: *Domino* model (0.8) (high-angle planar faults to seismogenic depth except where they intersect larger-throw fault); existence of H95 fault not dependent on domino model—considered as an independent source with low probability of being an active seismogenic structure. *Detachment* model (0.2) listric geometry detachment modeled at 6 km depth; includes hidden strike-slip fault sources.	Coalescing Fault Model (1.0) Bare Mountain fault, independent planar fault to seismogenic depths. Yucca Mountain faults are assumed to coalesce down dip at relatively shallow depth (2 to 5 km). Three faults (WW, SC, and PBC) are primary independent seismogenic faults in three-fault system. Coalescing Models: 12 km (0.2) and 15 km (0.7) seismogenic depth: 1-fault system (0.1) 2-fault system (0.5) 3-fault system (0.4) 20 km (0.1) seismogenic depth 1-fault system (0.3) 2-fault system (0.4) 3-fault system (0.3) Planar fault and detachment-decoupled model geometries are considered part of range of behavior for coalesced systems.	Within Crater Flat domain, included 11 individual faults (9 YM, BM, and Hwy 95); excluded 7 mapped faults ($P_A = 0$) based on no or low rates of Quaternary activity (including GD and SD). Model- local faults sole into detachment between 5 km and base of seismogenic zone (0.01). Model- block-bounding faults coalesce at depth either in one or two master faults (0.09) Model (end member) - 4 linked block-bounding faults (0.4) Model (end member) - faults behave independently (0.5) All of the above models include a simultaneous rupture scenario that acts as an additional source; weights on activity vary according to rupture model (0.1 on independent and linked; 0.5 on detachment and coalescing models).	Behavior models included: (1) single-fault (2) linked-fault (3) distributed-fault Single-fault scenarios - 6 major local faults 9 linked-fault scenarios 8 distributed fault scenarios
Local Faults—M_{max}	RLD (for buried structures) or SRL (all others) RA SRL + S Moment Equation	General weights SRL (0.3) SRL x D (0.3) MD (0.15) AD (0.15) RA (0.1)	RL (0.4) RA (0.6) ± 0.25 units	RL (0.5) RA (0.5) ± 0.5 units	SRL, RA, MD, AD, M_o inferred from stress drop; weights vary depending on available data.	RL (0.206) MD (0.104) RL x MD (0.207) RA (0.207) SRL + S (0.069) Seismic Moment (0.207)

TABLE 4-1
SUMMARY OF SEISMIC SOURCE CHARACTERIZATION MODELS
Page 7 of 9

Issue	AAR Team	ASM Team	DFS Team	RYA Team	SBK Team	SDO Team
	Different weights assigned depending on fault length (< or ≥ 25 km), tectonic model, and coalesced behavior model. M_{max} ± ¼ unit, M_{max} + ¼ = m^u	Modified on a fault basis depending on available data. M_{max} ± ¼ unit, M_{max} + ¼ = m^u			M_{max} ± ¼ unit, M_{max} + ¼ = m^u	M_{max} ± ¼ unit, M_{max} + ¼ = m^u
Local Faults—Recurrence	Slip-Rate Approach (0.6); Recurrence Interval Approach (0.4) - where data are available. Characteristic (0.7), Modified exponential (0.3) b-value 0.80 (0.3), 1.00 (0.4), 1.20 (0.3)	Slip-Rate Approach (0.5) Recurrence Interval Approach (0.5) Characteristic (0.7) Truncated Exponential (0.2) Maximum moment (0.1)	Slip-Rate Approach (1.0) Independent behavior- Characteristic (0.6) Maximum moment(0.3) Exponential (0.1) Distributed behavior- Characteristic (0.6) Maximum moment(0.2) Exponential (0.2)	Slip-Rate Approach (0.7) Recurrence Interval Approach (0.3) Characteristic and truncated exponential—weights vary depending on coalescing model used.	Slip-Rate Approach (0.7 to 1.0) Recurrence Interval Approach (used where data are available, but given lower weight, 0.2 to 0.3) Both characteristic and truncated exponential models used (weight varies depending on fault model)	Moment Rate (0.33) Average Recurrence Interval (0.33) Interseismic Recurrence Interval (0.33) Characteristic (0.7) Truncated exponential (0.3)
OTHER SOURCES						
Buried Regional Dextral Shear Zone	Included w/ P[s] = 1.0 for Tectonic Model A (0.05). Regional strike-slip fault 50 to 100 km in length Slip Rate 0.05 (0.3) 0.1 (0.4) 0.2 (0.3)	Yes; see above. M_{MAX} M_w 7.1 (0.3) 60-km rupture M_w .6.7 (0.7) 25-km rupture Slip Rate 0.1 mm/yr (0.6) 0.025 mm/yr (0.2) 0.24 mm/yr (0.2)	Includes a hypothetical strike-slip fault of regional or local extent, with low probability (0.05) that it is a seismogenic source. Local strike-slip fault (0.5) 30-km length. Regional strike-slip fault (0.5) 200-km length.	Not included as fault source; possible buried strike-slip fault judged incapable of producing earthquakes larger than the maximum background earthquake or any other source included in the source model.	Not included as fault source; possibility is covered by seismic source zone.	Yes; see above. Fault Length 20 km (minimum) 27 km (preferred) 120 km (maximum) Slip Rate 0.001 (minimum) 0.005 (preferred) 0.02 (maximum)

TABLE 4-1
SUMMARY OF SEISMIC SOURCE CHARACTERIZATION MODELS

Issue	AAR Team	ASM Team	DFS Team	RYA Team	SBK Team	SDO Team
Seismogenic Detachment (modeled as independent source)	No (possibility is covered by areal source zone).	Detachment Model (0.15) Probability—seismogenic (0.01) Depth to detachment 6 km (0.25) (BD-6) / 2- 6 km (0.5) BD (0.25) BD=brittle-ductile transition Maximum magnitude 7.1 (0.15) 7.6 (0.7) 8.0 (0.15) Slip Rate 0.05 mm/yr (0.6) 0.013 mm/yr (0.2) 0.12 mm/yr (0.2) Mean Recurrence 25 kyr (0.15) 75 kyr (0.7) 200 kyr (0.15) Characteristic (1.0)	Yes (Paintbrush Canyon /Stagecoach fault in the detachment model (0.2) is modeled as a shallow-dipping, seismogenic source that extends beneath the Crater Flat Basin).	Possibility of a seismic detachment is excluded.	No (shallow and deeper detachments as active seismogenic structures are given no weight). Hypothesized detachments affect only down-dip fault extent of Yucca Mountain faults; depth is dependent on Bare Mountain fault.	A seismogenic detachment (modeled as an independent source) was thoroughly considered but could not be substantiated by the available evidence.
Volcanic Source Zone (basaltic)	No (possibility is covered by areal source zone).	No (maximum magnitudes for volcanic-related earthquakes are less than M_{max} for fault and background seismic zones, and recurrence rate for volcanic eruptive events is estimated to be insignificant compared to seismicity rates).	No (possibility is covered by seismic source zones).	Yes (0.7) Spatial location (basaltic cones in site vicinity). Preferred return periods 2×10^5 and 2×10^6 $M_{max} = 5.5$.	No (possibility is covered by seismic source zones).	Defines two volcanic sources with probabilities of 0.25 and 0.7. Recurrence—2 to 3 volcanic events per Ma Maximum magnitude distribution for volcanic events: 6.0 ± 0.2 (0.1) 5.8 ± 0.4 (0.6) 5.5 ± 0.3 (0.3)

TABLE 4-1
SUMMARY OF SEISMIC SOURCE CHARACTERIZATION MODELS
Page 9 of 9

Issue	AAR Team	ASM Team	DFS Team	RYA Team	SBK Team	SDO Team
Gravity Fault	Considered distinct from Ash Meadows fault, which is included as a regional fault; accounted for in assessment of M_{max} for background source zones >20 km from site.	Not discussed. Ash Meadows fault is included as regional fault source (probability of activity 1.0).	Amargosa/Gravity (Ash Meadows) fault is included as regional fault source (probability of activity 1.0).	Not discussed. Ash Meadows fault included as regional fault.	Included as potential northern extension of the Ash Meadows fault (0.1).	Characterized as a regional fault source, probability of activity (0.9).
Cross-Basin Fault	Included w/ P[s] = 1 in Tectonic Model C (0.35)	Includes local buried strike-slip fault with low probability (see above); preferred length (25-km) (0.7) based on down-on-east segments along the west side of Crater Flat.	A local hidden strike-slip fault is included with a low probability (P_A = 0.05) in the detachment model for local faults.	Not explicitly included in SSC model; see comment above regarding buried strike-slip faults.	Not included.	Based on evidence for distributed dextral faulting, the hingeline-Pahrump-Stewart Valley fault is characterized as a buried strike-slip fault.
Highway 95 or Carrara Fault	Included w/: P[s] = 0.5 for Tectonic Model A P[s] = 0.8 for Tectonic Models B & C.	Carrara fault characterized as active (P_A = 0.85) regional fault source.	Included with low probability (P_A = 0.1) as a hypothetical regional source.	Not included.	Included as independent fault source (P_A = 0.4).	Highway 95 fault assigned a probability of 0.2 (regional fault source).

TABLE 4-2
ACRONYMS FOR FAULT SOURCES

LOCAL FAULT SOURCES	
AW	Abandoned Wash Fault
BC	Black Cone Fault
BM	Bare Mountain Fault
BWR	Bow Ridge Fault
CF	Crater Flat Fault
CCF	Central Crater Flat Fault
CWW	Central Windy Wash Fault
E-SIDE (ES)	East Side Fault (PC+SR+BWR+MWV+GD+WD1+WD2+EB (Team AAR)
EB	East Busted Butte Fault
ELC	East Lathrop Cone Fault
FW	Fatigue Wash Fault
GD	Ghost Dance Fault
H95	Carrara (Highway 95) Fault
IR	Iron Ridge Fault
MWV	Midway Valley Fault
NCF	Northern Crater Flat Fault
NPC	Northern Paintbrush Canyon Fault
NWW	Northern Windy Wash Fault
PBC	Paintbrush Canyon Fault
SC	Solitario Canyon Fault
SCF	Southern Crater Flat Fault
SPC	Southern Paintbrush Canyon Fault
SR	Stagecoach Road Fault
SWW	Southern Windy Wash Fault
WD1	West Dune Wash Fault #1
WD2	West Dune Wash Fault #2
W-SIDE 1	West Side Fault #1 (SC+IR) (Team AAR)
W-SIDE 2	West Side Fault #2 (WW+FW+CF) (Team AAR)
WW	Windy Wash Fault
WSIDE	West Side Fault (Team RYA)

Table 4-3
SUMMARY OF SSFD EXPERT TEAM FAULT DISPLACEMENT HAZARD CHARACTERIZATIONS

Issue	AAR team	ASM team	DFS team	RYA team	SBK team	SDO team
PRINCIPAL FAULTING APPROACH	Displacement approach [0.67]; Earthquake approach [0.33]	Earthquake approach [1.0]	Displacement approach [1.0]	Displacement approach [1.0]	Displacement approach [0.85-0.9] Earthquake approach [0.1-0.15]	Earthquake approach [1.0]
Displacement Approach for Principal Faulting						
Probability That Principal Faulting Can Occur P(C)	Evaluate P(C) based on probability fault is seismogenic	NA	Evaluate P(C) based on probability fault being seismogenic	Evaluate P(C) based on probability fault is seismogenic	Evaluate P(C) based on probability fault being seismogenic	Evaluate P(C) based on probability fault being seismogenic
Frequency of Displacement Events	Slip rate, (*SR*) [1.0]	NA	$SR/\overline{D}_E$ [0.5]; Recurrence intervals (*RI*) [0.5]	Slip rate [0.2]; Recurrence intervals [0.8]	Slip rate [0.8]; Recurrence intervals [0.2]	NA
Slip Rate (*SR*)	Quaternary slip rates used in SSC model	NA	Paleoseismic data [0.7]; uniform post-Tiva Canyon [0.1]; uniform post-Rainier Mesa [0.1]; decreasing slip rate model [0.1]	Quaternary slip rates used in SSC model	Quaternary paleoseismic data point specific or interpolated	NA
Average Displacement Per Event, $\overline{D}_E$	$\overline{D}_E = 0.83\ MD^{max}$ MD^{max} from fault length [0.3]; D_{cum} [0.3]; paleoseismicity data [0.4]	NA	Paleoseismologic data [0.5]; $SR \times RI$ [0.5]	Paleoseismic data [1.0]	Paleoseismic data [0.8]; From *AD-RL* [0.1]; From *MD-RL* [0.1];	NA
Conditional Probability of Exceedance, *P(D>d)*	Distribution for D/MD^{max} [1.0]	NA	Distribution for *D/AD* [1.0]	Distribution for *D/AD* [0.5]; Distribution for D/MD^{max} [0.5]	D/AD_{paleo} $D/AD_{F(RL)}$ $D/MD_{F(RL)}$ correlated with $\overline{D}_E$	NA

Issue	AAR team	ASM team	DFS team	RYA team	SBK team	SDO team
Earthquake Approach for Principal Faulting						
Probability That Principal Faulting Can Occur, P(C)	P(C) = P(S) from SSC model	P(C) = P(S) from SSC model	NA	NA	P(C) = P(S) from SSC model	P(C) = P(S) from SSC model
Frequency of Earthquakes on Principal Faulting Source	Earthquake frequency from SSC model	Earthquake frequency from SSC model	NA	NA	Earthquake frequency from SSC model	Earthquake frequency from SSC model
Probability of Surface Rupture	Randomization of rupture depth with rupture width based on *RL*/aspect ratio; *RL* specified by magnitude-*RL* [0.5]; magnitude-rupture area [0.5]	Empirical models 32 GB earthquakes [0.5]; 105 EC earthquakes [0.5]	NA	NA	Empirical model 32 GB earthquakes [1.0]	Empirical models 32 GB earthquakes [0.5]; 47 NB&R earthquakes [0.5]

Table 4-3
SUMMARY OF SSFD EXPERT TEAM FAULT DISPLACEMENT HAZARD CHARACTERIZATIONS

Issue	AAR team	ASM team	DFS team	RYA team	SBK team	SDO team
Conditional Probability of Exceedance, *P(D>d)*	Maximum displacement per event, *MD*, from *SRL* [0.33]; M_w [0.33]; and *RLD* [0.34]; *D/MD* from Wheeler data [1.0]	*MD* from M_w [1.0] *D/MD* from Wheeler data [1.0]	NA	NA	*MD* from M_w [1.0] *D/MD* from Wheeler data [0.5]; fractal model [0.5]	*AD* and distribution for *D/AD* [0.5]; *AD* from* M_w [0.2]; *RL* [0.4]; and Paleoseismic data [0.4] *MD* and distribution for *D/MD* [0.5]; *MD* from* M_w [0.2]; *RL* [0.4]; and Paleoseismic data [0.4]; *D/MD* from Wheeler data [0.8], and fractal model [0.2] * for $m<m^U$-½ use only M_w Ramelli curve also was used for Solitario Canyon fault

Issue	AAR team	ASM team	DFS team	RYA team	SBK team	SDO team
DISTRIBUTED FAULTING APPROACH	Displacement approach [0.67]; Earthquake approach [0.33]	Earthquake approach [1.0]	Displacement approach [1.0]	Displacement approach [1.0]	Displacement approach [0.8]; Earthquake approach [0.2]	*On Principal Faults–* Earthquake approach [1.0]; *Other Sites–* Displacement approach [0.3, Earthquake approach [0.7]
Earthquake Approach for Distributed Faulting						
Probability of Occurrence P(C)	If capable of principal faulting P(C) = P(S) Otherwise, P(C) based on slip-tendency	Function of the category and orientation of feature, cos(strike azimuth)	NA	NA	P(C)=1.0	Slip tendency [1.0]
Frequency of Earthquakes on Seismic Sources	Earthquake frequency from SSC model	Earthquake frequency from SSC model	NA	NA	Earthquake frequency from SSC model	Earthquake frequency from SSC model
Probability of Slip Per Event, P_i(Slip|Event on j)	Logistic regression of historical faulting data [1.0]	Probability a function of r and hanging wall-footwall location; preferred model [0.6]; upper-bound model [0.4]	NA	NA	$P(\theta)\times F(event)$ $P(\theta)$ based on slip tendency [0.5]; Relative orientation [0.5] $F(event)$ based on logistic regression of historical surface faulting data [0.5], peak velocity [0.5]	$P(\theta)\times F(event)$ $P(\theta)$ based on relative orientation [1.0] $F(event)$ based on logistic regression of historical surface faulting data [1.0]

Table 4-3
SUMMARY OF SSFD EXPERT TEAM FAULT DISPLACEMENT HAZARD CHARACTERIZATIONS
Page 5 of 6

Issue	AAR team	ASM team	DFS team	RYA team	SBK team	SDO team
Conditional Probability of Exceedance, *P(D>d)*	*For site of principal faulting* use principal faulting–distribution times *RF* [1.0] *For other sites–* Distribution of D/MD^{max}; MD^{max} from *RL* [0.5], D_{cum} [0.5]	*RF* times principal faulting distribution; *RF* from Displacement potential [0.7], Relative cumulative displacement [0.3]	NA	NA	D/D_{cum} [1.0]	Distribution for *D/MD* on principal rupture as a function of distance from rupture [0.8], Distribution for *D/MD* on principal rupture times function of relative D_{cum} [0.2]
Displacement Approach for Distributed Faulting						
P(C)	Evaluate P(C) based on orientation.	NA	Evaluate P(C) based on orientation, location, and P(S)	Evaluate P(C) based on orientation, location, and P(S)	P(C)=1.0	Based on slip tendency [1.0]
Frequency of Dstributed Faulting Events	Slip rate [1.0]	NA	$SR/\overline{D}_E$ [0.5], and Recurrence intervals (*RI*) [0.5]	Slip rate [1.0]	Slip rate [1.0]	Slip rate [1.0]
Slip Rate	Uniform post 11.6 Ma [0.1], Uniform post 3.7 Ma [0.3], and 3.26×10^{-5} D_{cum} [0.6]	NA	Uniform post-Tiva Canyon [0.33], Uniform post-Rainier Mesa [0.33], and Decreasing slip rate model [0.34]	D_{cum}/12.7 [0.1], 0.02 D_{cum}/1.6 [0.6], and 0.2 D_{cum}/3.7 [0.3]	Geologic history [0.75] with D_{cum}/12.5 [0.1], 0.2 D_{cum}/11.6 [0.3], and 0.8 D_{cum} x 0.21/0.9 [0.6]; Ratio of cumulative slip to that of block-bounding faults and their slip rates [0.25]	0.02 D_{cum}/1.6Ma [0.3]; 0.006 D_{cum}/1.6Ma [0.4]; 0.002 D_{cum}/1.6Ma [0.3]
Average Displacement Per Event, $\overline{D}_E$	$0.83MD^{max}$ from Length [0.5], D_{cum} [0.5]	NA	Direct estimate [0.5] SR*RI [0.5]	Fault length [0.5] D_{cum} [0.5]	D_{cum} [1.0]	Based on D_{cum} and AAR scaling relationship [0.5]; SBK distribution [0.5]

Table 4-3
SUMMARY OF SSFD EXPERT TEAM FAULT DISPLACEMENT HAZARD CHARACTERIZATIONS

Issue	AAR team	ASM team	DFS team	RYA team	SBK team	SDO team
Conditional Probability of Exceedance, $P(D>d)$	Distribution for D/MD^{max} [1.0]		Distribution for D/AD [1.0]	Distribution for D/AD [0.5] Distribution for D/MD^{max} [0.5] with $MD^{max} = AD/0.83$	Distribution for D/D_{cum} [1.0]	For AAR scaling distribution for D/MD^{max}, for SBK scaling distribution for D/D_{cum}

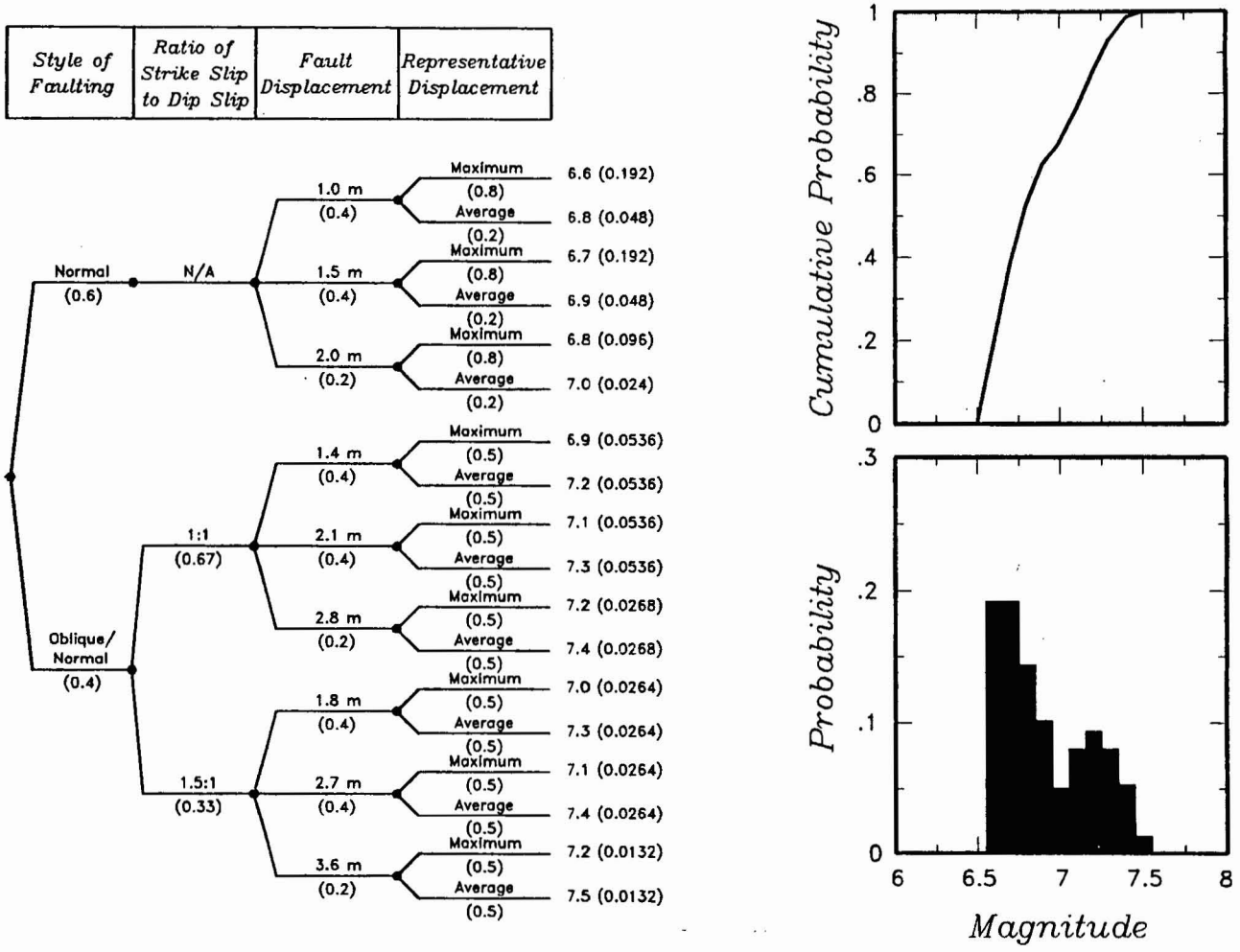

Figure 4-1 Example logic tree and resulting discrete probability distributions for assessing the magnitudes of paleoearthquakes

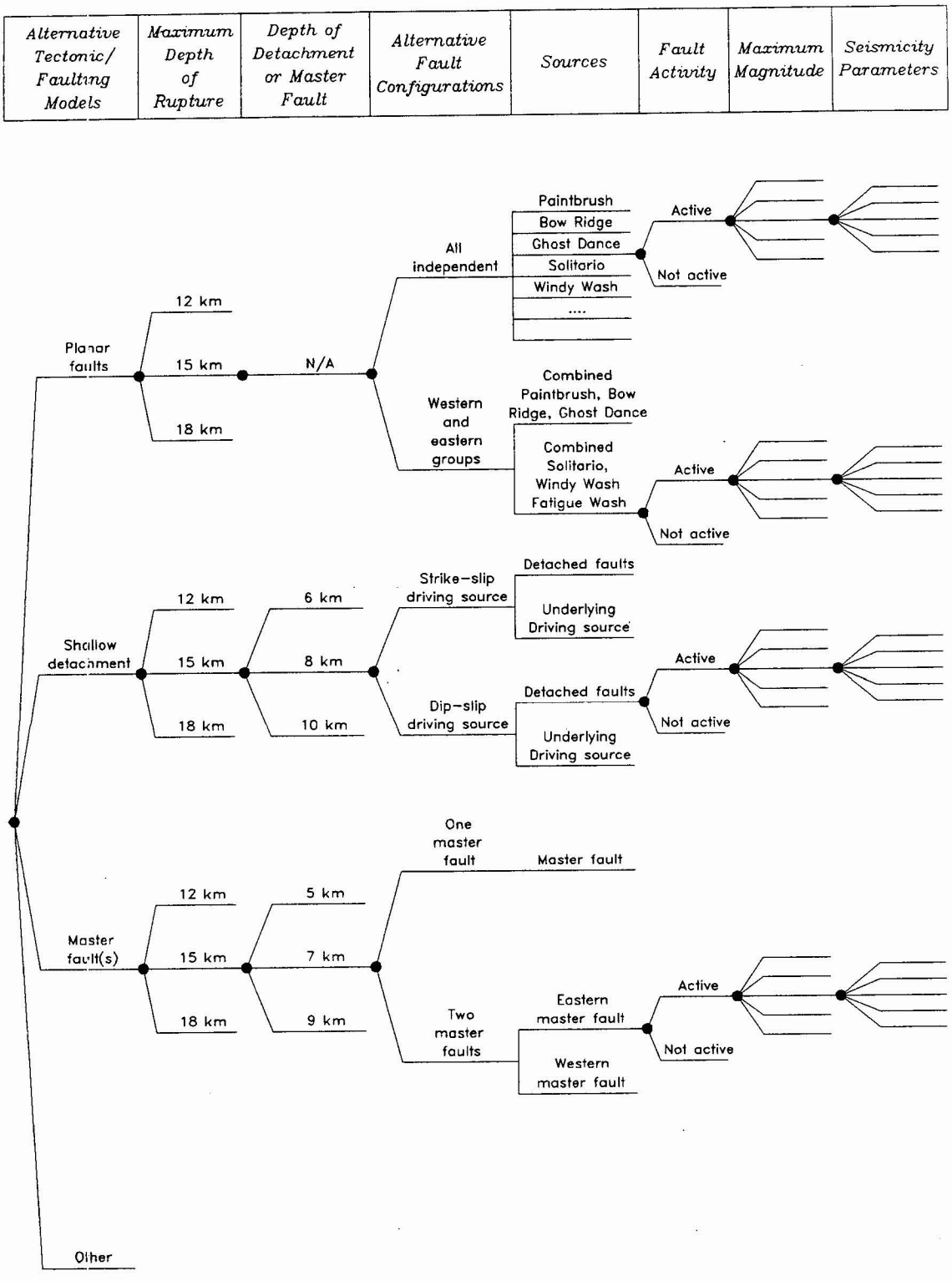

Figure 4-2. Example logic tree for expressing the uncertainty in characterizing local fault sources

TABLE 4-2 (Continued)

REGIONAL FAULT SOURCES	
AH	Ash Hill Fault
AM	Ash Meadows Fault
AR	Amargosa River Fault
BH	Buried Hills Fault
BLR	Belted Range Fault
BM	Bare Mountain Fault
CB	Carpetbag Fault
CS	Cane Spring Fault
DV	Death Valley Fault
EDV	Eastern Death Valley Fault
EM	Emigrant Fault
EN	East Nopah Fault
EPR	East Pintwater Range Fault
ER	Eleana Range Fault
ESR	East Spector Range Fault
EVN	Emigrant Valley North Fault
EVS	Emigrant Valley South Fault
FC	Furnace Creek Fault
FLV	Fish Lake Valley Fault
GM	Grapevine Mountains Fault
GV	Grapevine Fault
H95	Cararra (Highway 95) Fault
HM	Hunter Mountains Fault
JFG	Jackass Flats Gravity Fault
KR	Kawich Range Fault
KW	Keane Wonder Fault
MDV	Middle Death Valley Fault
MM	Mine Mountain Fault
OAK	Oak Springs Fault
OSV	Oasis Valley Fault
PAN	Panamint Valley Fault
PC	Peace Camp Fault
PM1	Pahute Mesa Fault
PRP	Pahrump Fault
RV	Rock Valley Fault
RWBW	Rocket Wash-Beatty Wash Fault
SF	Sarcobatus Flat Fault
SPR	Spotted Range Fault
SPRP	South Pahrump Fault
SSC	South Silent Canyon Fault

TABLE 4-2 (Concluded)

REGIONAL FAULT SOURCES (Cont'd.)	
TOL	Tolicha Pass Fault
TP	Towne Pass Fault
WAH	Wahmonie Fault
WDV	Western Death Valley Fault
WPR	West Pintwater Range Fault
WSM	West Spring Mountains Fault
WSR	West Spector Range Fault
YB	Yucca Butte Fault
YC	Yucca Fault
YCL	Yucca Lake Fault

INFERRED STRIKE-SLIP FAULT SOURCES	
TI-BSS	Team ASM Buried Strike-Slip Fault
T2-HSS	Team DFS Hidden Strike-Slip Fault
T4-CB	Team AAR Cross Basin Fault
T4-PA2	Team AAR North-Bounding Strike-Slip Fault
T4-SS	Team AAR Regional Strike-Slip Fault
T6-SS	Team SDO Strike-Slip Fault

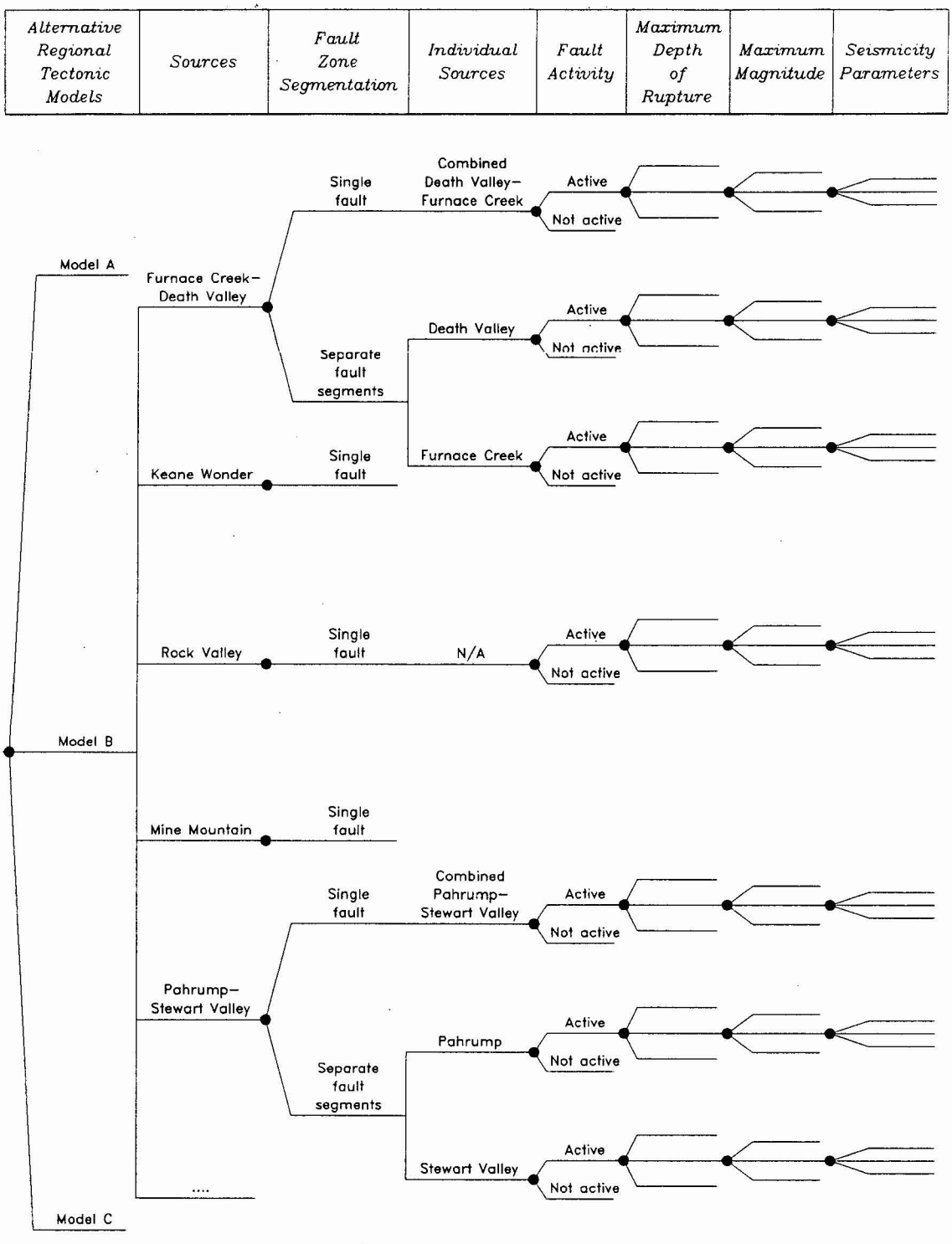

Figure 4-3. Example logic tree for expressing the uncertainty in characterizing regional fault sources

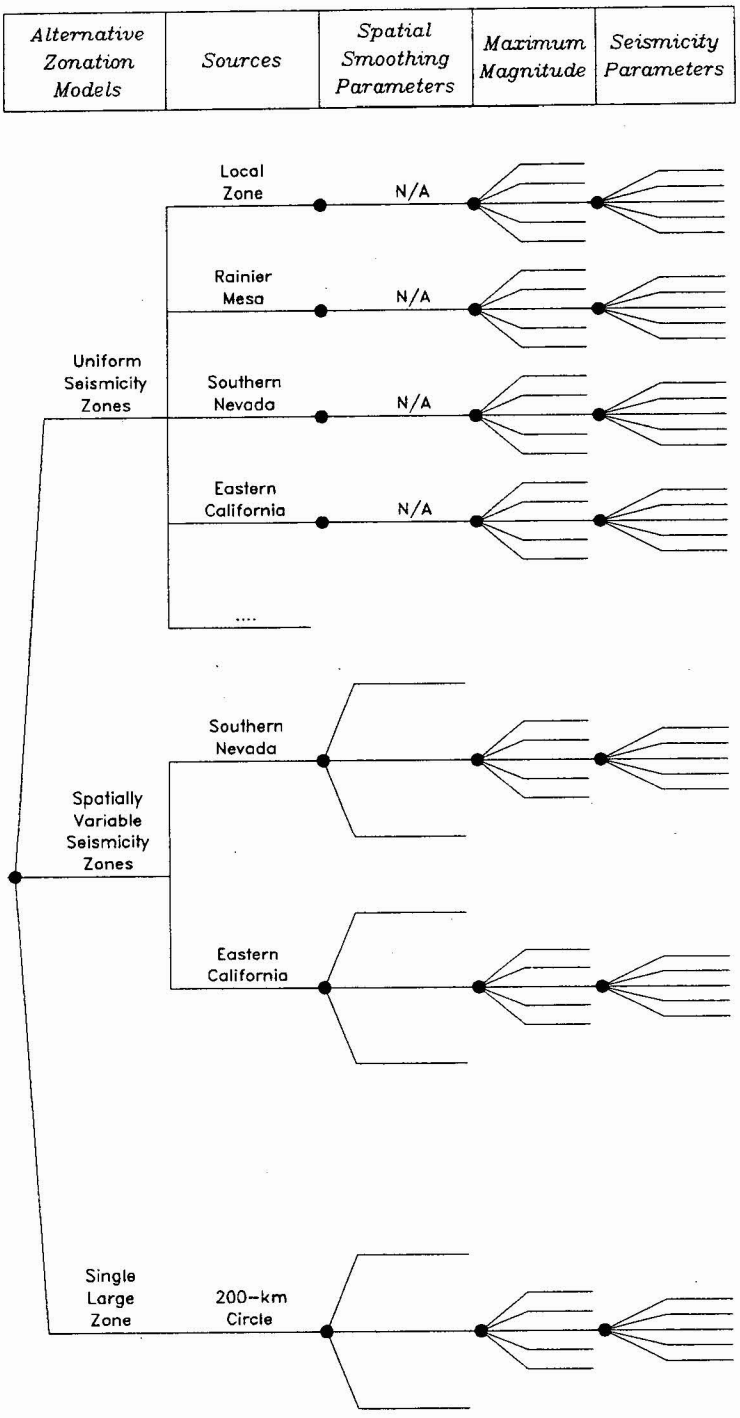

Figure 4-4. Example logic tree for expressing the uncertainty in characterizing regional areal source zones

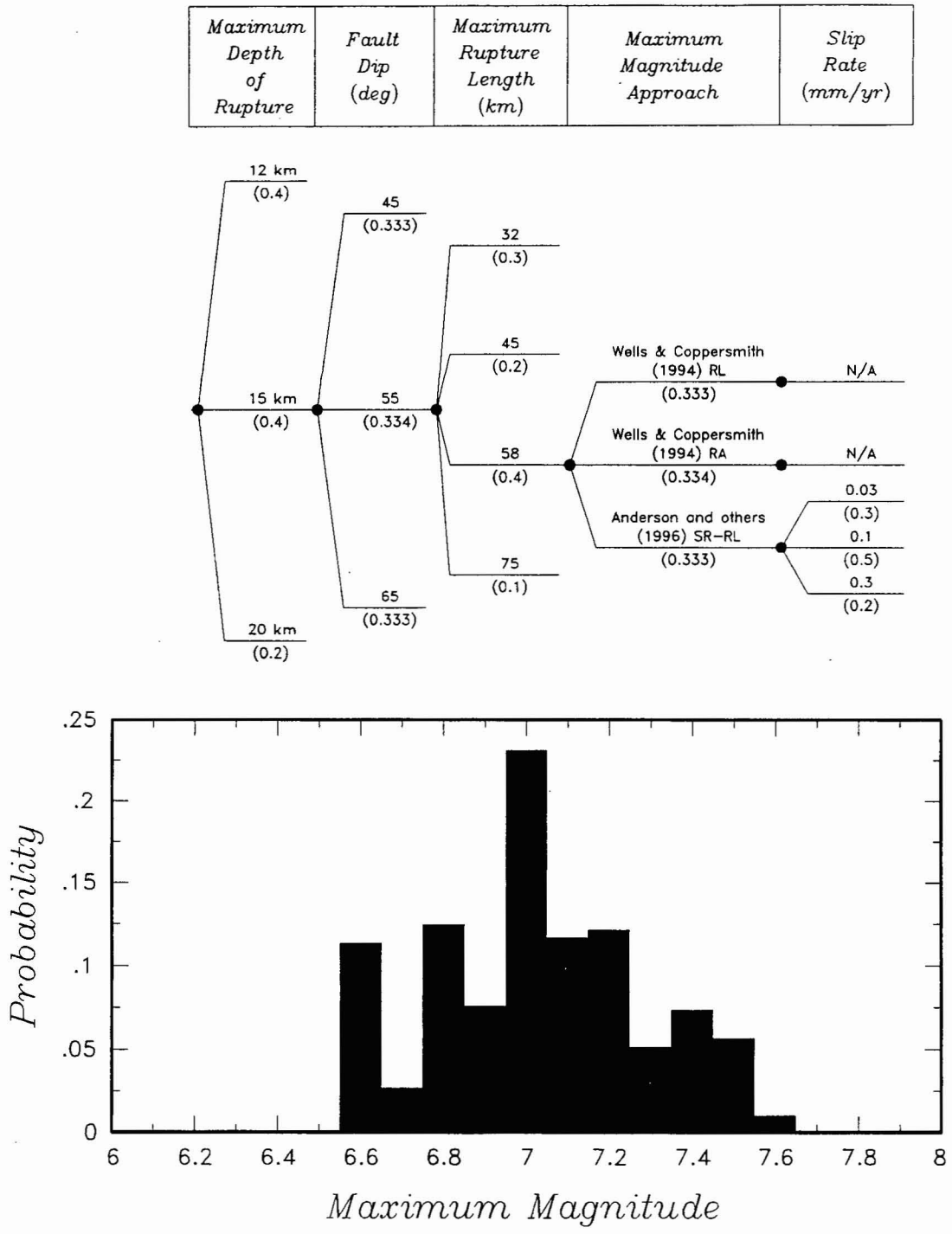

Figure 4-5. Example assessment of maximum magnitude for a fault source. Top, logic tree for uncertainty assessment. Bottom, resulting discrete distribution for maximum magnitude.

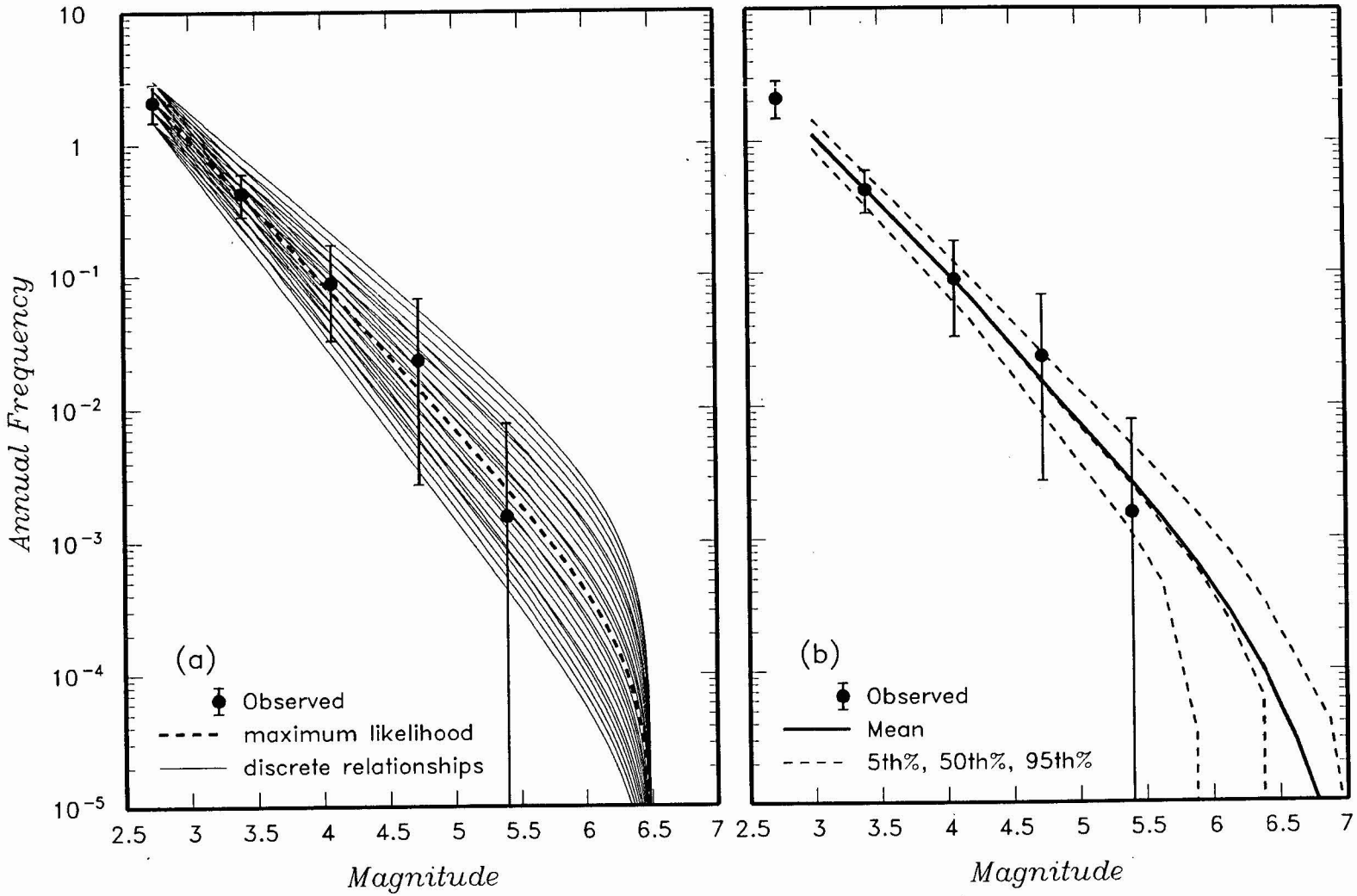

Figure 4-6 Example assessment of the recurrence relationships for an areal source zone. Left, 25 alternative recurrence relationships defined from maximum likelihood fit to observed seismicity. Right, resulting mean and percentile recurrence relationships for source zone.

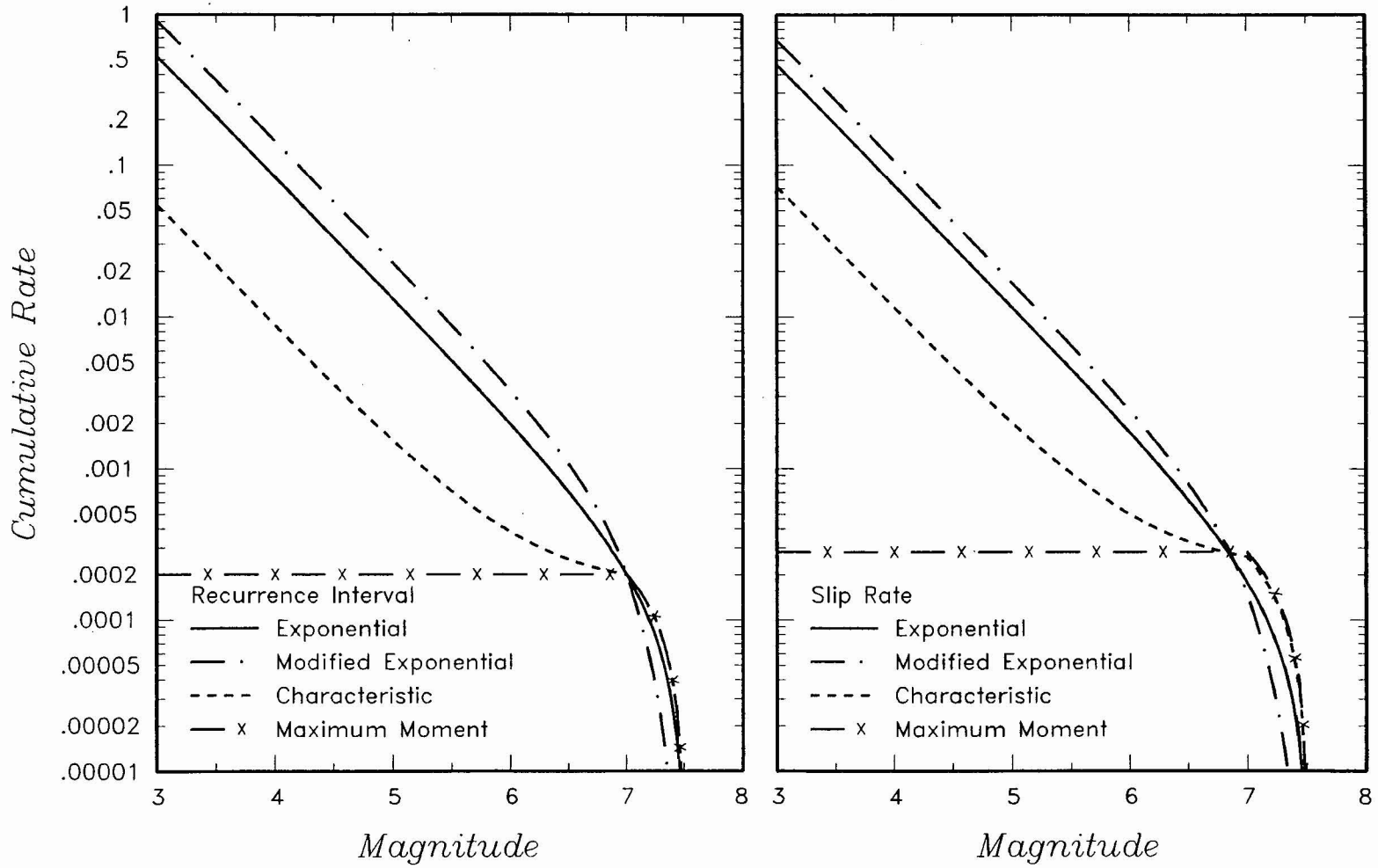

Figure 4-7. Alternative recurrence models constrained by either the recurrence interval for large events (left) or by fault slip rate converted to moment rate (right)

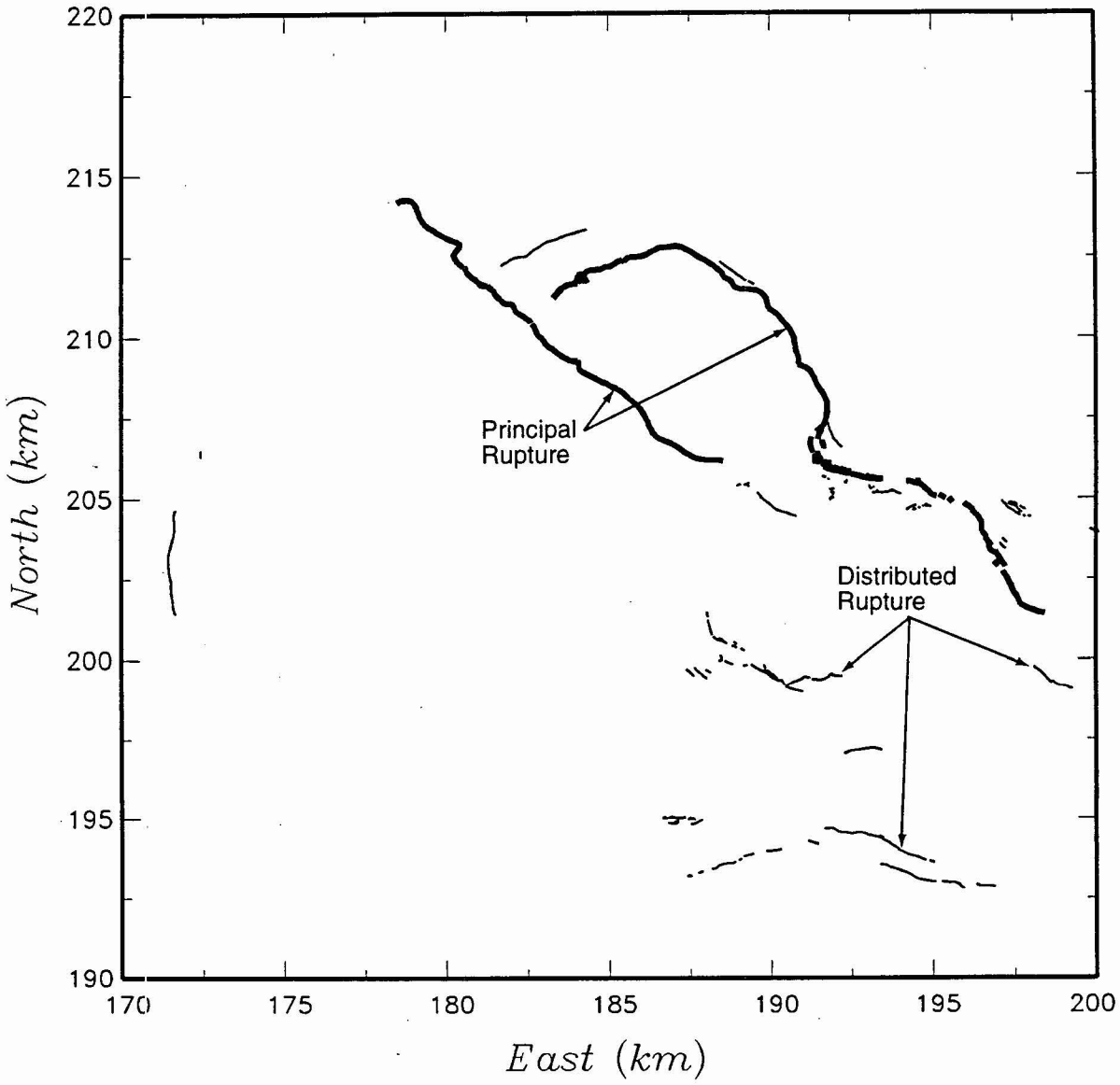

Figure 4-8 Examples of principal and distributed rupture in an earthquake

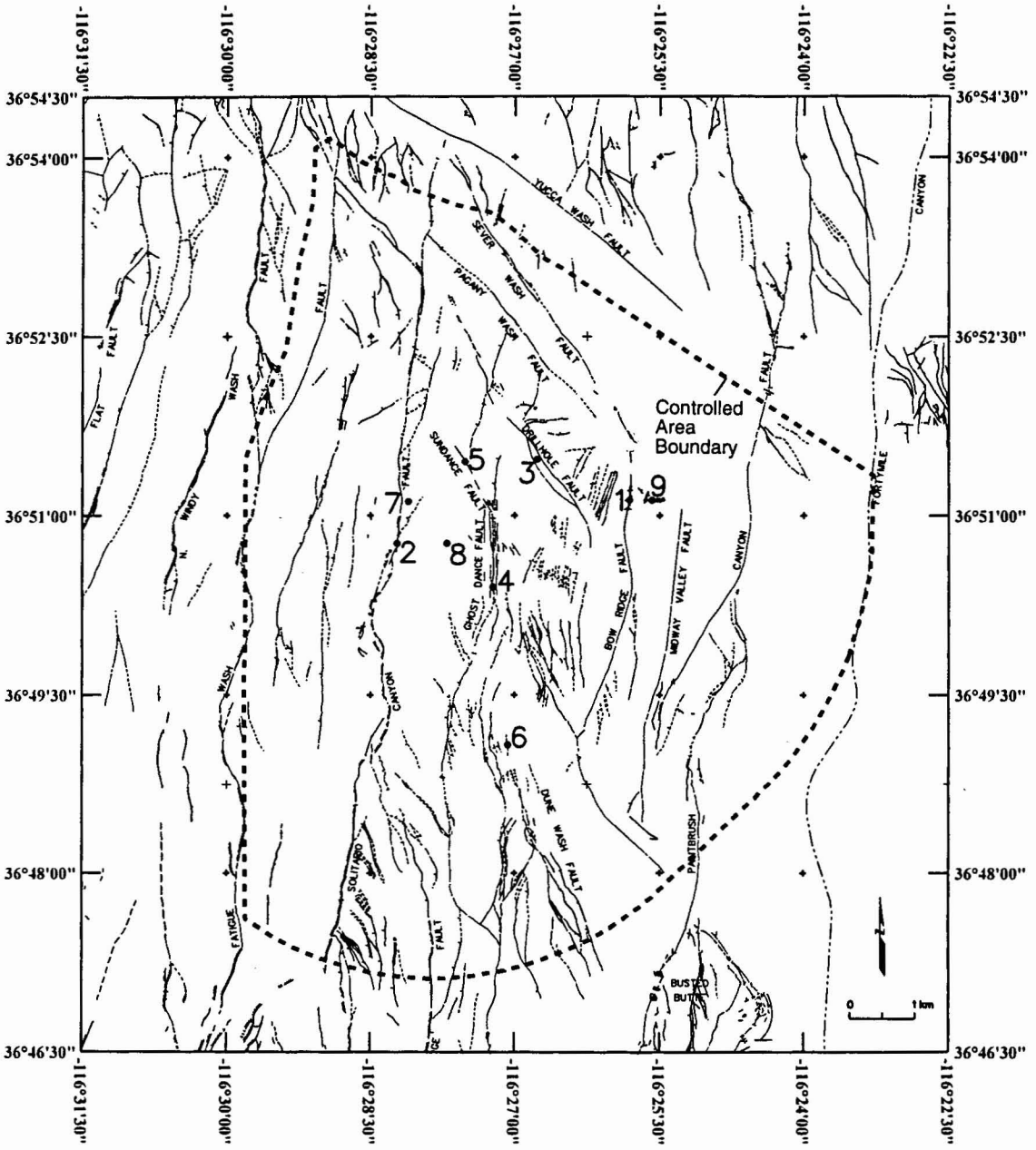

Figure 4-9 Location of nine points for demonstration of fault displacement hazard assessment

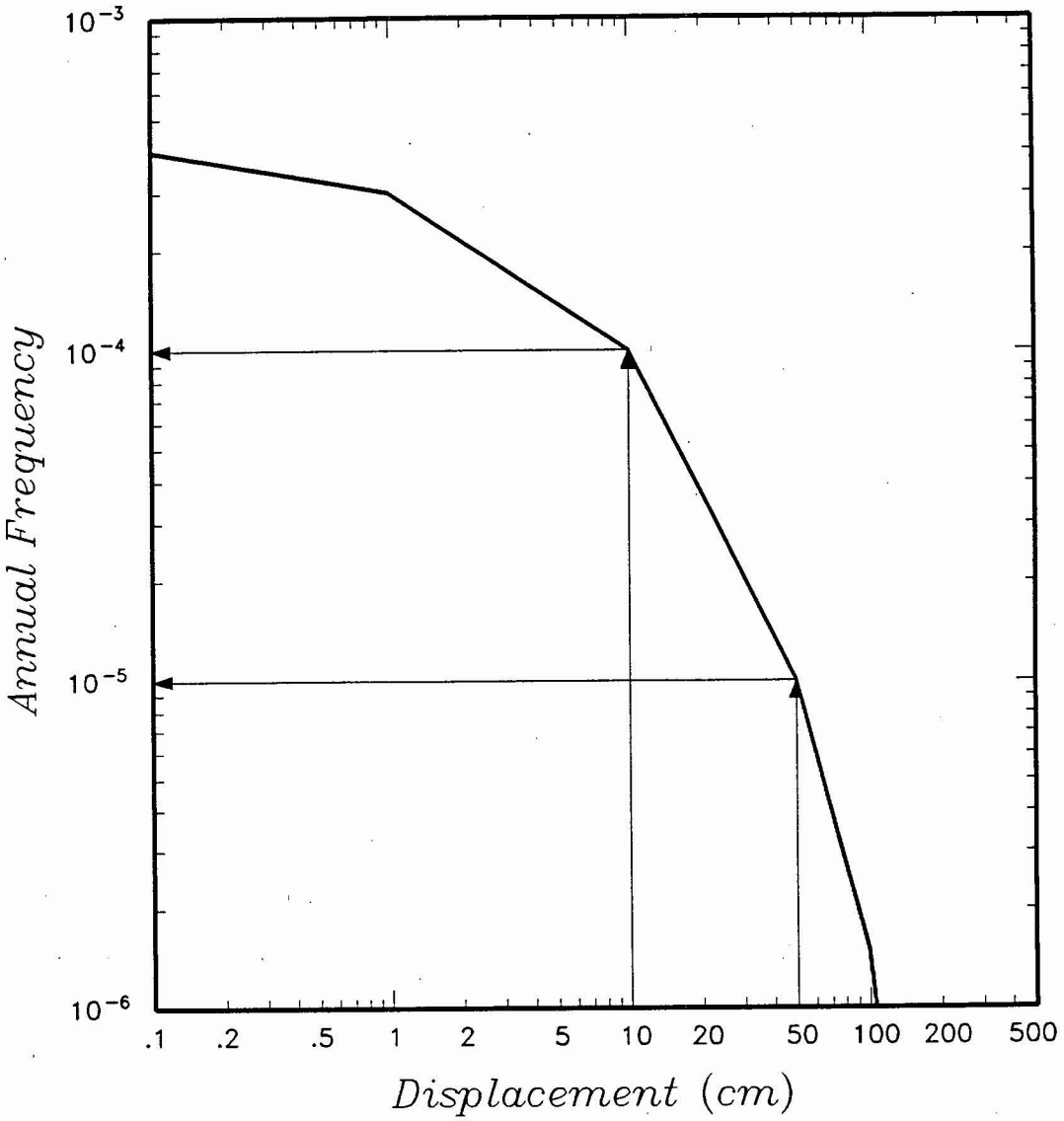

Figure 4-10 Example fault displacement hazard curve

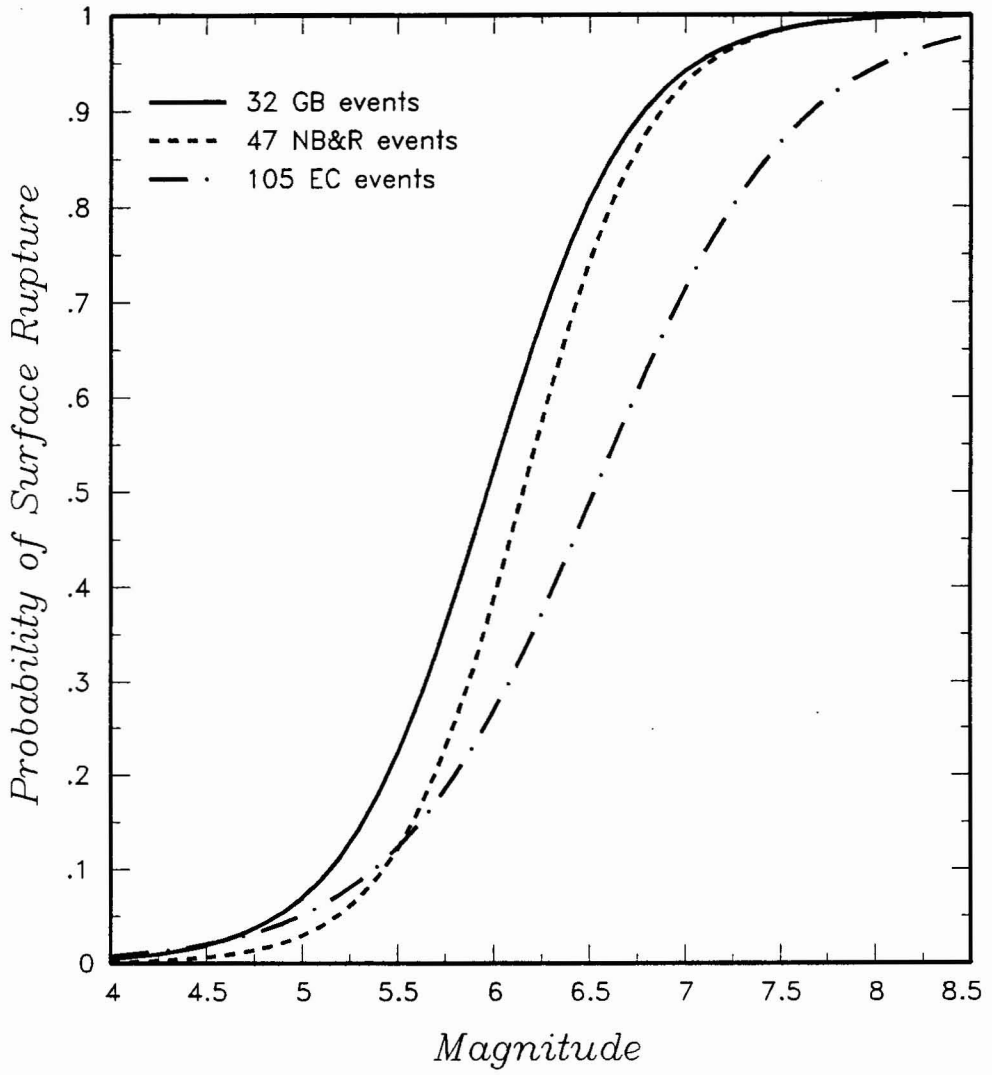

Figure 4-11 Probability of surface rupture as a function of earthquake magnitude computed from various data sets given in S.K. Pezzopane and T.E. Dawson (USGS, written communication, 1996)

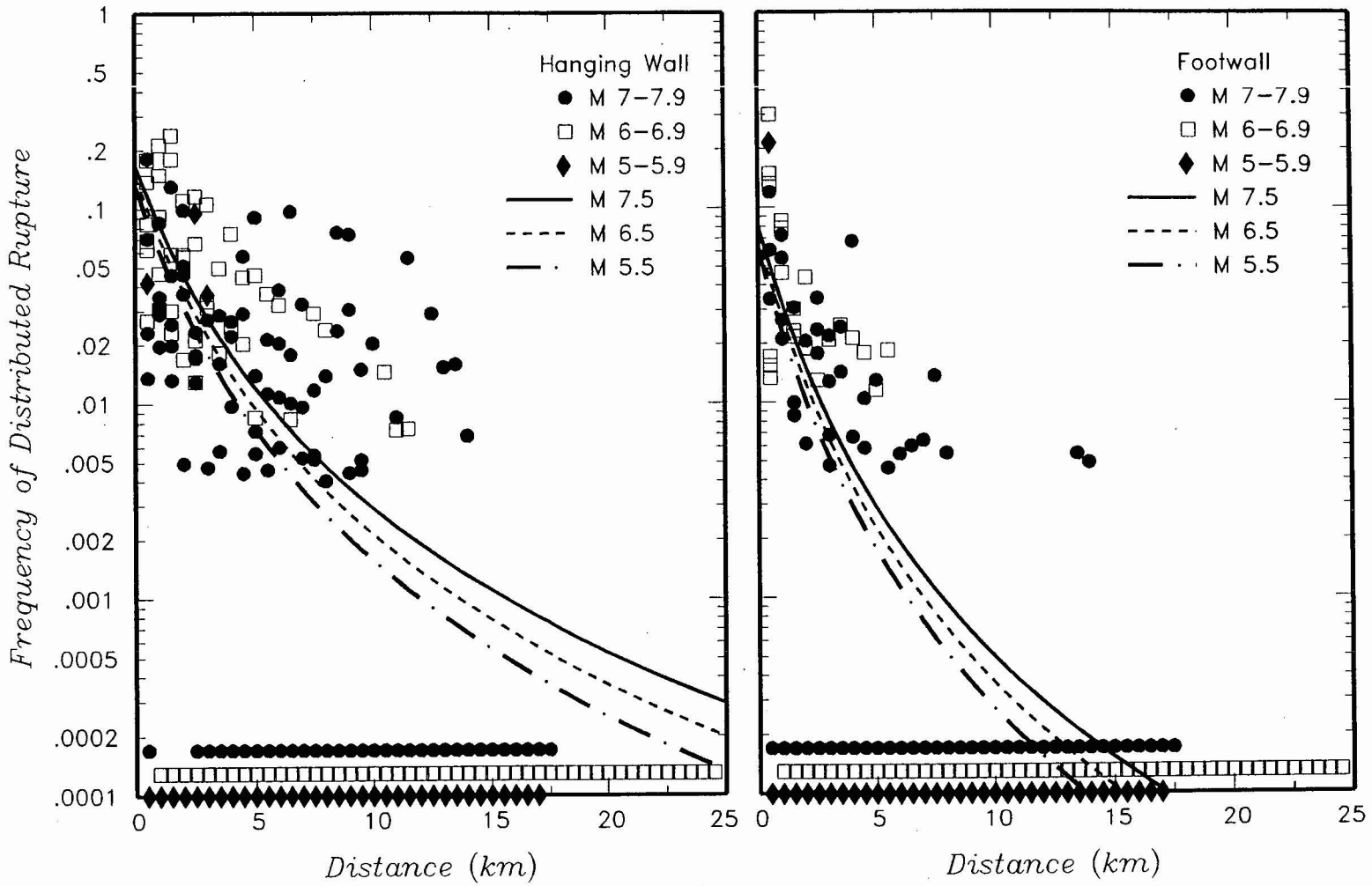

Figure 4-12. Probability of induced distributed slip as a function of distance from the rupture and hanging wall/footwall location computed from the data presented in S.K. Pezzopane and T.E. Dawson (USGS, written communication, 1996). Curves show logistic regression fits to the data.

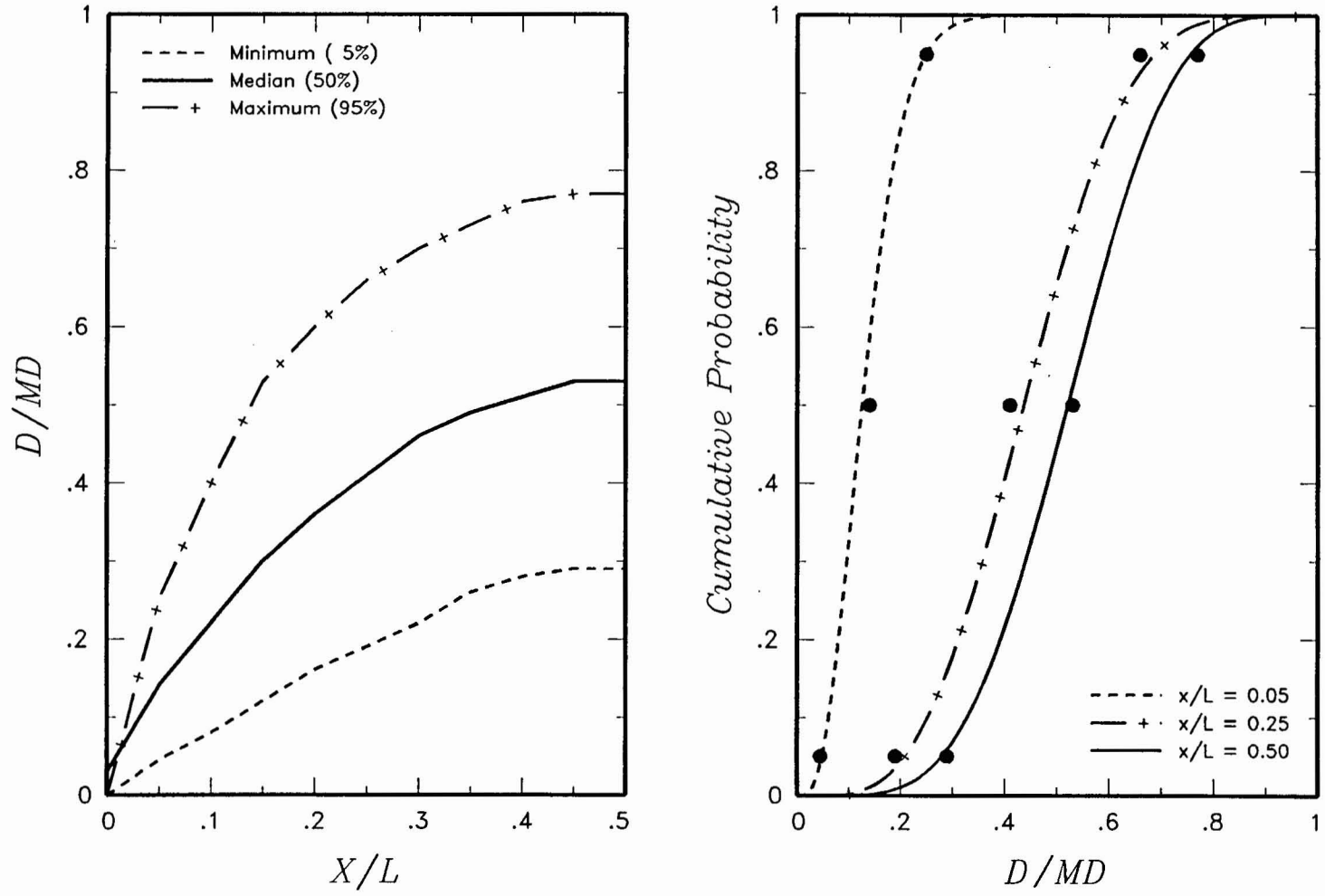

Figure 4-13 Probability distributions for D/MD as a function of location along a principal rupture. Left, smooth curves for minimum, median, and maximum values of D/MD developed by the ASM team from analysis of historical ruptures. Right, Beta distributions fit to the D/MD values at specific values of x/L.

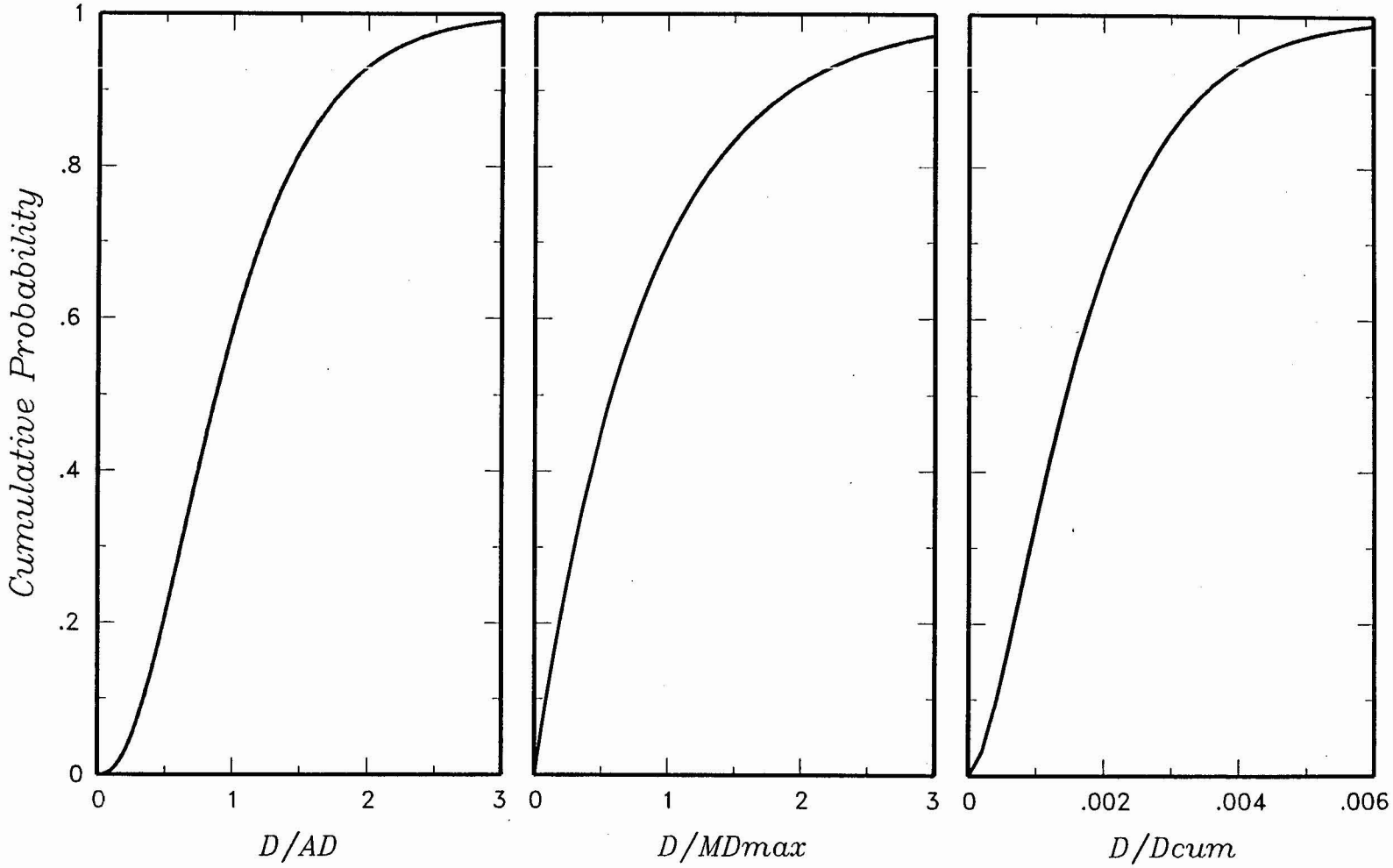

Figure 4-14 Example distributions for computing the conditional probability of exceeding a specific displacement, *d*

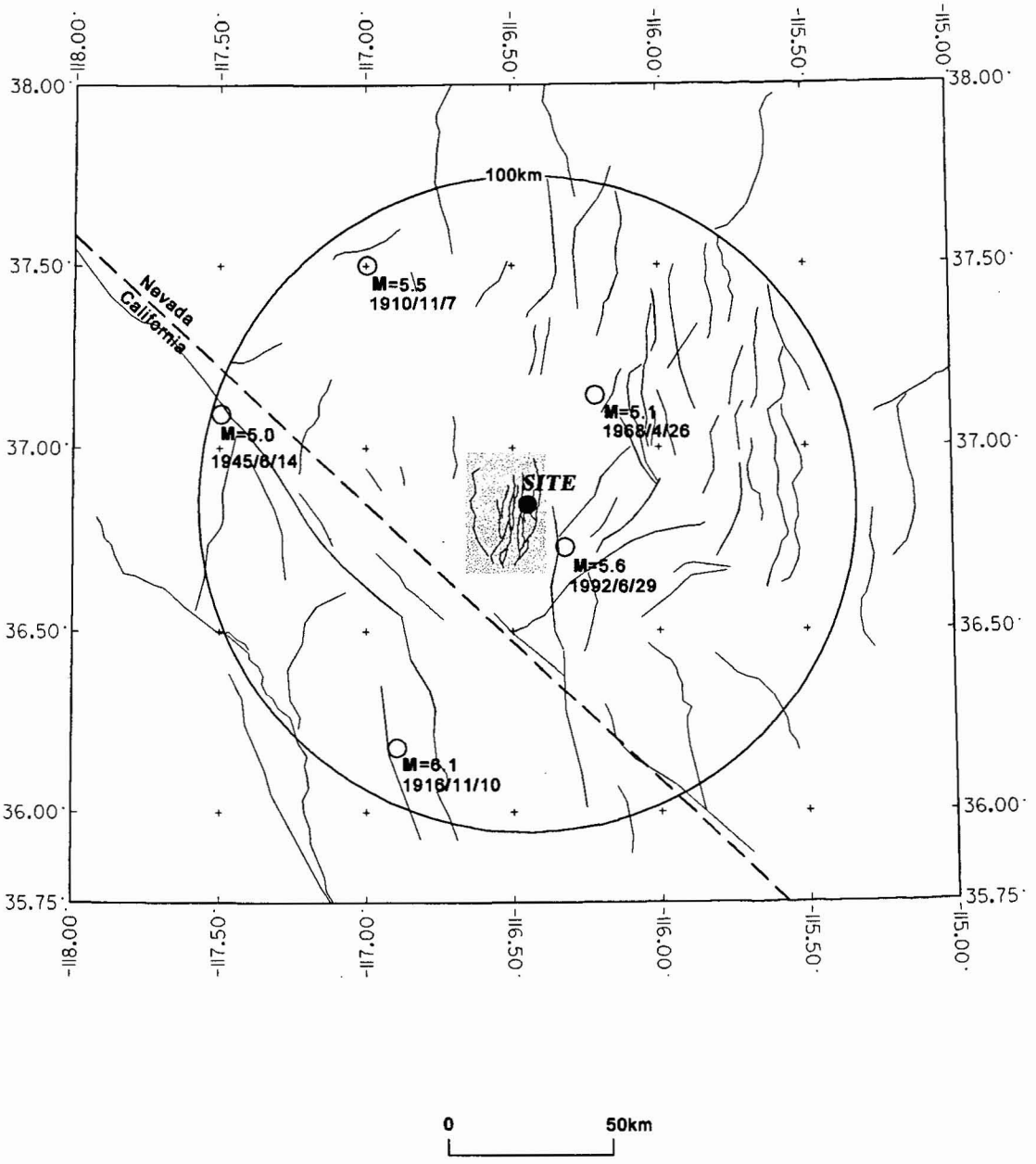

Figure 4-15 Region used for comparison of earthquake recurrence relationships developed from SSFD team models. Also shown are recorded earthquakes of magnitude M_W5 and greater.

Existing Tectonic Framework	*Significant NW–SE Dextral Shear Structure(s)?*	*Dextral–Shear Structure*	*Local Detachment Beneath Crater Flat Domain?*	*Depth of Detachment*	*SOURCE INVENTORY See Table AAR–2, Figure 4-16b*

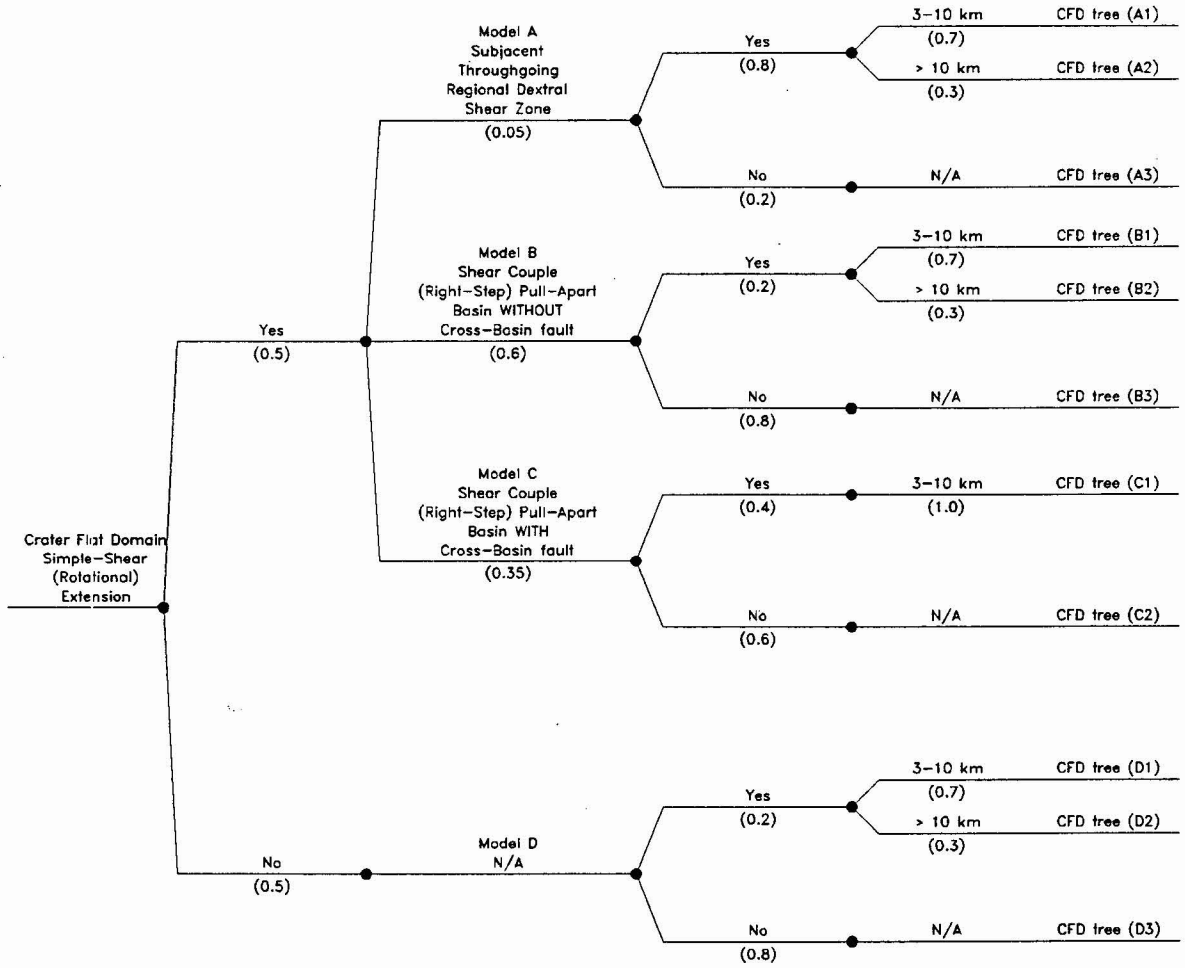

Figure 4-16a Logic tree for local fault source models developed by the AAR team

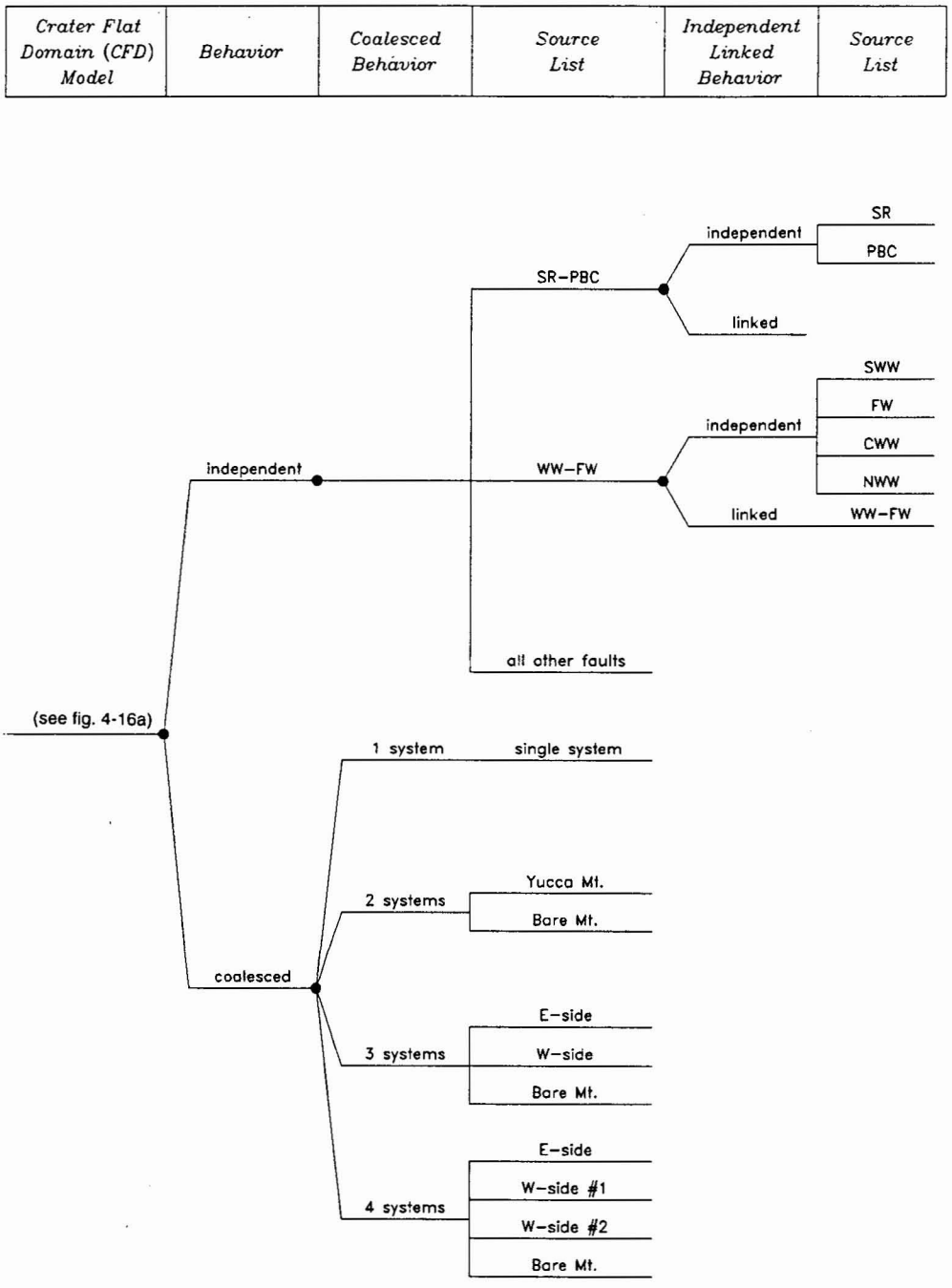

Figure 4-16b Logic tree for local fault source behavior developed by the AAR team

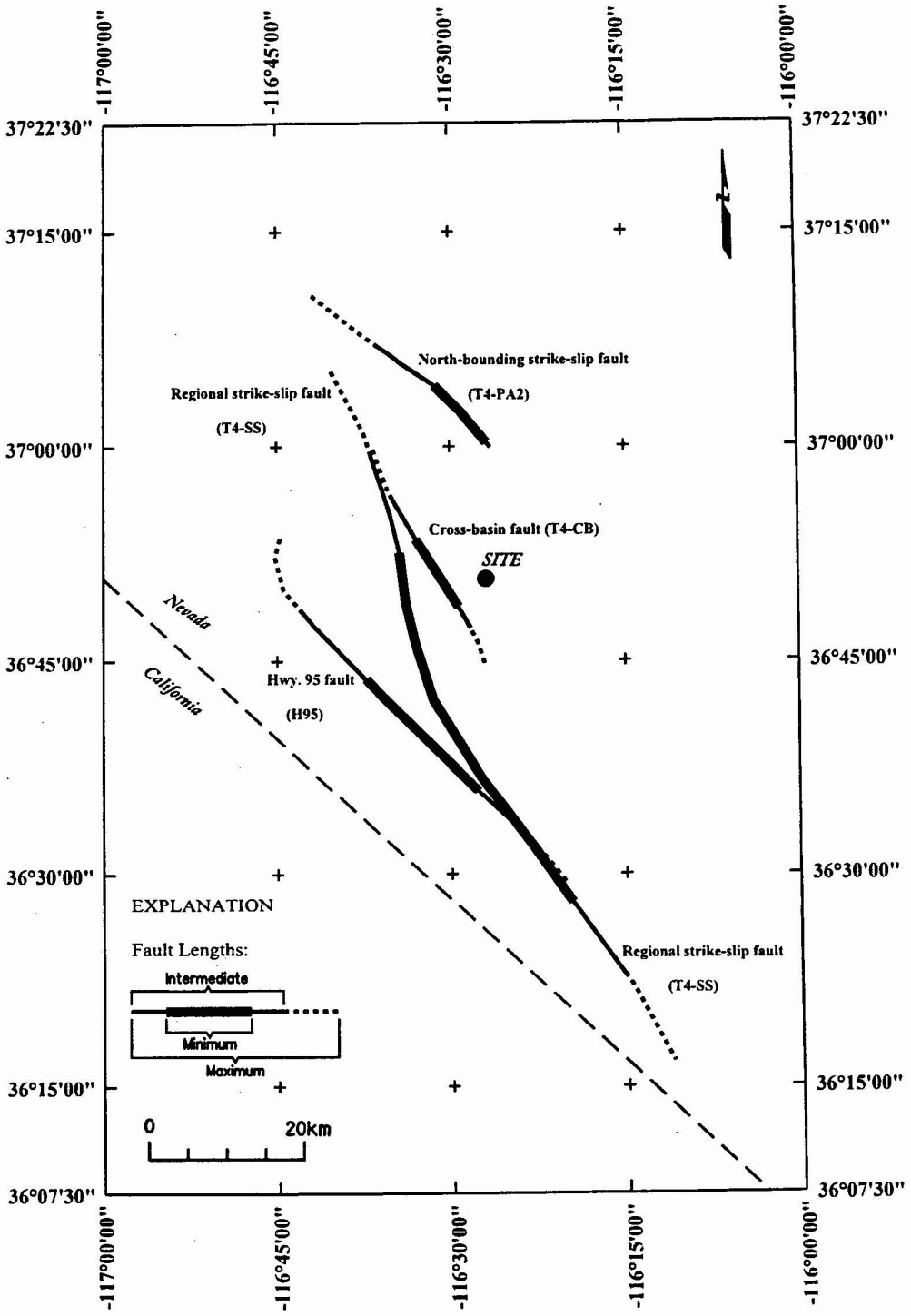

Figure 4-17 Location of AAR team's inferred local dextral shear sources

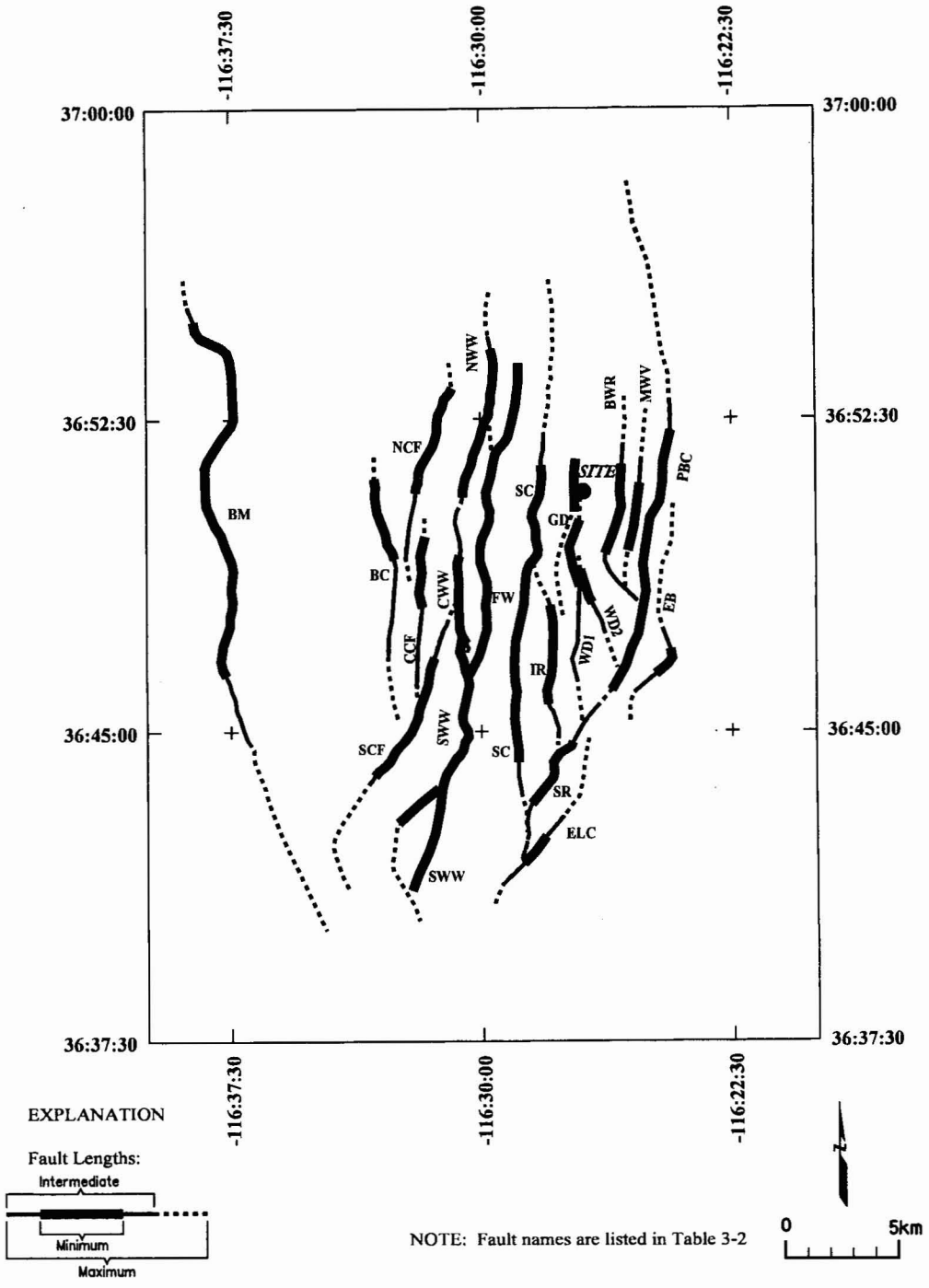

Figure 4-18. Location of local faults considered by the AAR team to be acting as independent sources

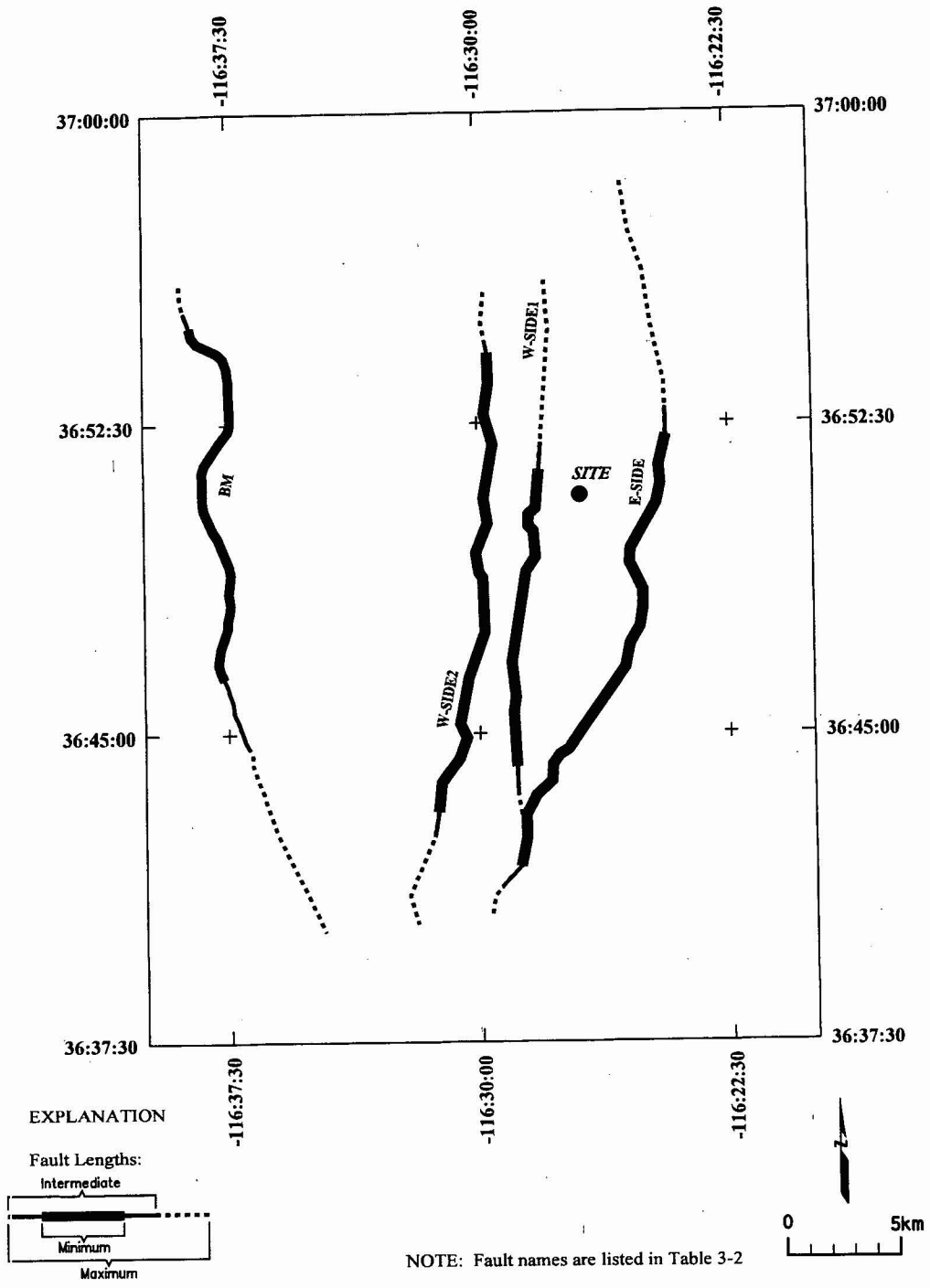

Figure 4-19. Location of coalesced faults considered by the AAR team

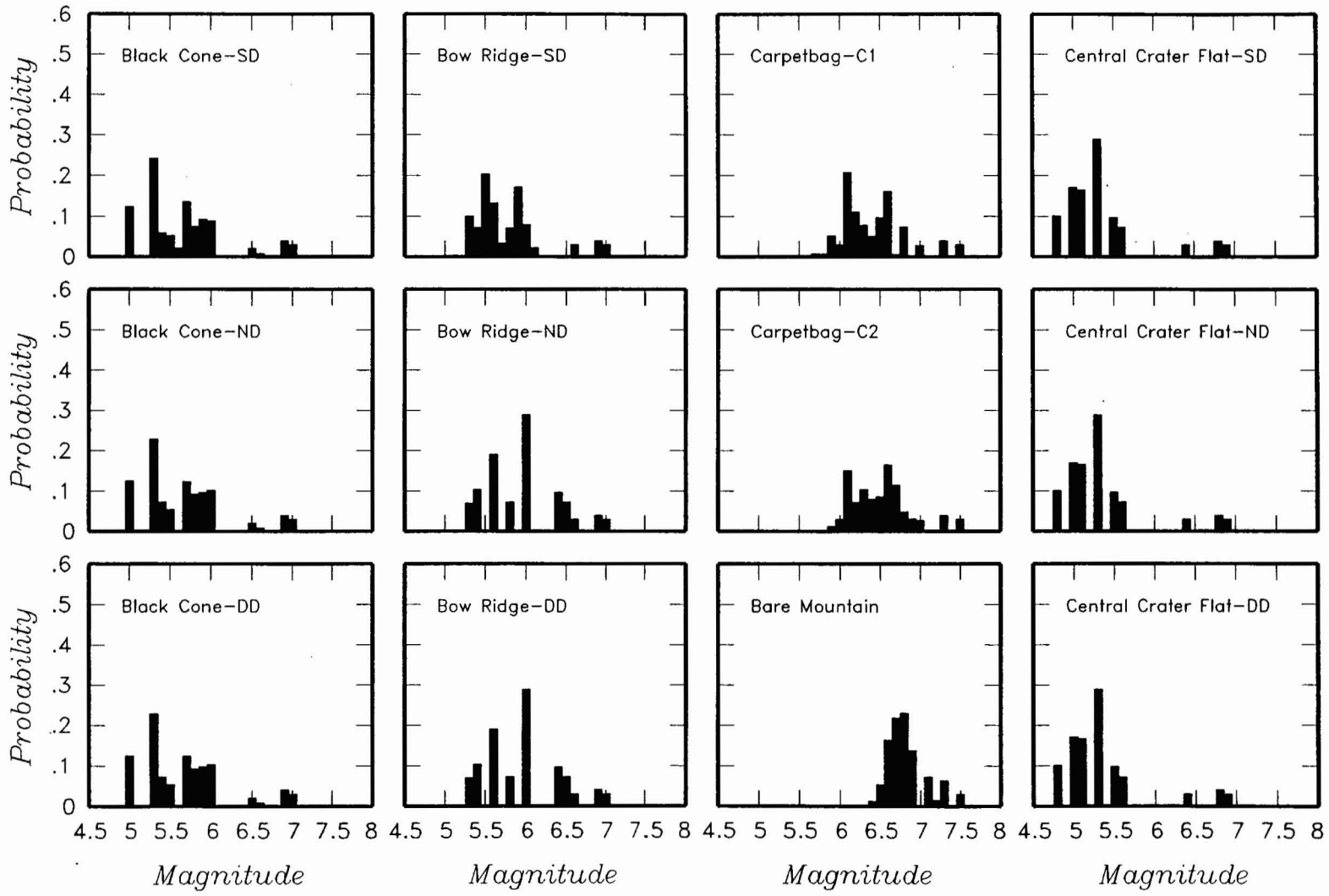

Figure 4-20a. Maximum magnitude distributions for AAR team's local fault sources. A, B, and C and numbers refer to variations of tectonic models A, B, and C; DD–deep detachment, ND–no detachment, SD-shallow detachment, SINGLE–single rupture (BM and YM faults), Single west-side rupture of west-side faults (WS1+WS2), Single Yucca Mountain–coalesced single YM system.

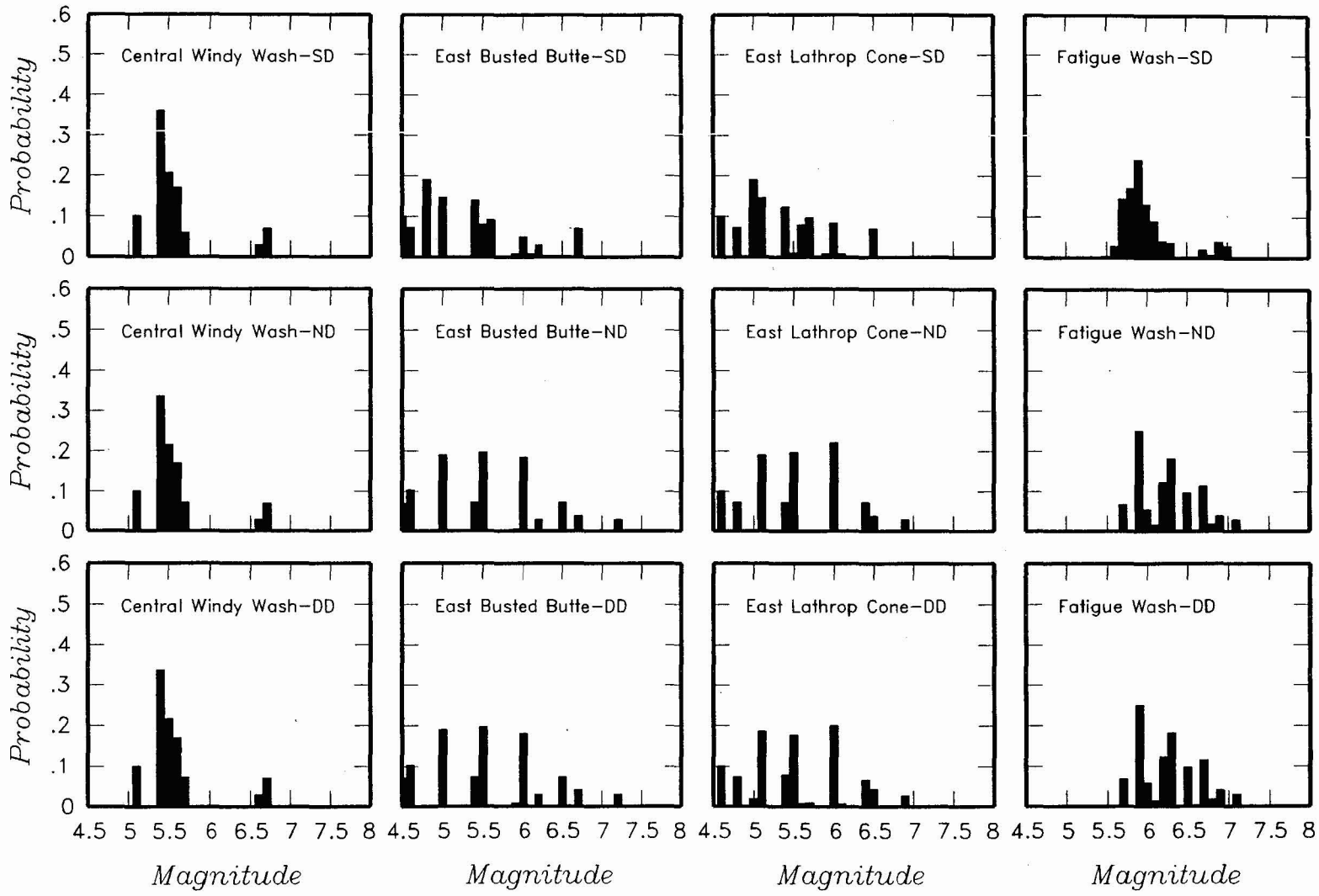

Figure 4-20b. Maximum magnitude distributions for AAR team's local fault sources

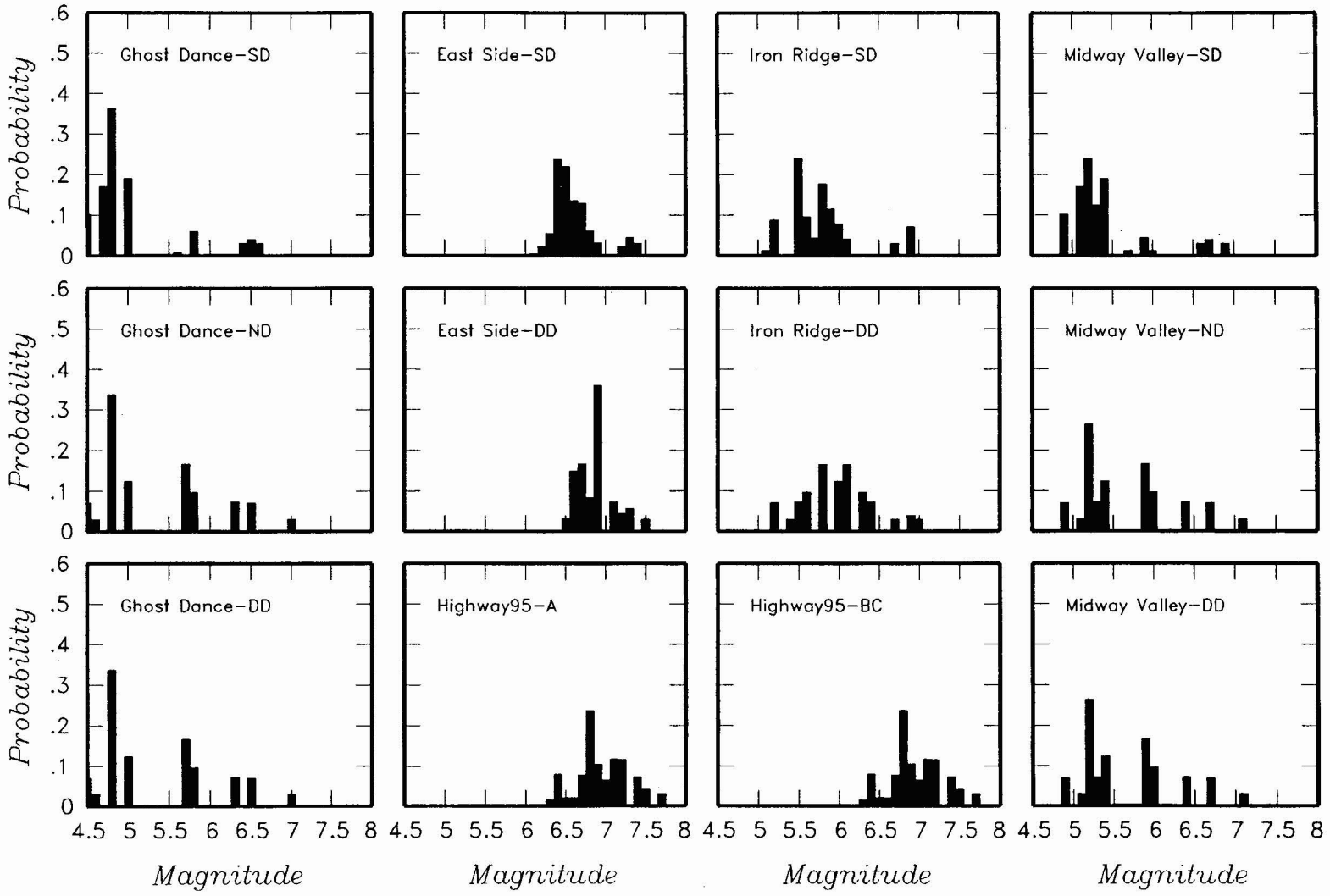

Figure 4-20c. Maximum magnitude distributions for AAR team's local fault sources

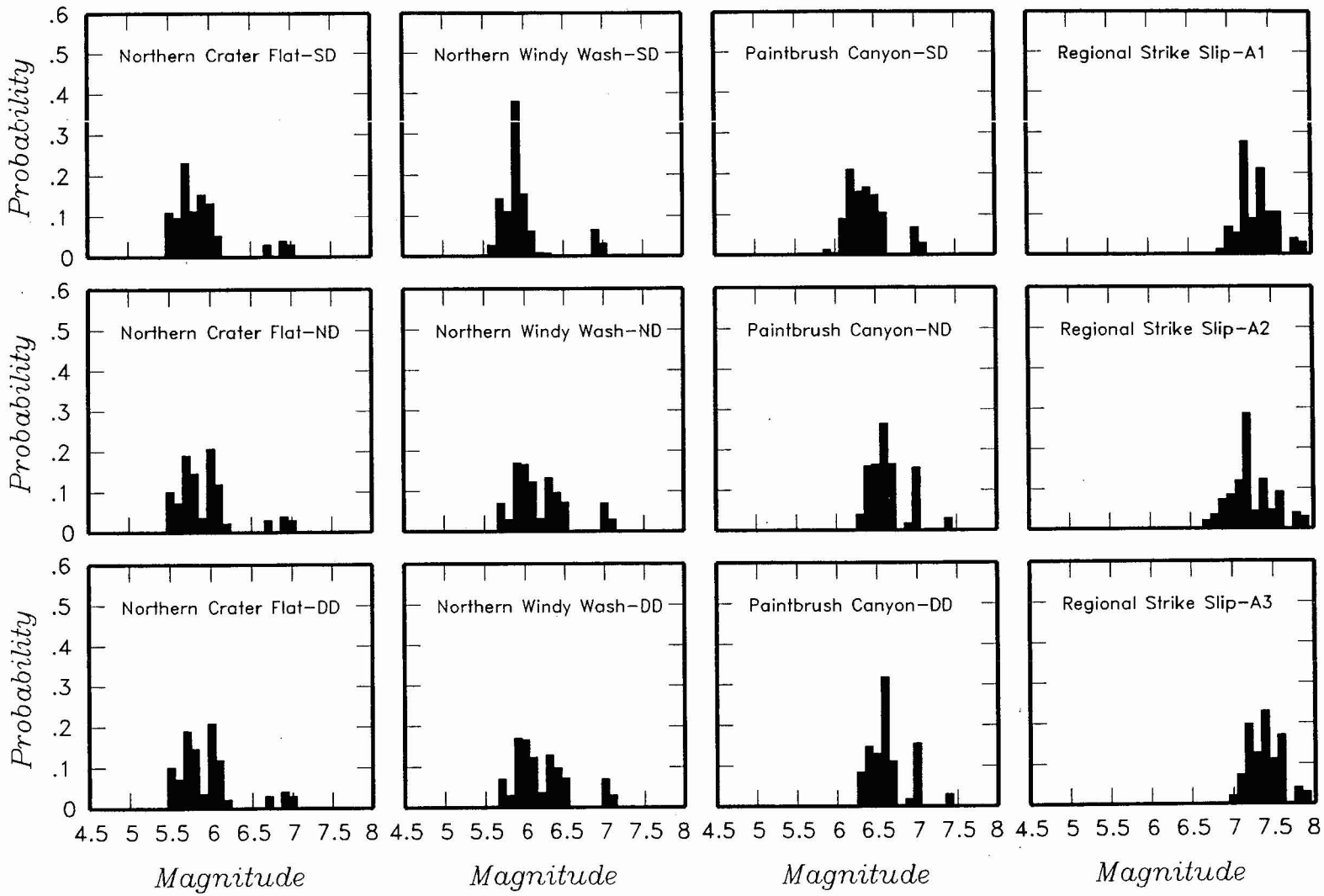

Figure 4-20d. Maximum magnitude distributions for AAR team's local fault sources

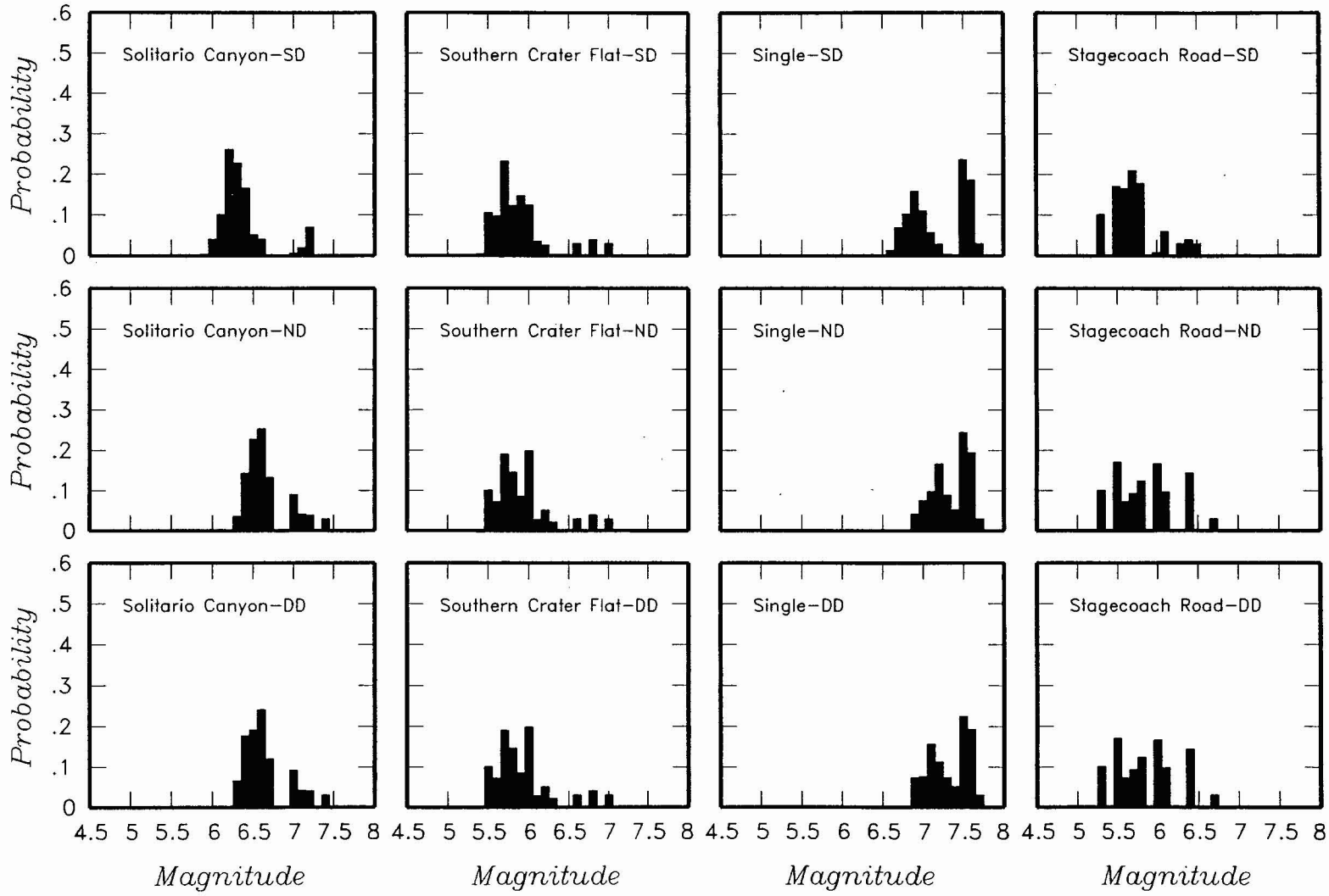

Figure 4-20e. Maximum magnitude distributions for AAR team's local fault sources

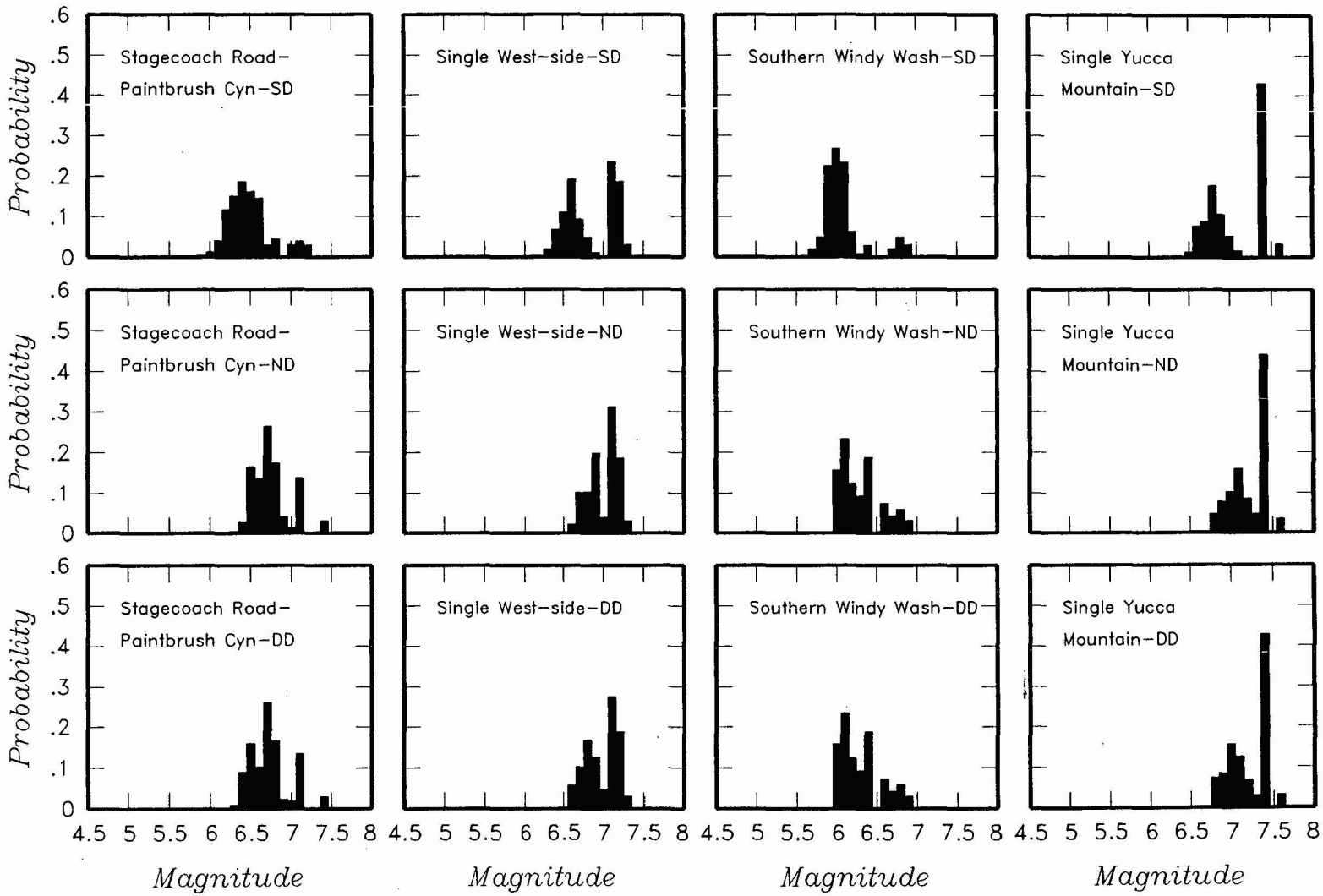

Figure 4-20f. Maximum magnitude distributions for AAR team's local fault sources

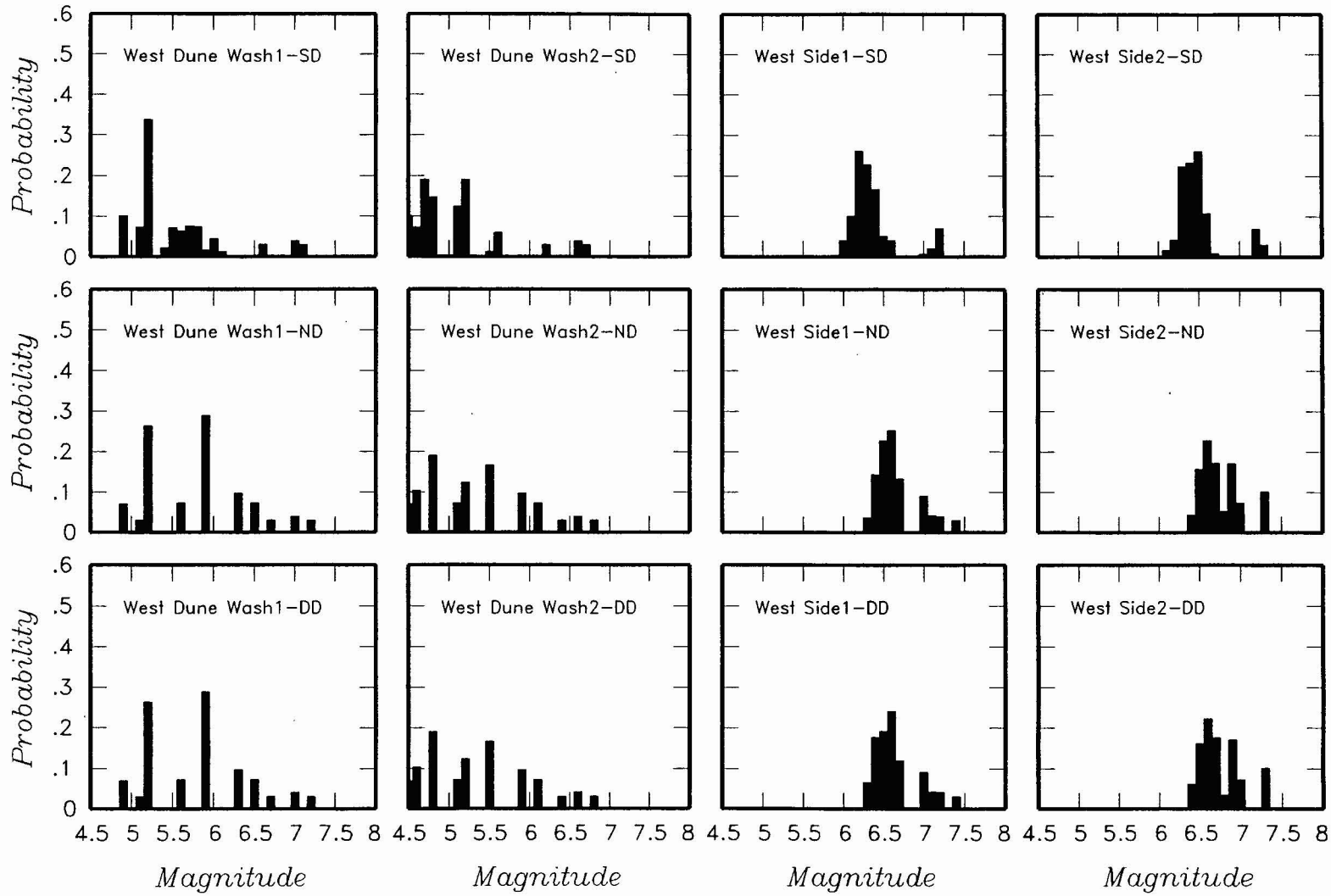

Figure 4-20g. Maximum magnitude distributions for AAR team's local fault sources

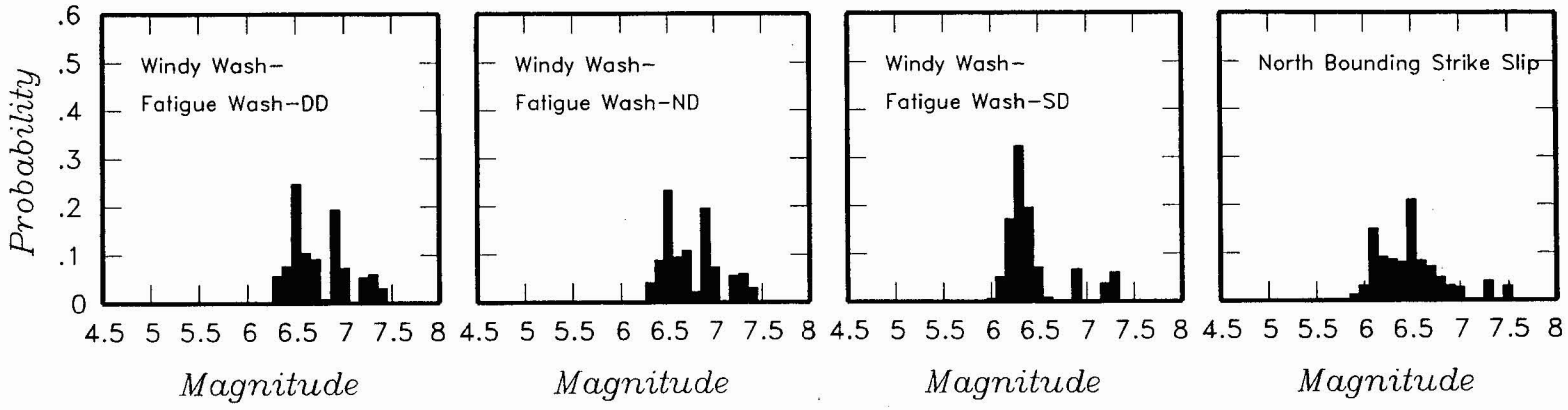

Figure 4-20h. Maximum magnitude distributions for AAR team's local fault sources

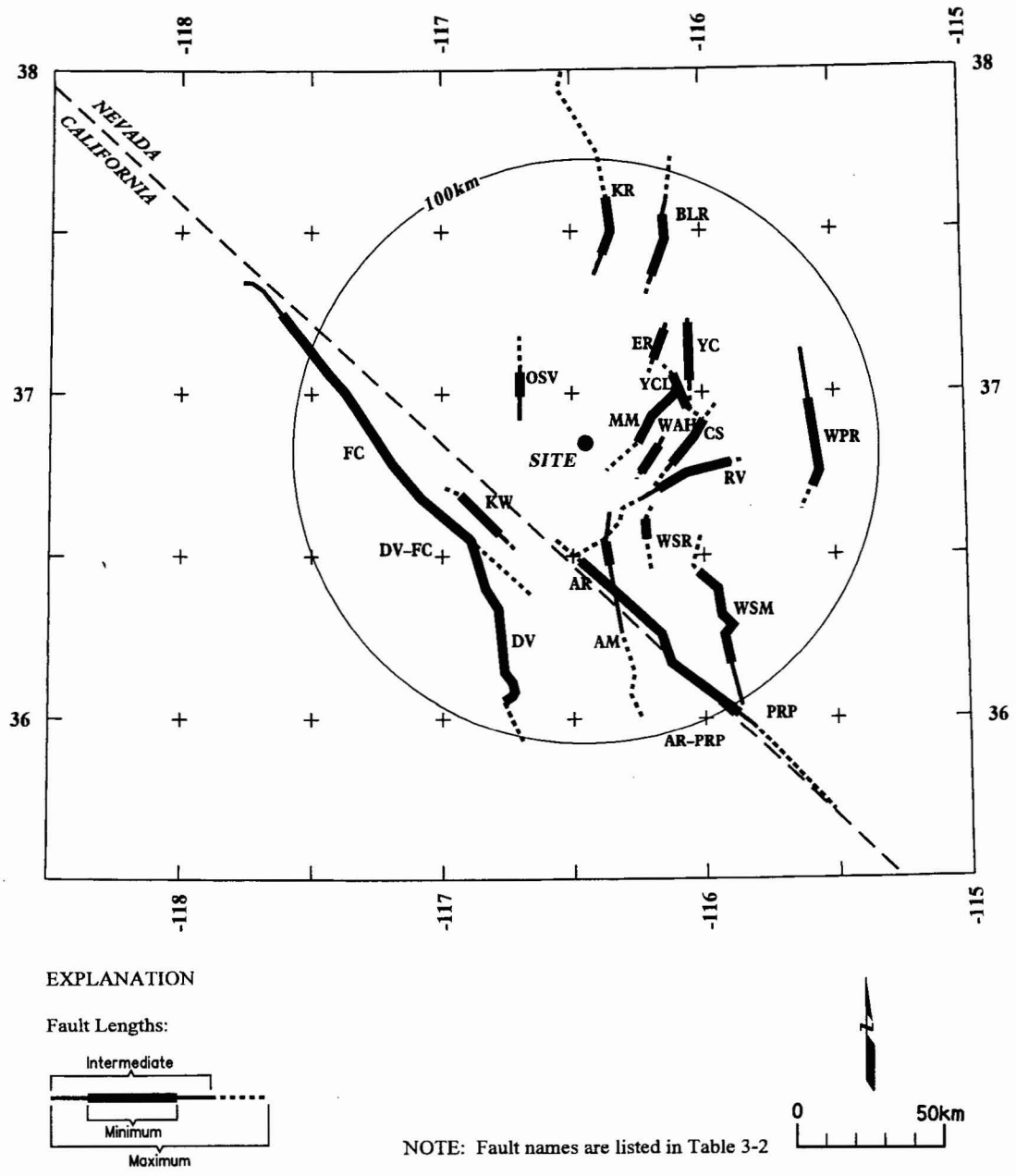

Figure 4-21. Regional fault sources considered by the AAR team

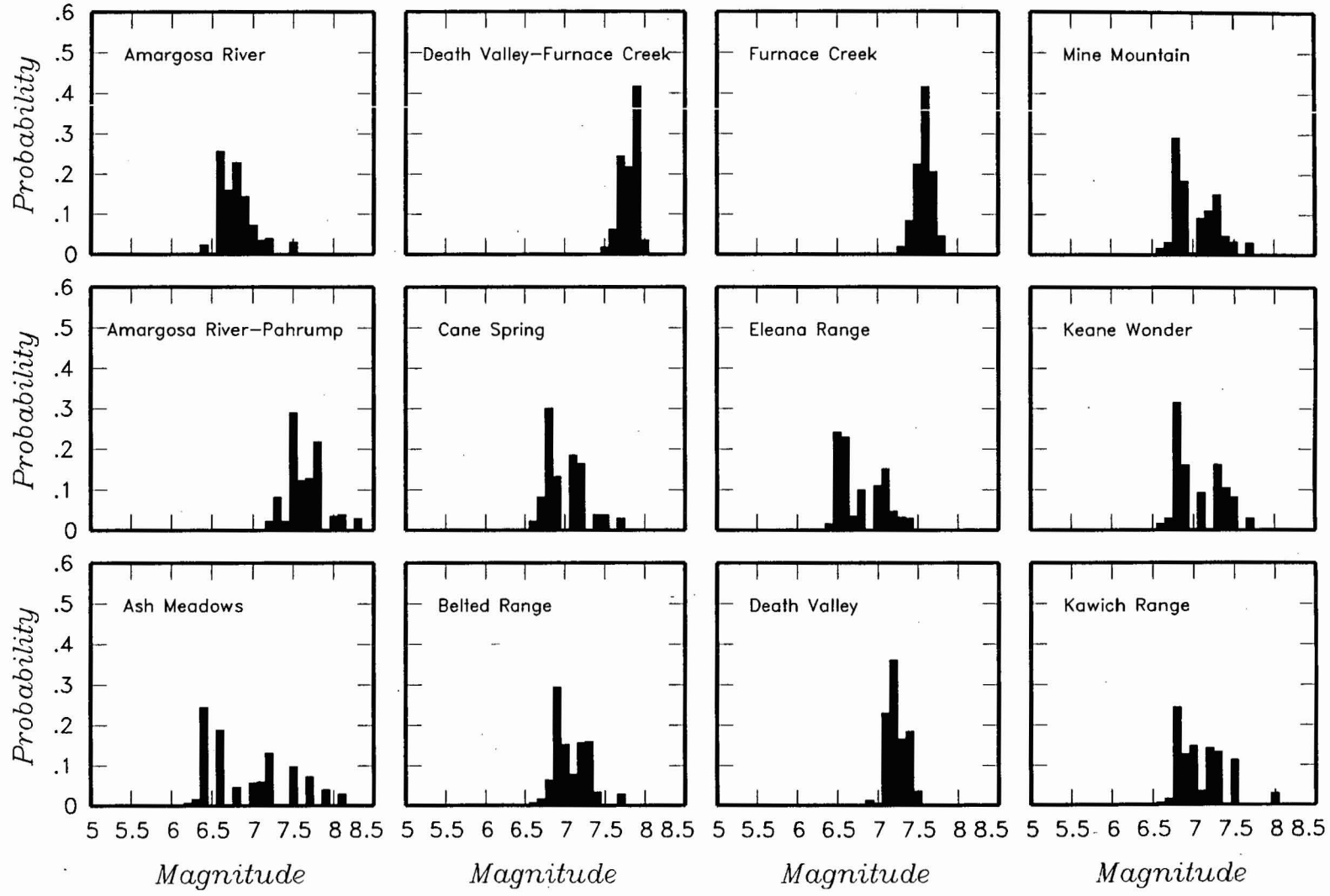

Figure 4-22 Maximum magnitude distributions for AAR team's regional fault sources

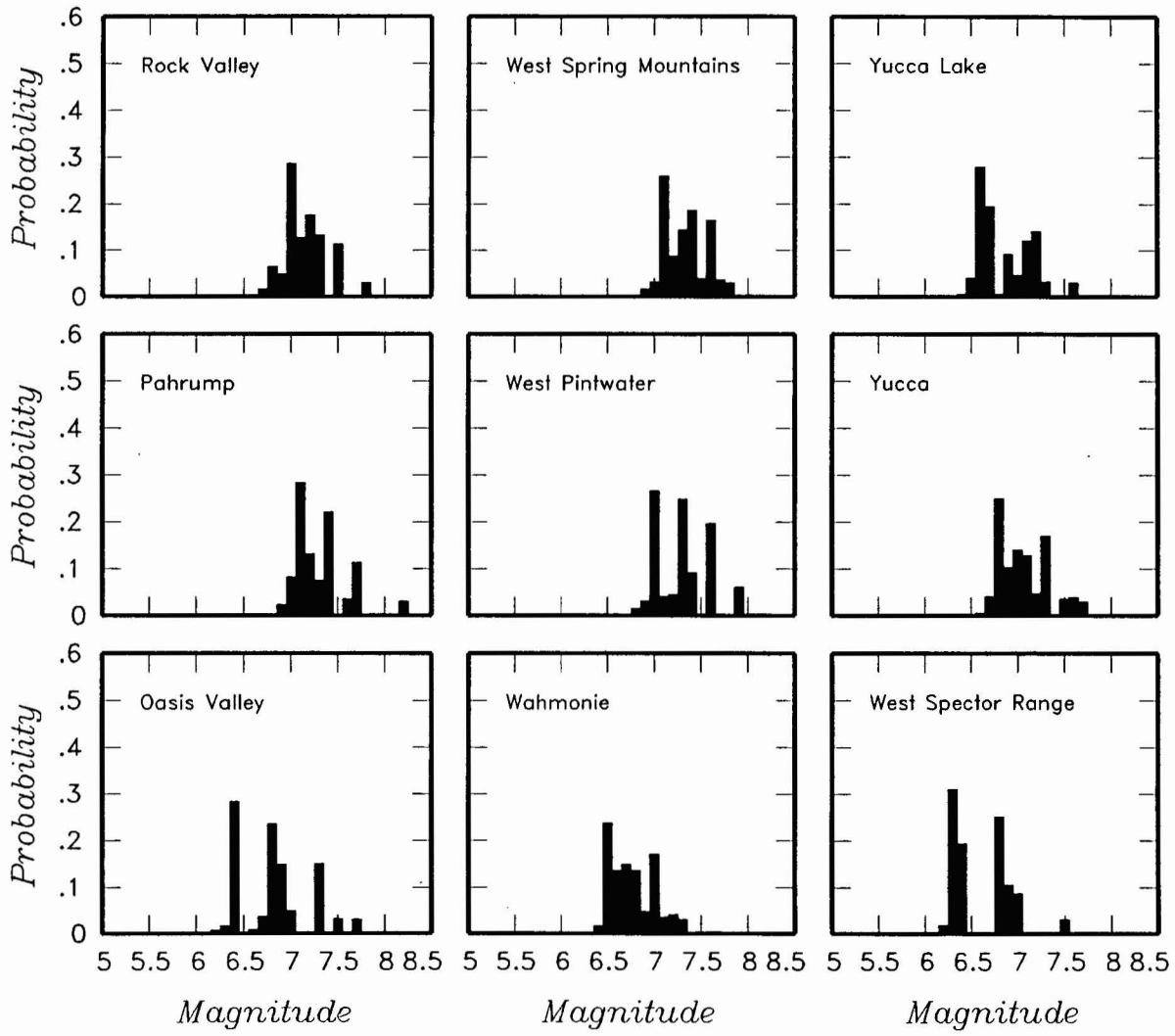

Figure 4-22 (Cont'd.) Maximum magnitude distributions for AAR team's regional fault sources

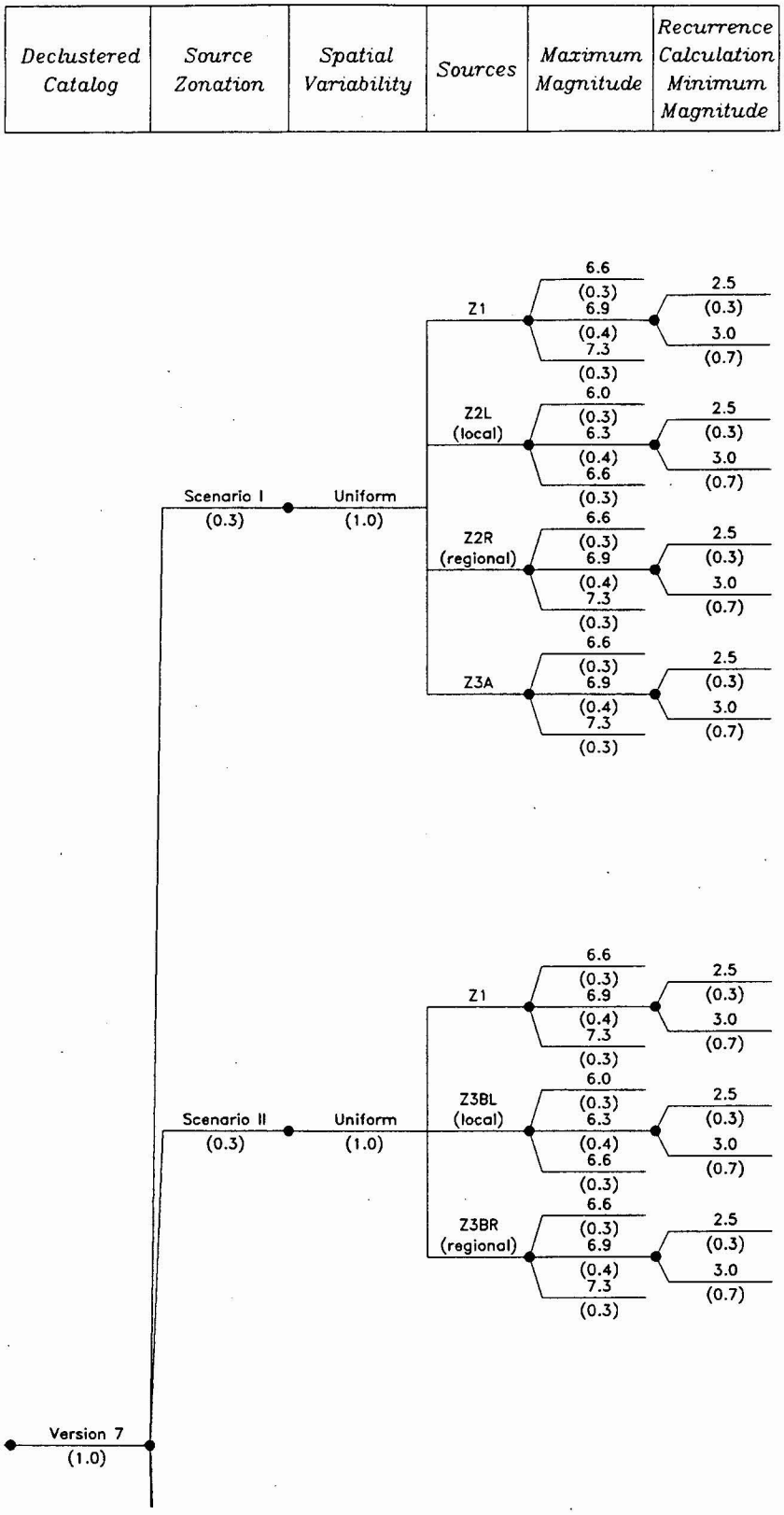

Figure 4-23 Logic tree for regional source zones developed by the AAR team

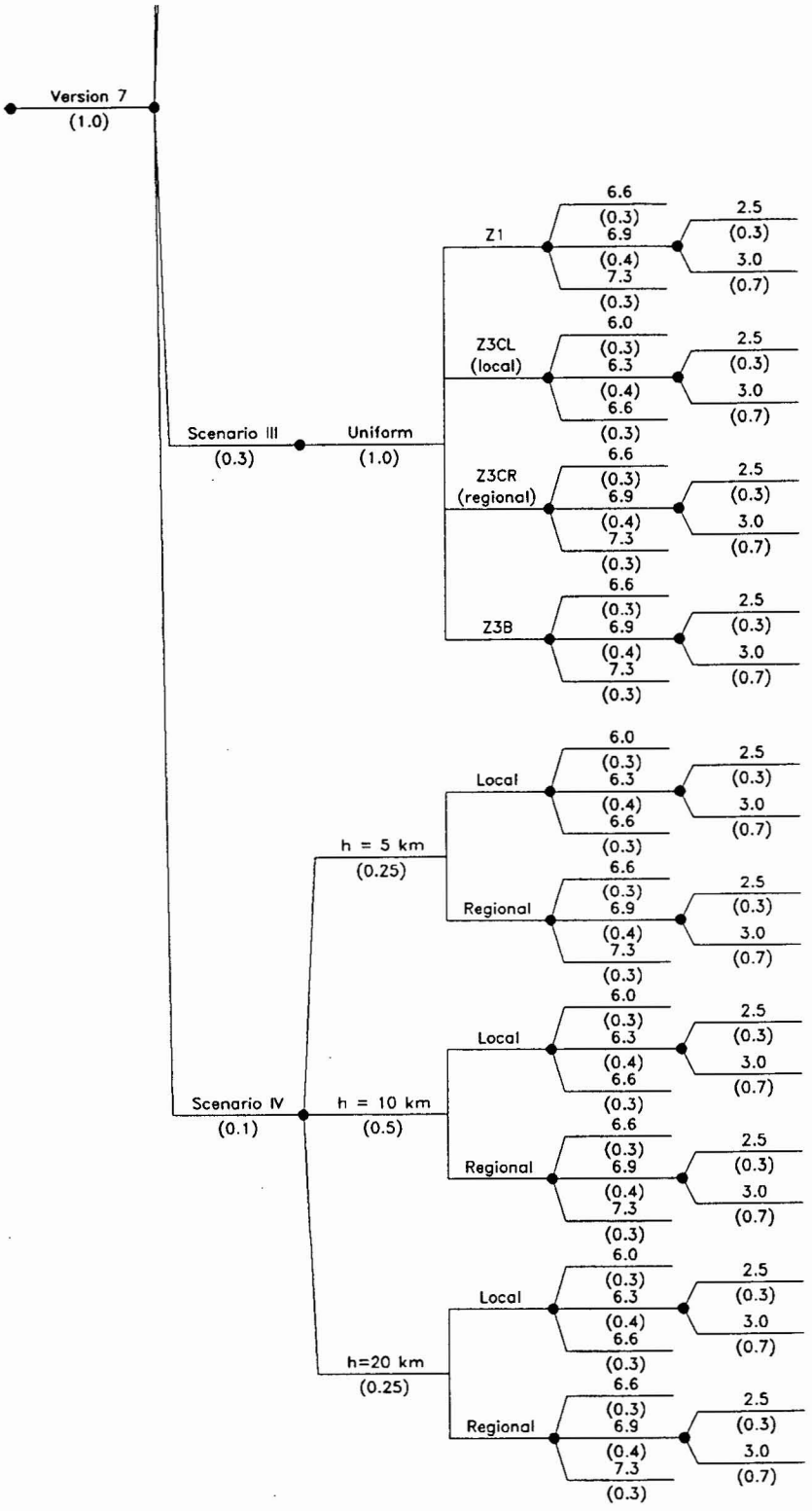

Figure 4-23 (Cont'd.) Logic tree for regional source zones developed by the AAR team

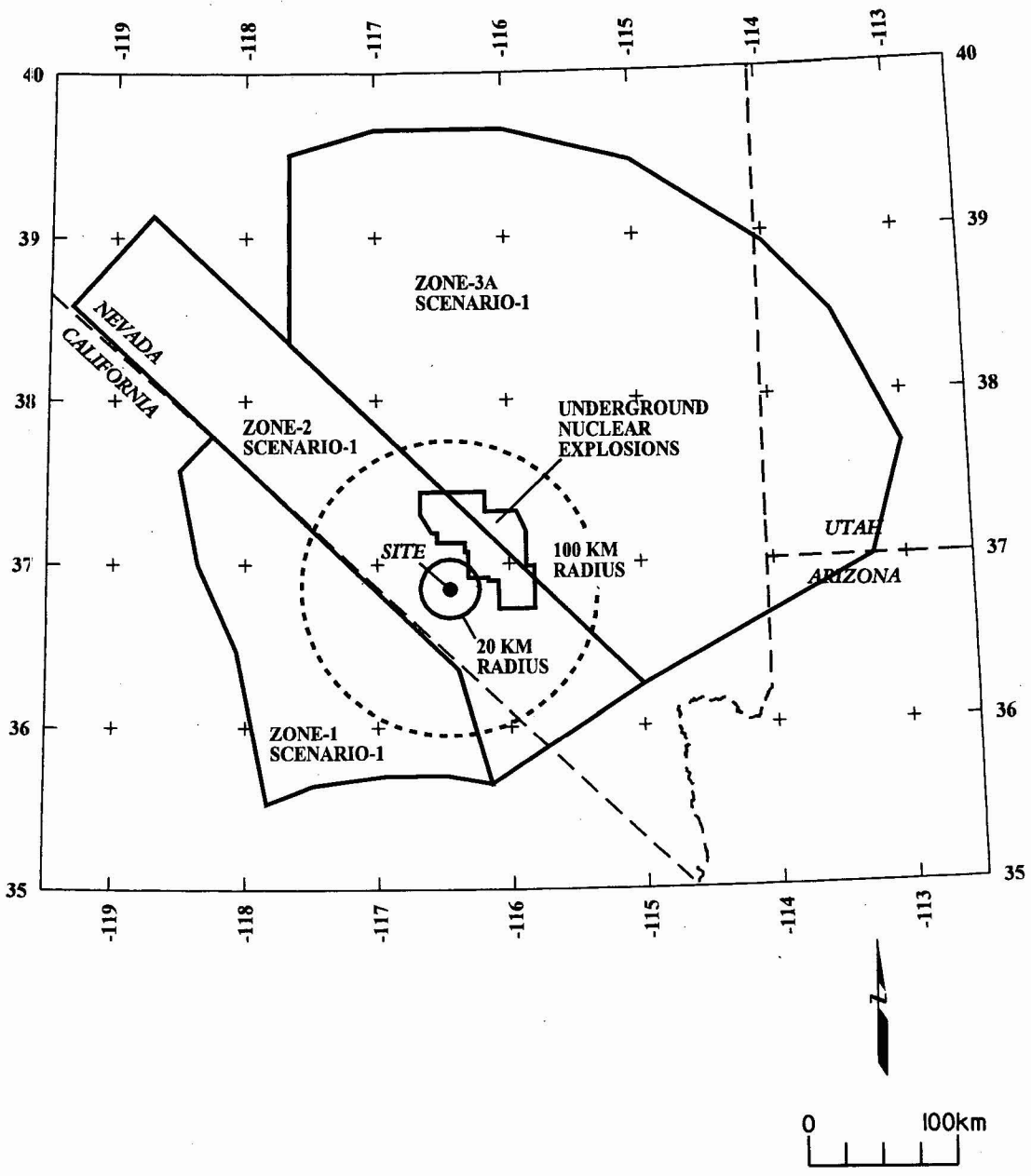

Figure 4-24a. Alternative regional source zone models considered by the AAR team

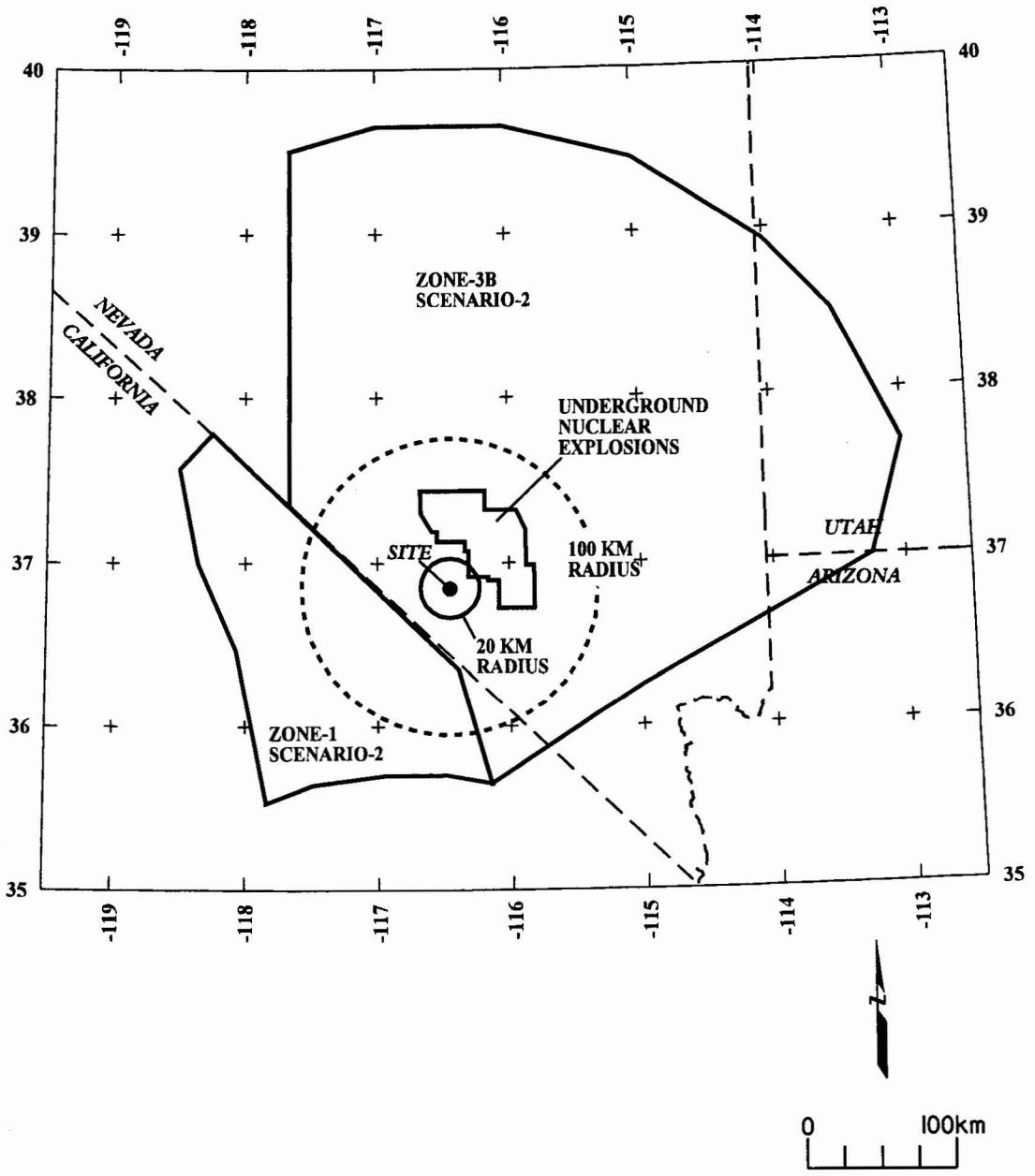

Figure 4-24b. Alternative regional source zone models considered by the AAR team

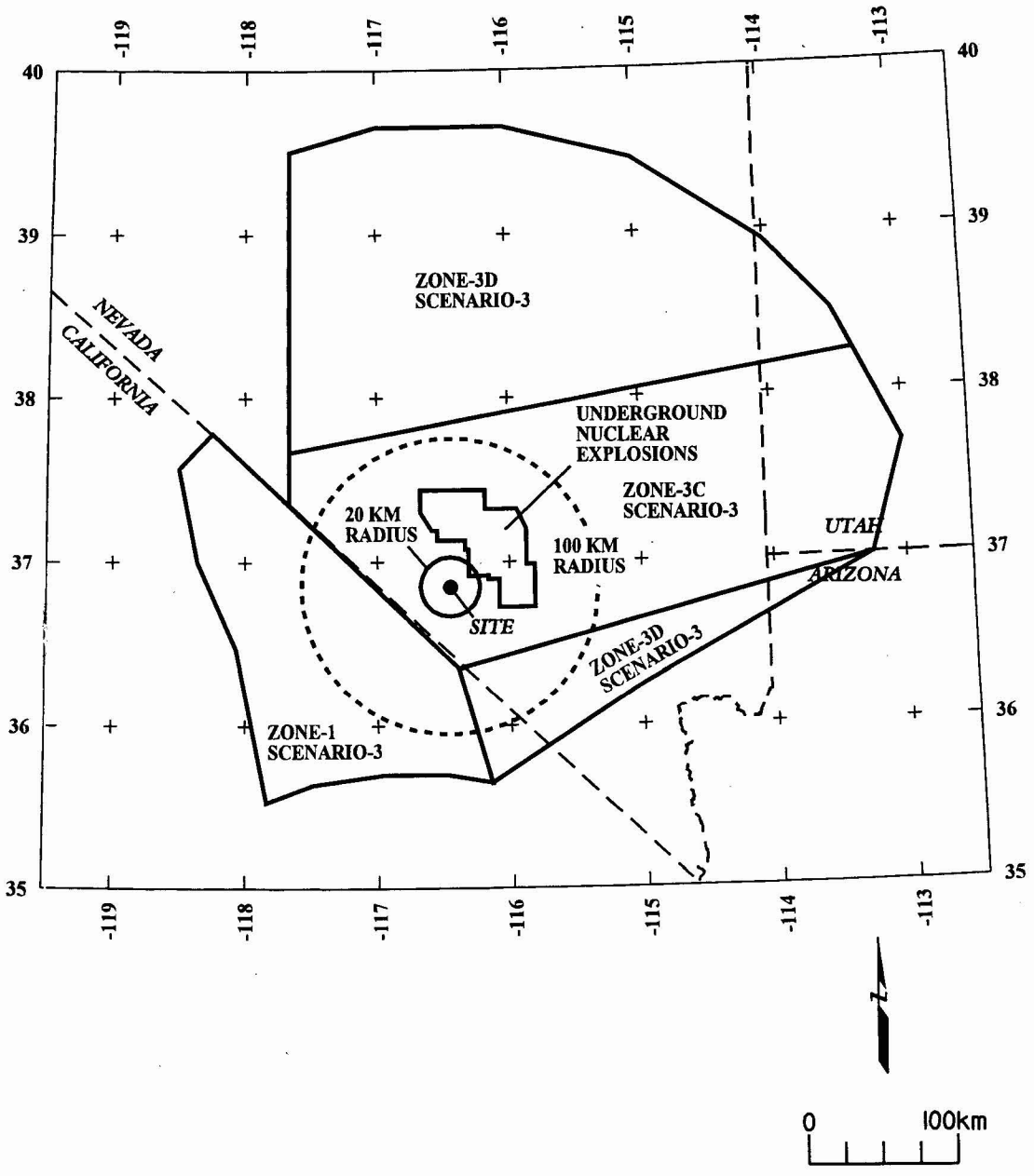

Figure 4-24c. Alternative regional source zone models considered by the AAR team

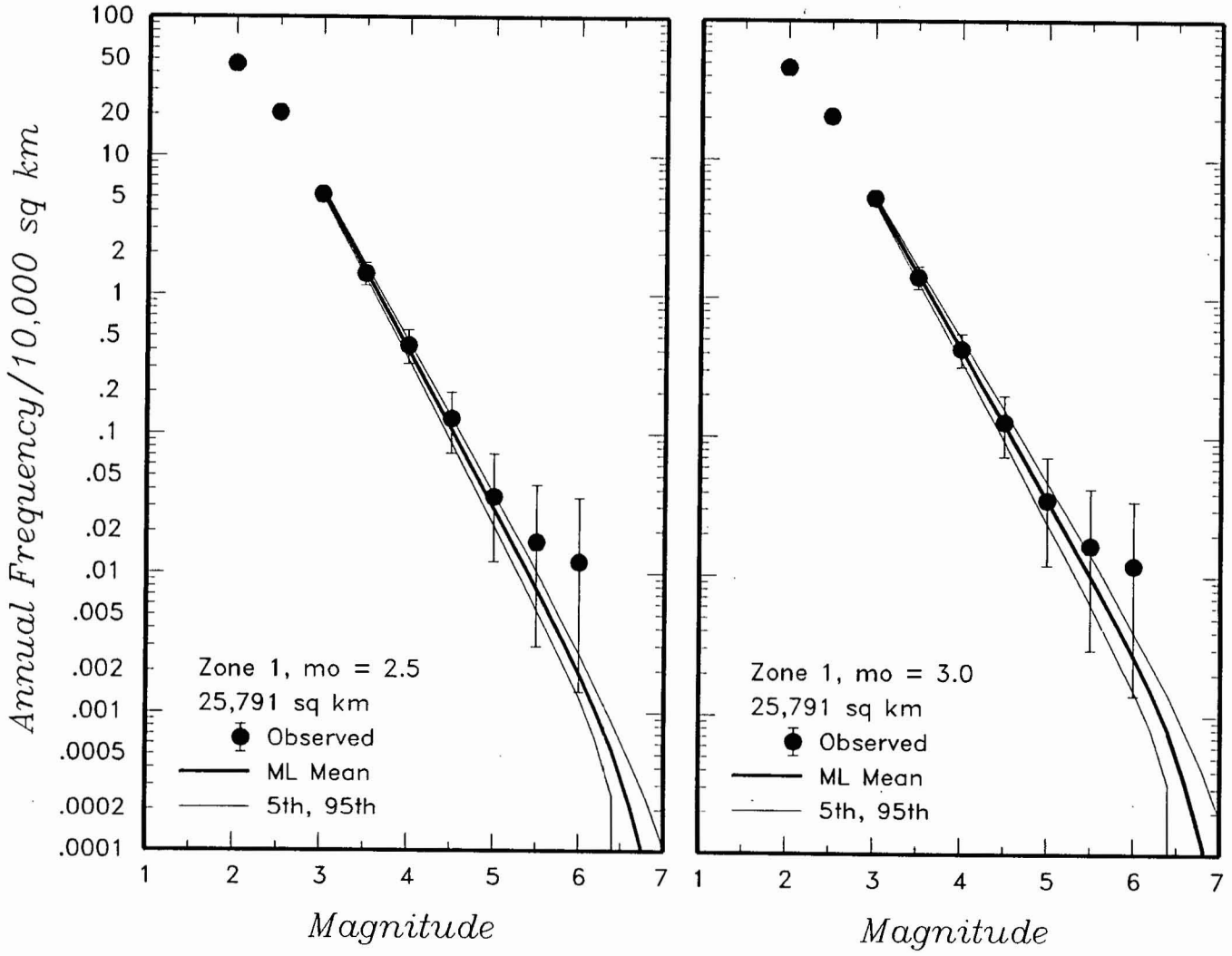

Figure 4-25 Earthquake recurrence relationships for the regional source zones defined by the AAR team. The solid dots with vertical error bars represent the observed data. The thick and thin solid curves are the mean, 5th, and 95th percentiles of the recurrence rates based on the uncertainty in recurrence parameters and maximum magnitude.

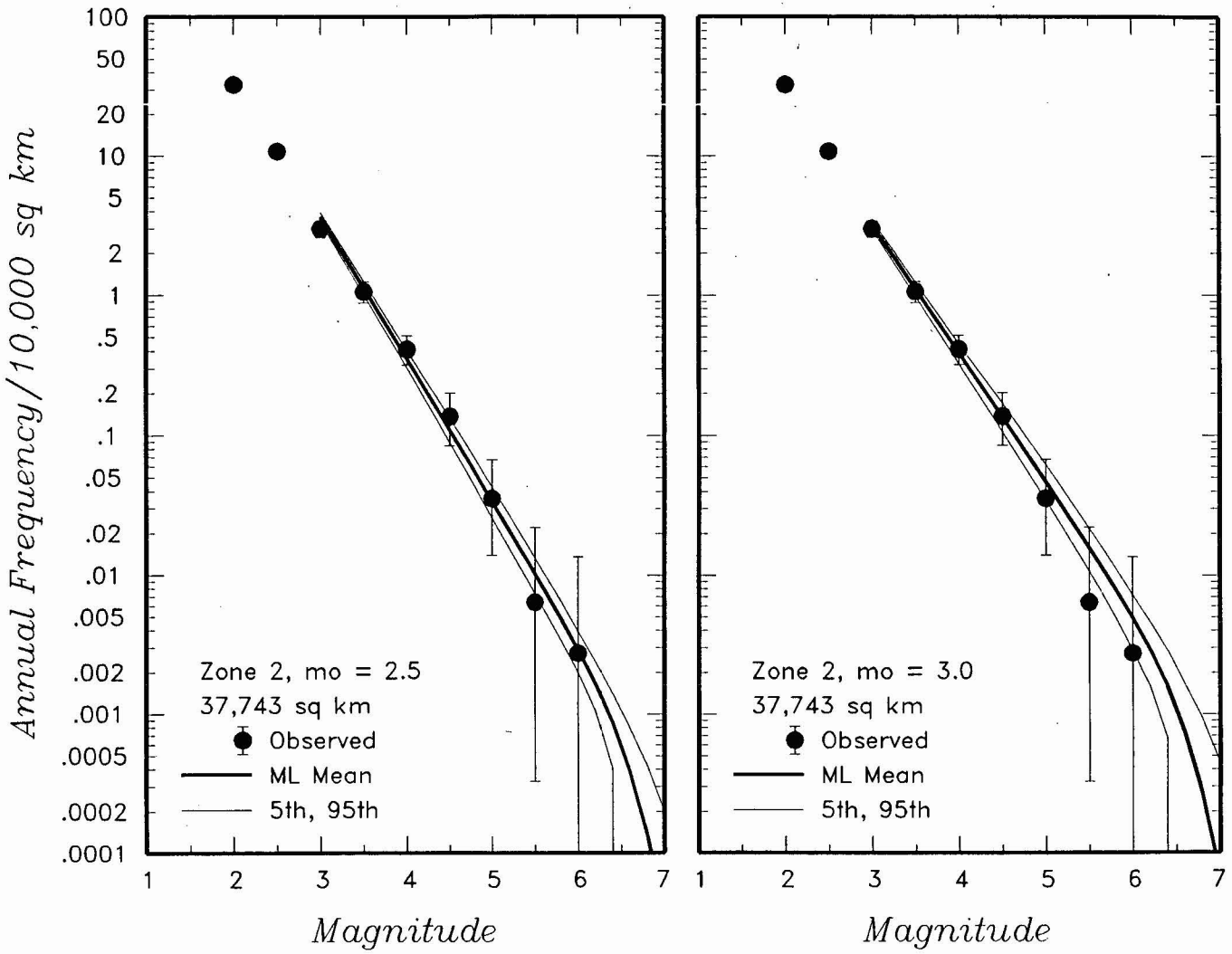

Figure 4-25 (Cont'd.) Earthquake recurrence relationships for the regional source zones defined by the AAR team

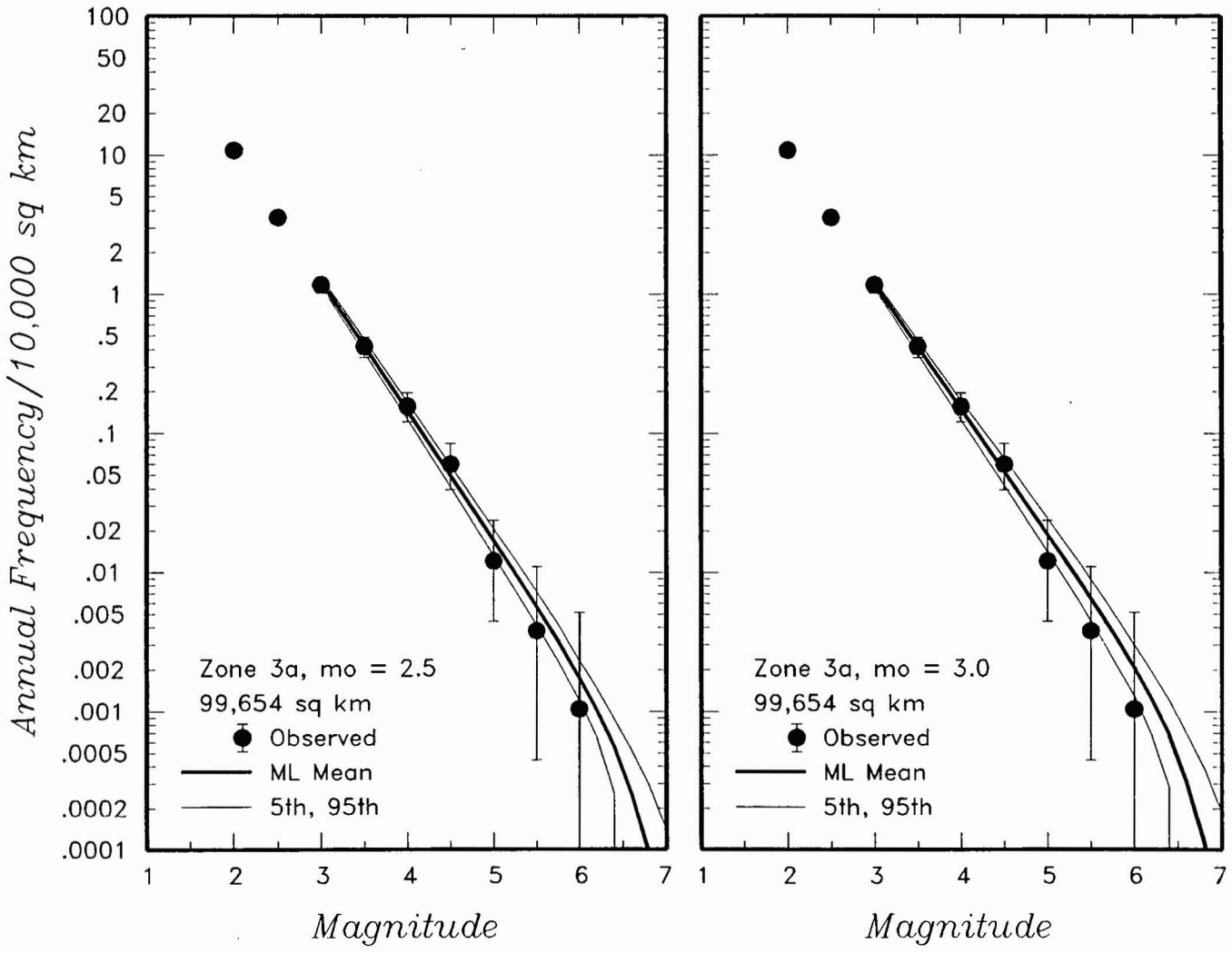

Figure 4-25 (Cont'd.) Earthquake recurrence relationships for the regional source zones defined by the AAR team

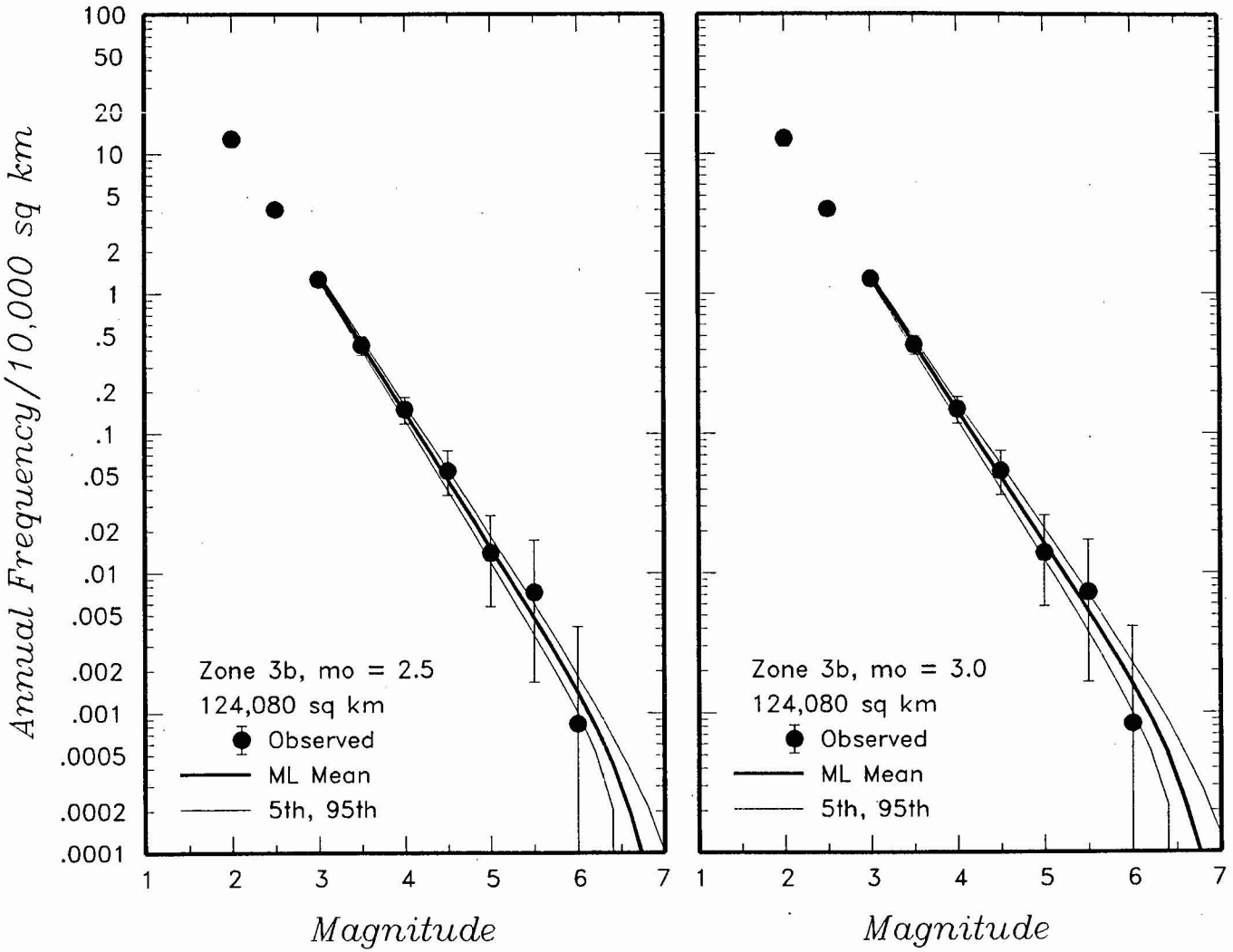

Figure 4-25 (Cont'd.) Earthquake recurrence relationships for the regional source zones defined by the AAR team

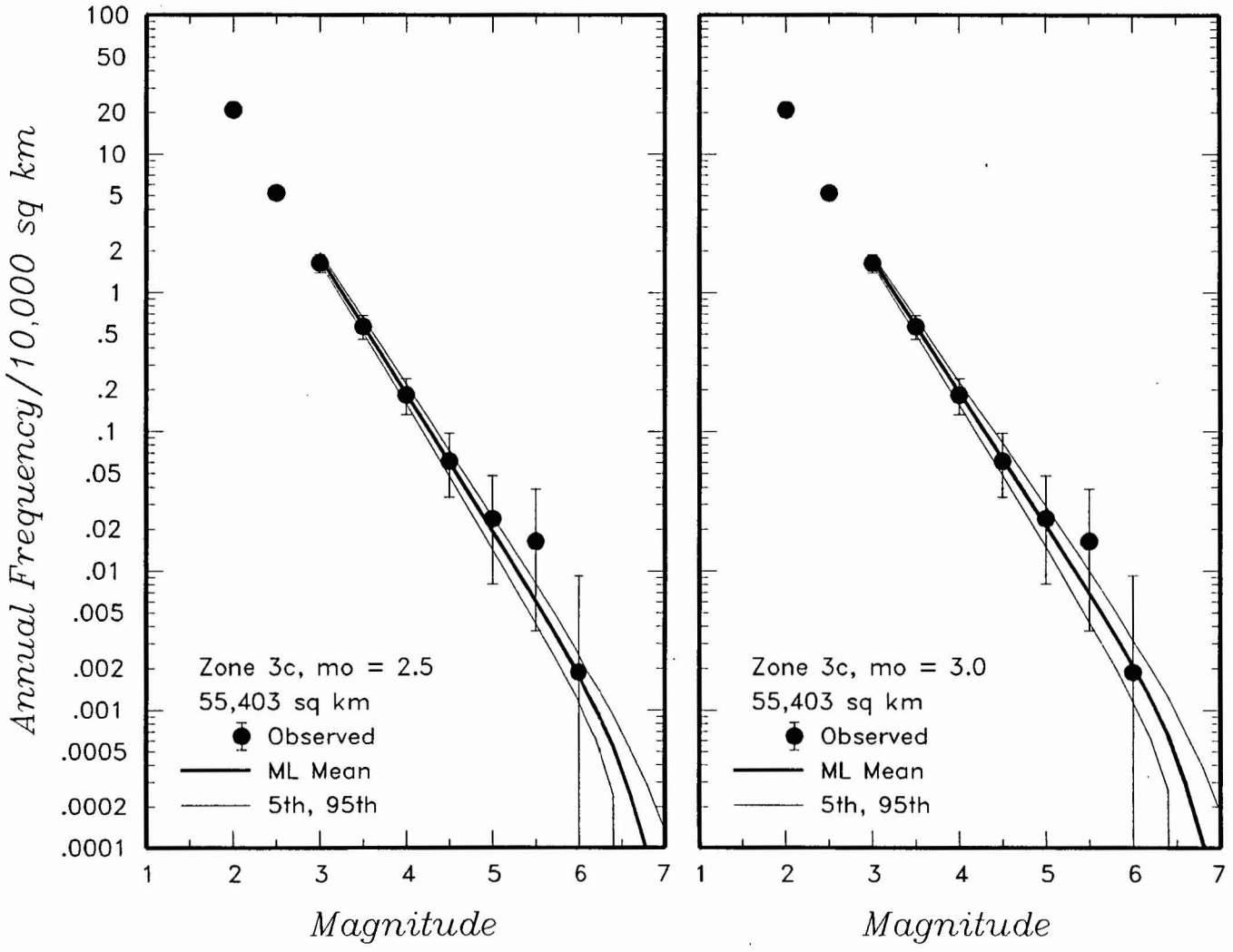

Figure 4-25 (Cont'd.) Earthquake recurrence relationships for the regional source zones defined by the AAR team

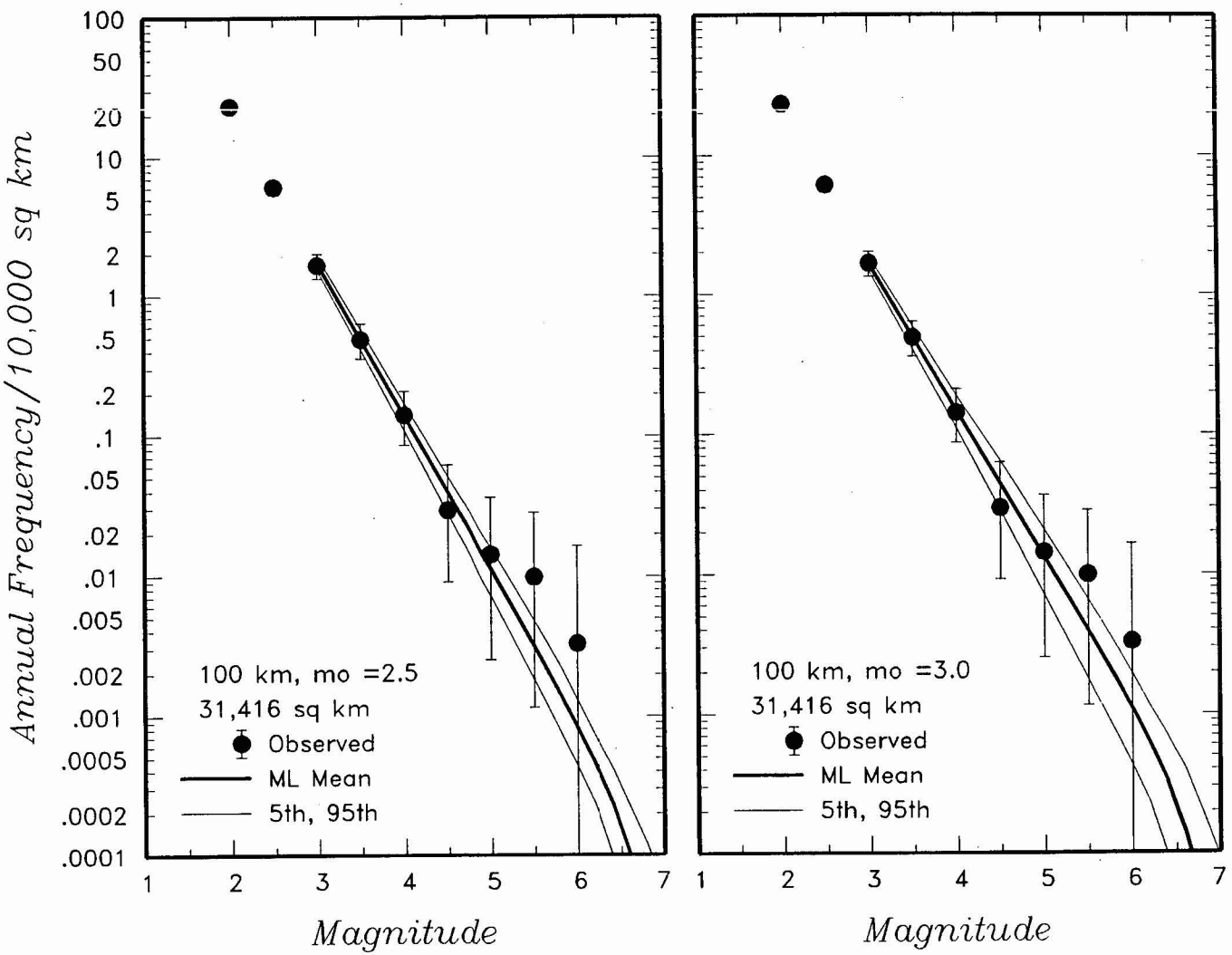

Figure 4-25 (Cont'd.) Earthquake recurrence relationships for the regional source zones defined by the AAR team

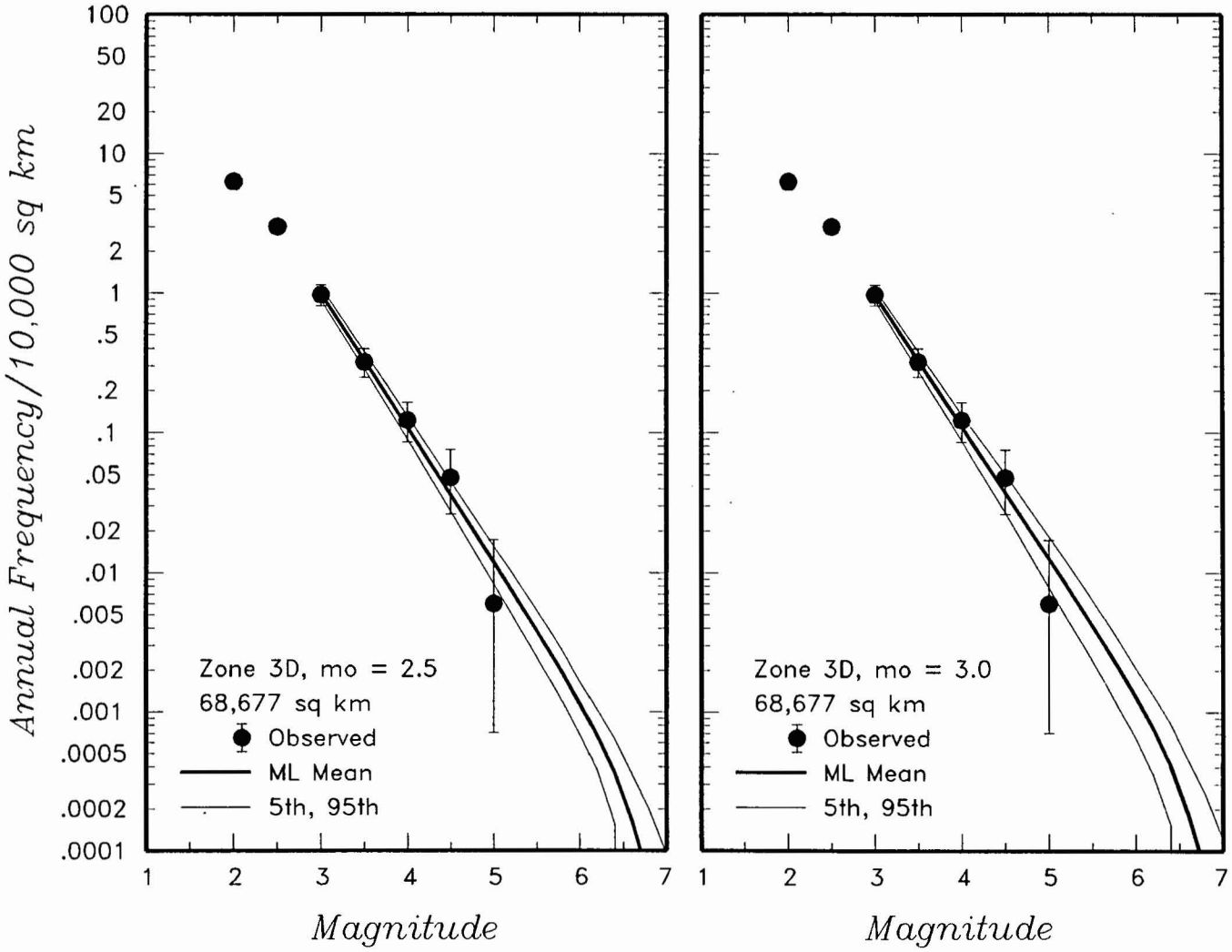

Figure 4-25 (Cont'd.) Earthquake recurrence relationships for the regional source zones defined by the AAR team

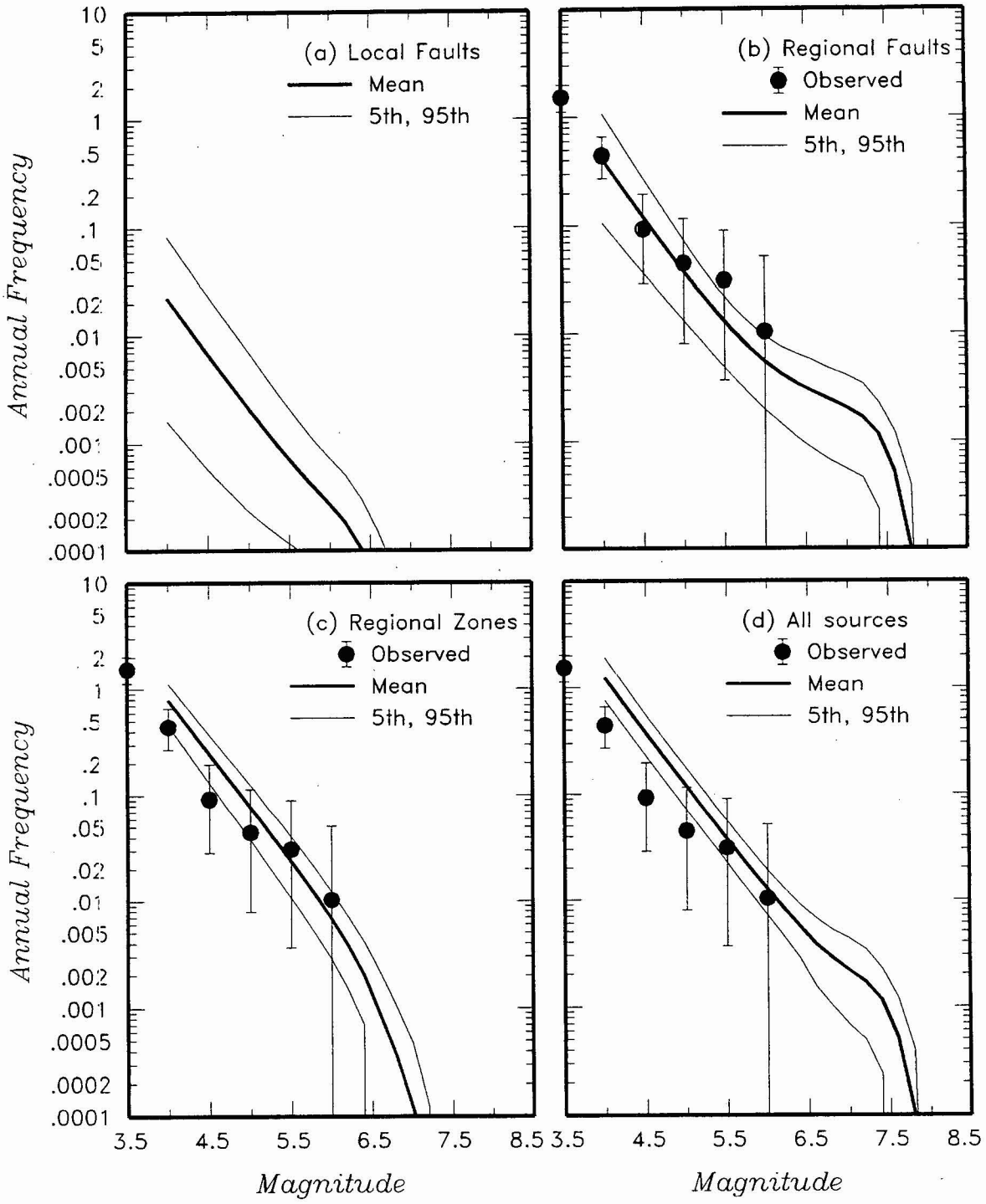

Figure 4-26. Predicted mean, 5th-, and 95th-percentile recurrence rates for (a) local fault sources, (b) regional fault sources, (c) regional source zones, and (d) all sources combined for the AAR team. The solid dots with vertical error bars show the observed frequency of earthquakes occurring within 100 km of the Yucca Mountain site.

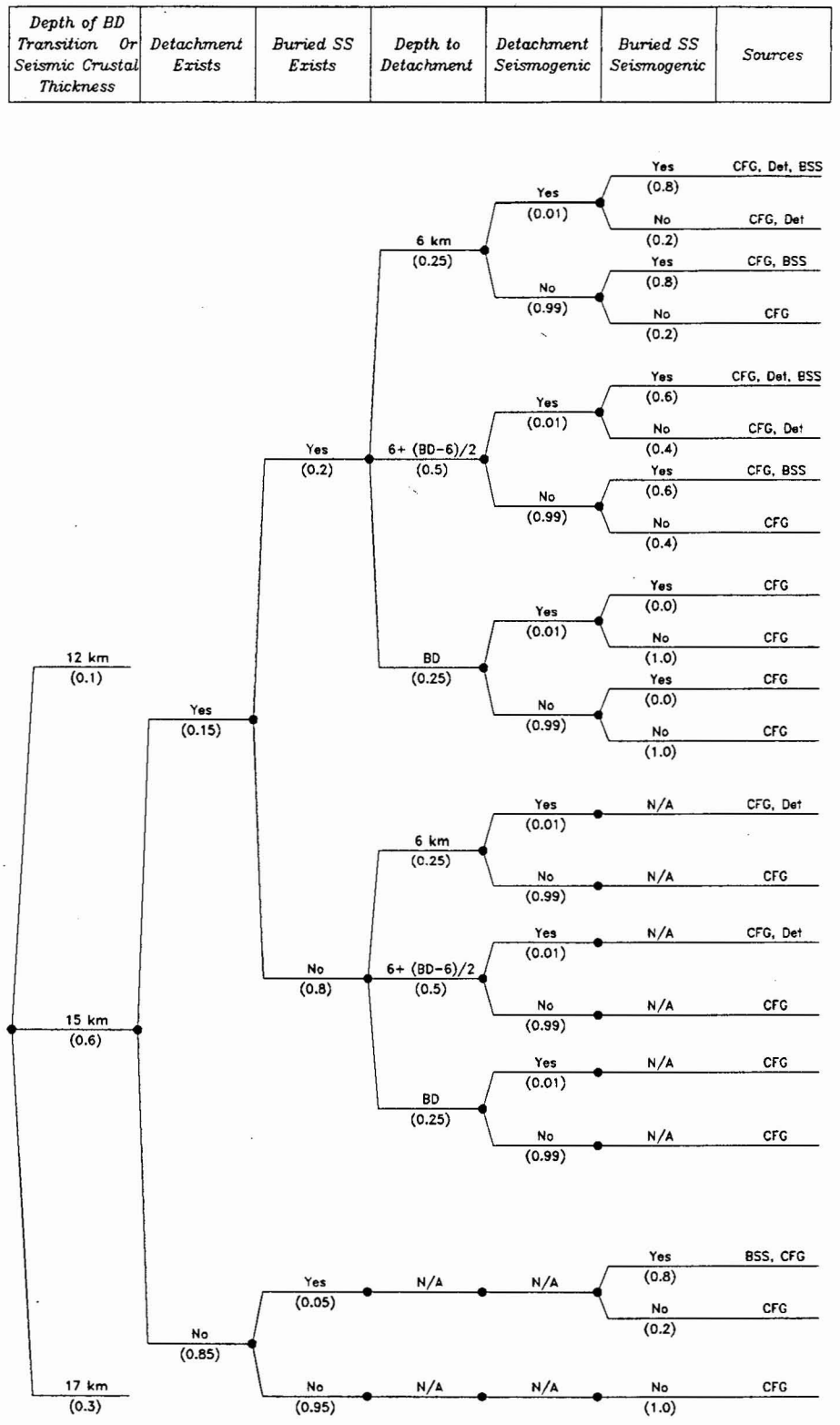

Figure 4-27a Logic tree for local fault sources developed by the ASM team

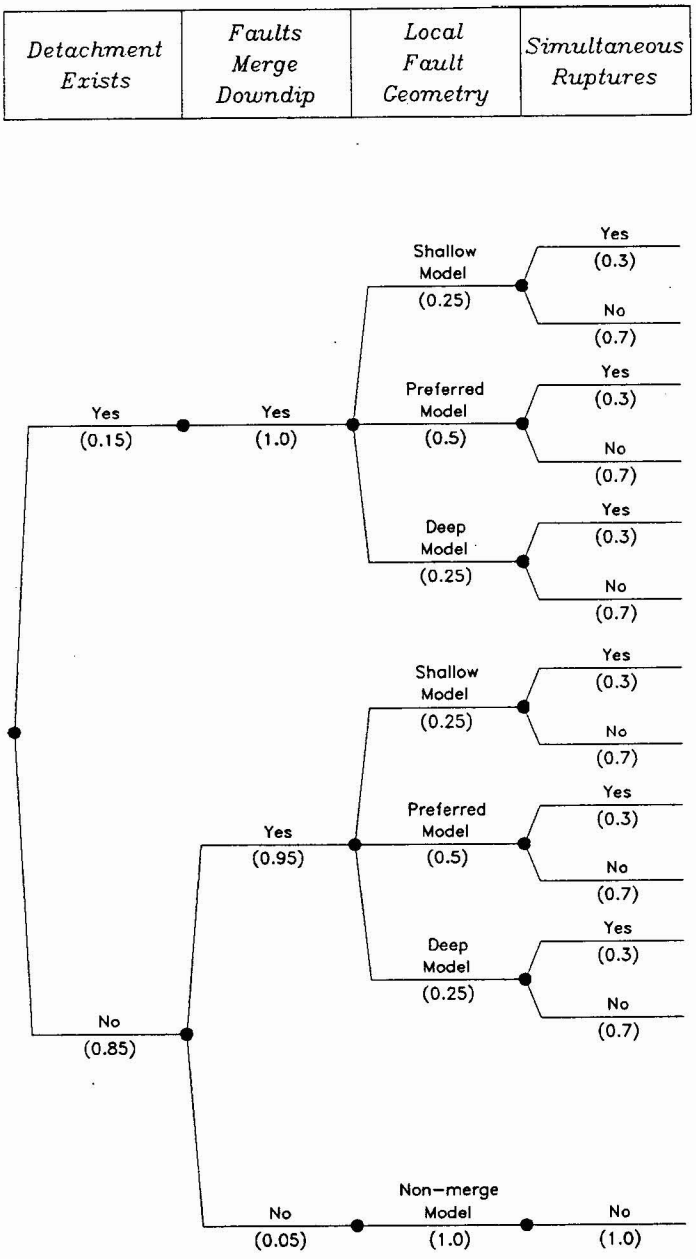

Figure 4-27b Logic tree for rupture behavior of Crater Flat group of faults

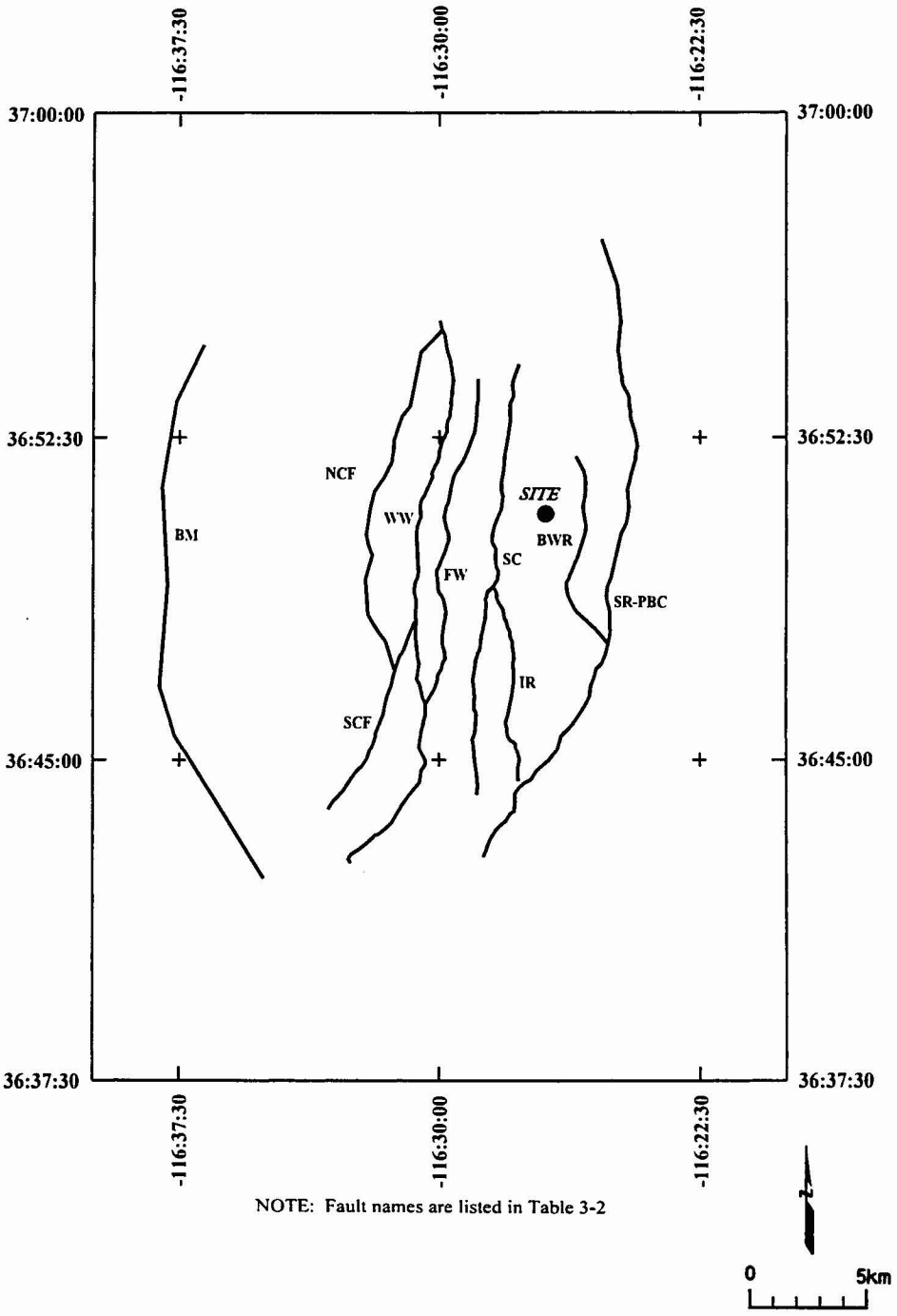

NOTE: Fault names are listed in Table 3-2

Figure 4-28 Location of fault sources considered by the ASM team

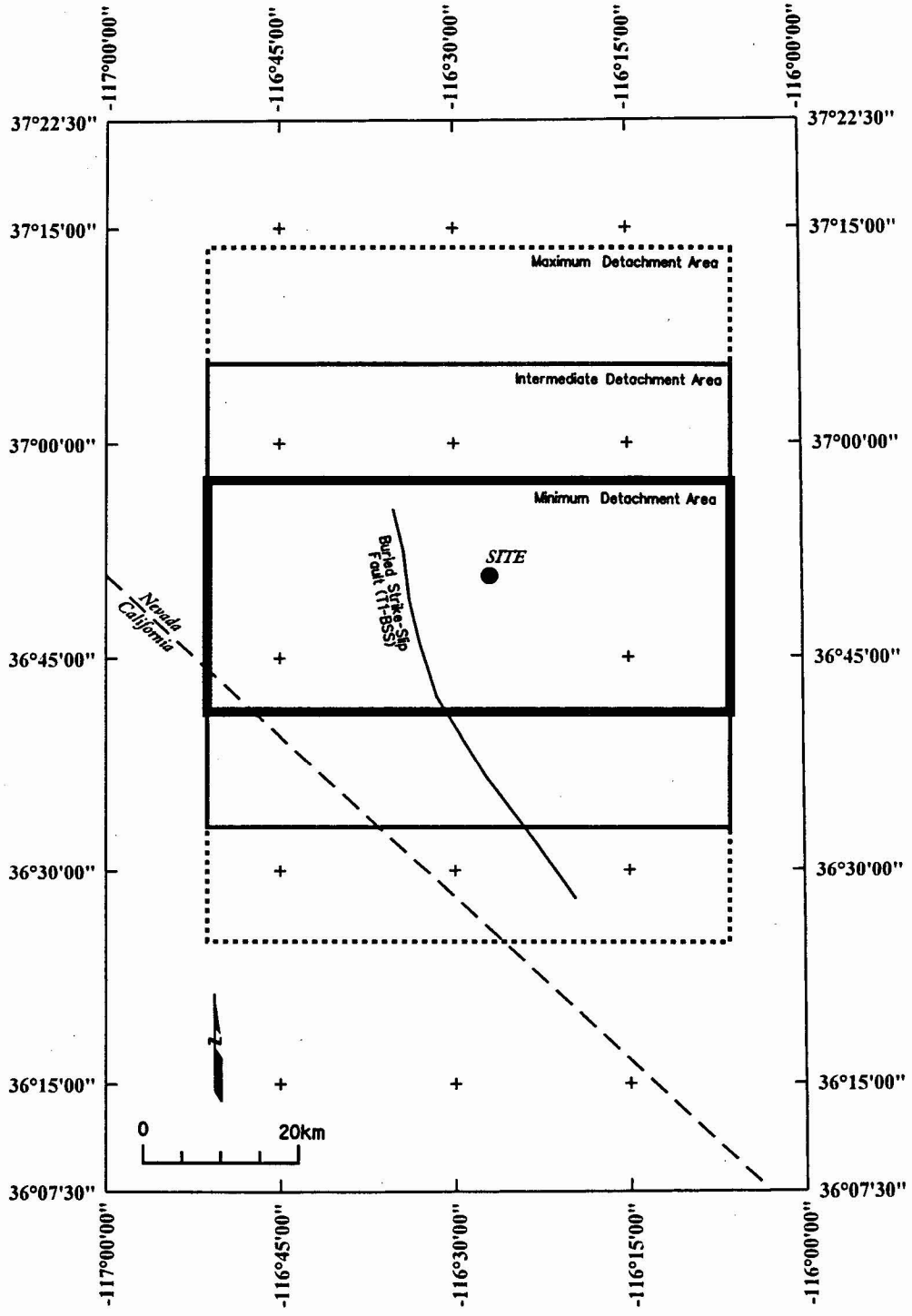

Figure 4-29 Location of hypothetical buried strike-slip and detachment faults in the vicinity of Yucca Mountain included in the ASM seismic source model

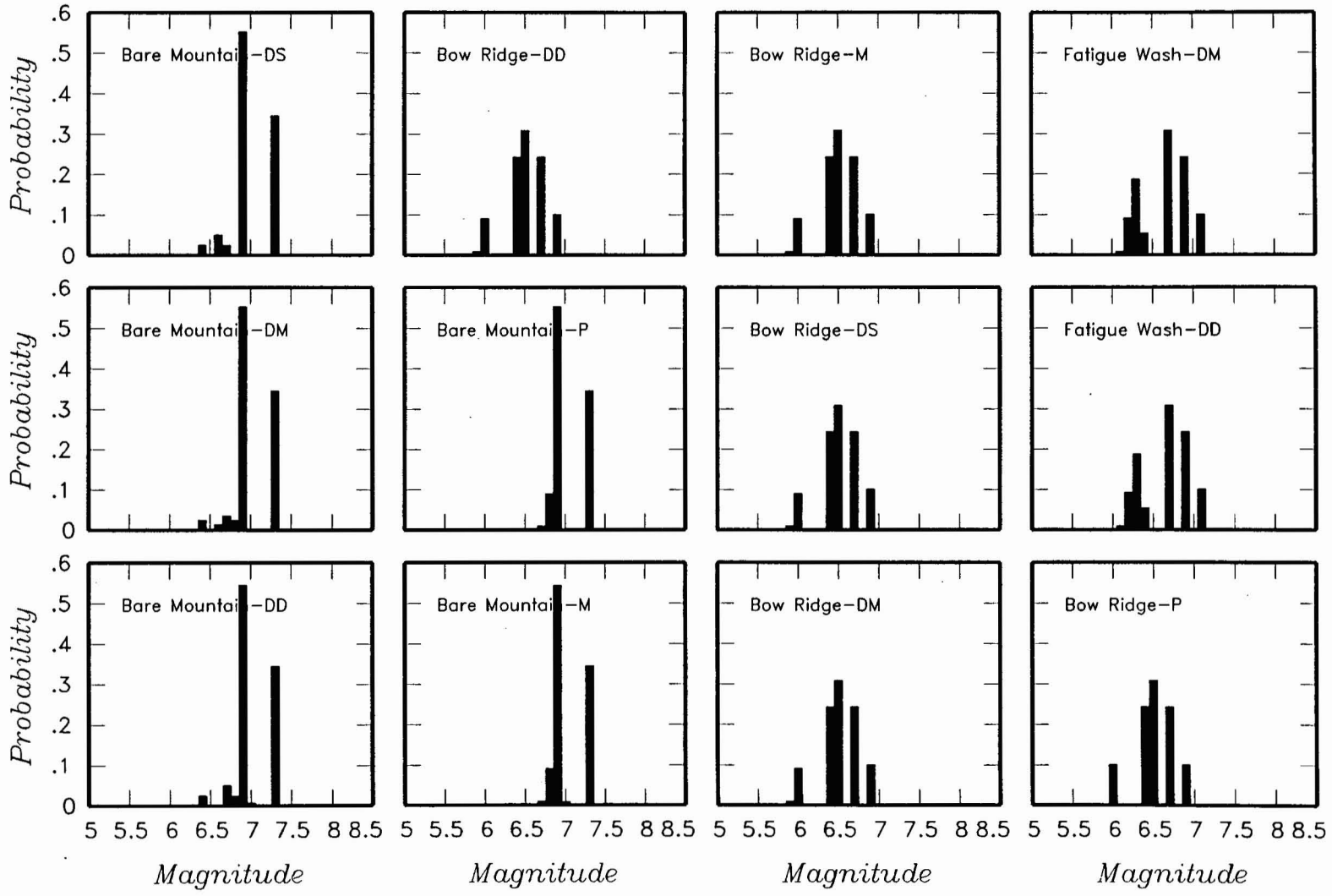

Figure 4-30 Maximum magnitude distributions for ASM team's local fault sources. DS–shallow detachment, DM–preferred detachment, DD–deep detachment; M–merging model, P–planar model; BM–Bare Mountain, W–Windy Wash, SRPBC–Stagecoach Road-Paintbrush Canyon.

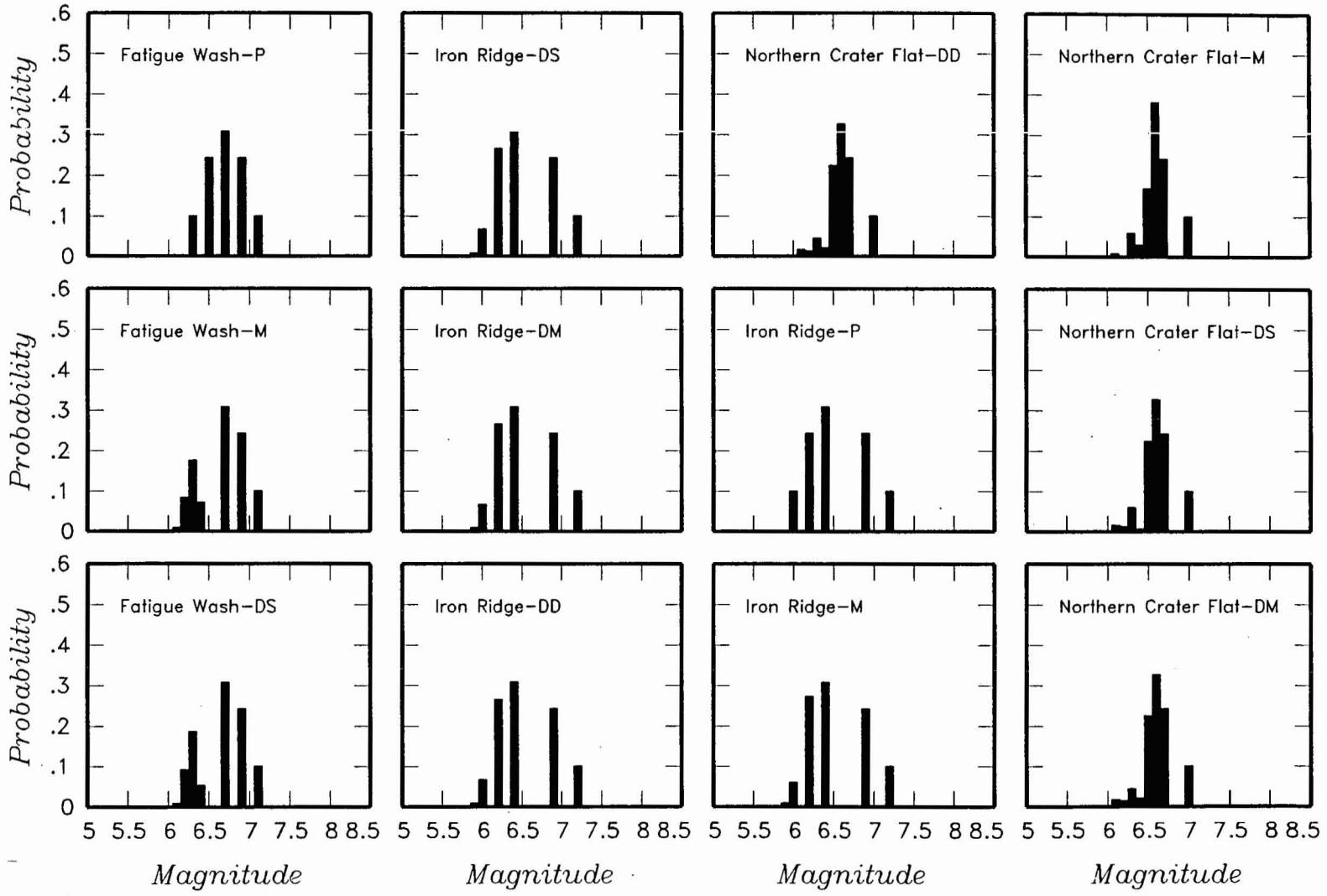

Figure 4-30 (Cont'd.) Maximum magnitude distributions for ASM team's local fault sources

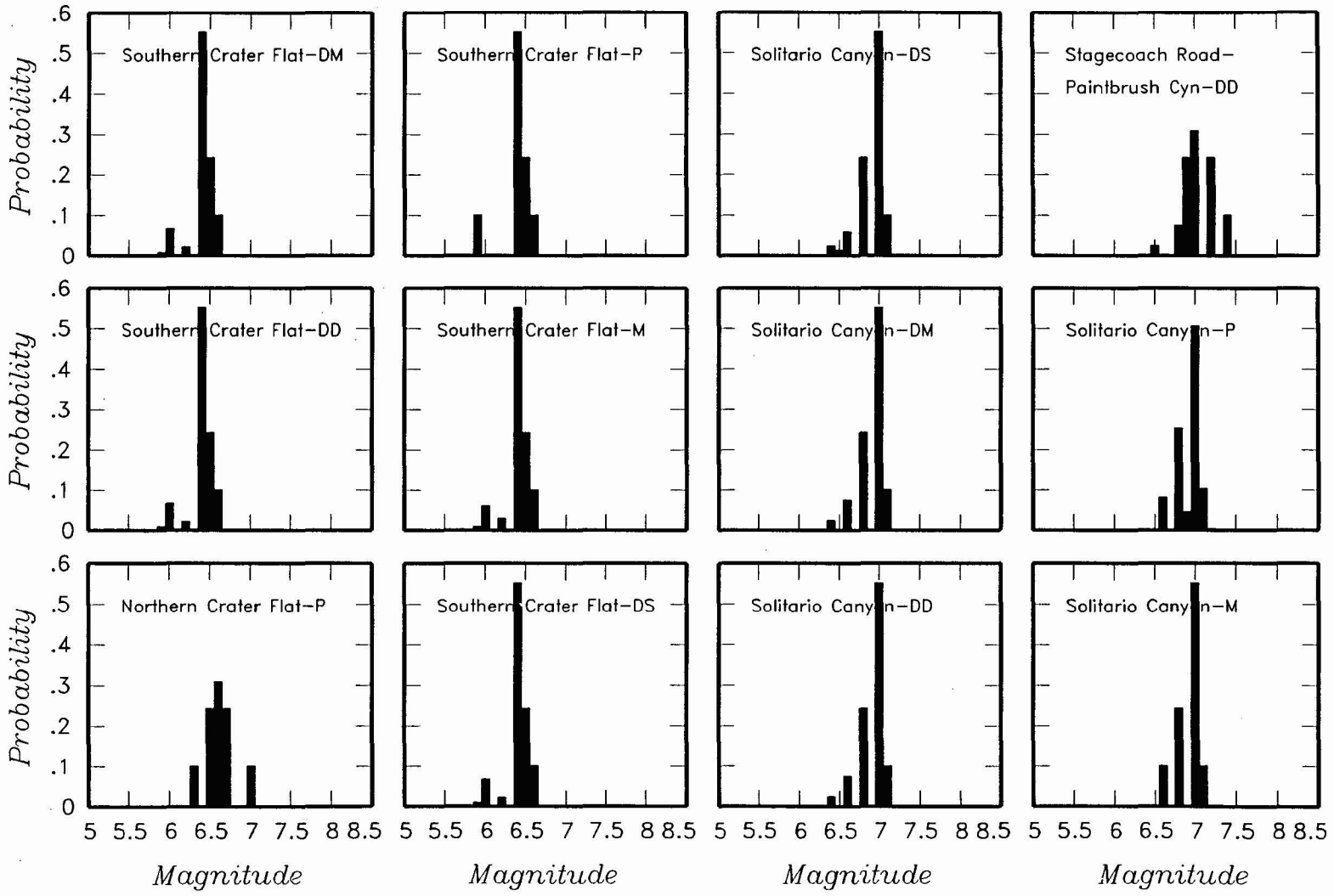

Figure 4-30 (Cont'd.) Maximum magnitude distributions for ASM team's local fault sources

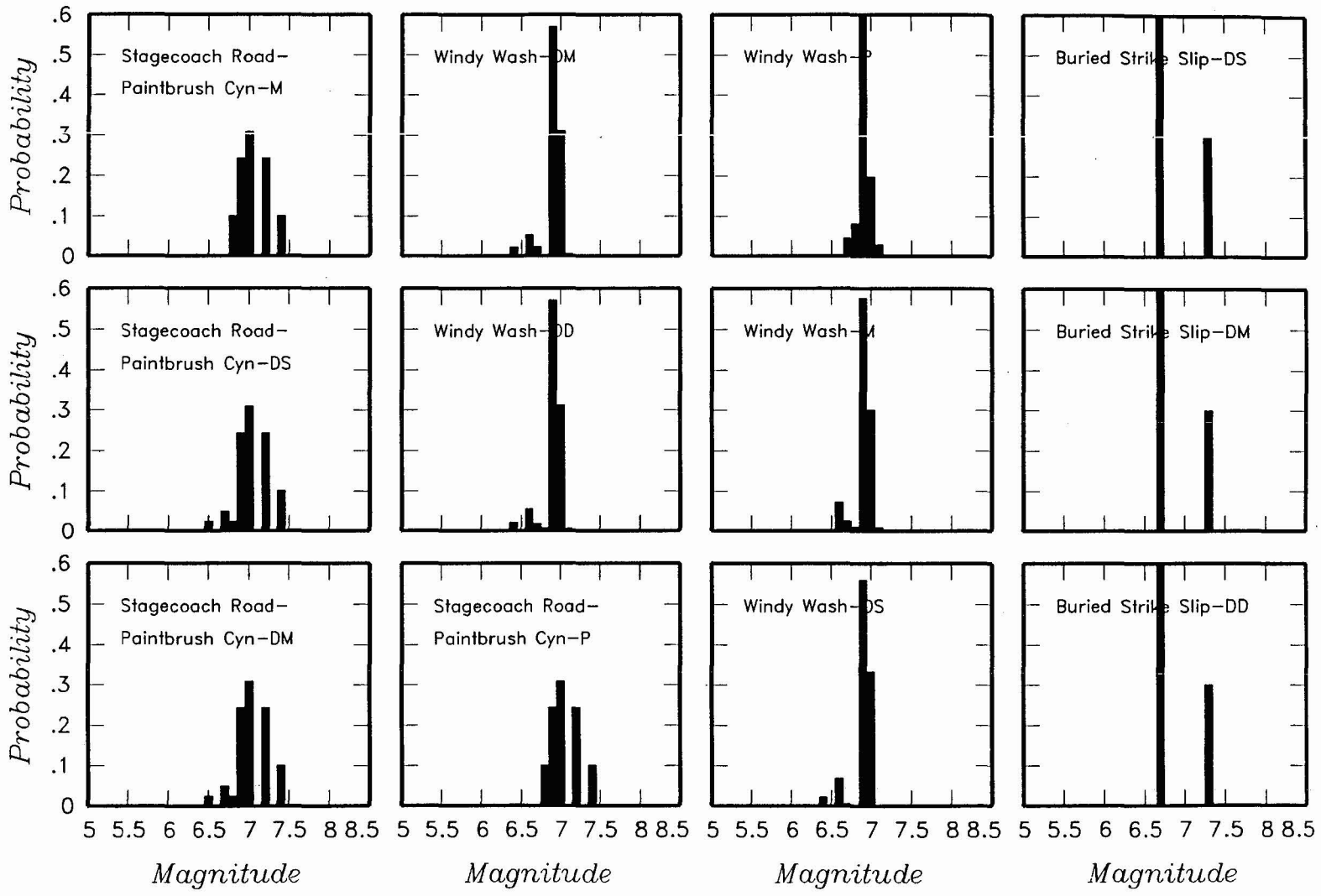

Figure 4-30 (Cont'd.) Maximum magnitude distributions for ASM team's local fault sources

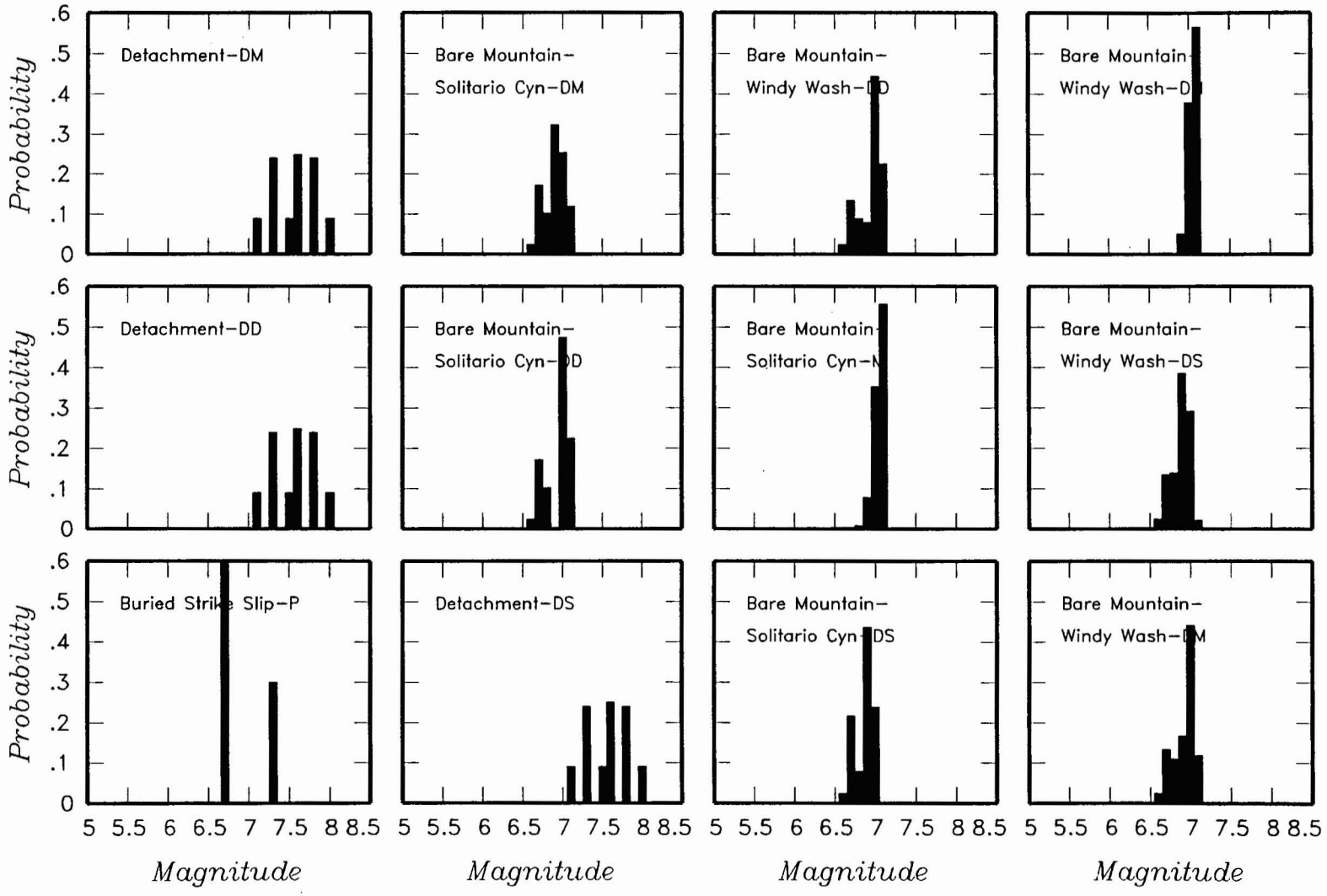

Figure 4-30 (Cont'd.) Maximum magnitude distributions for ASM team's local fault sources

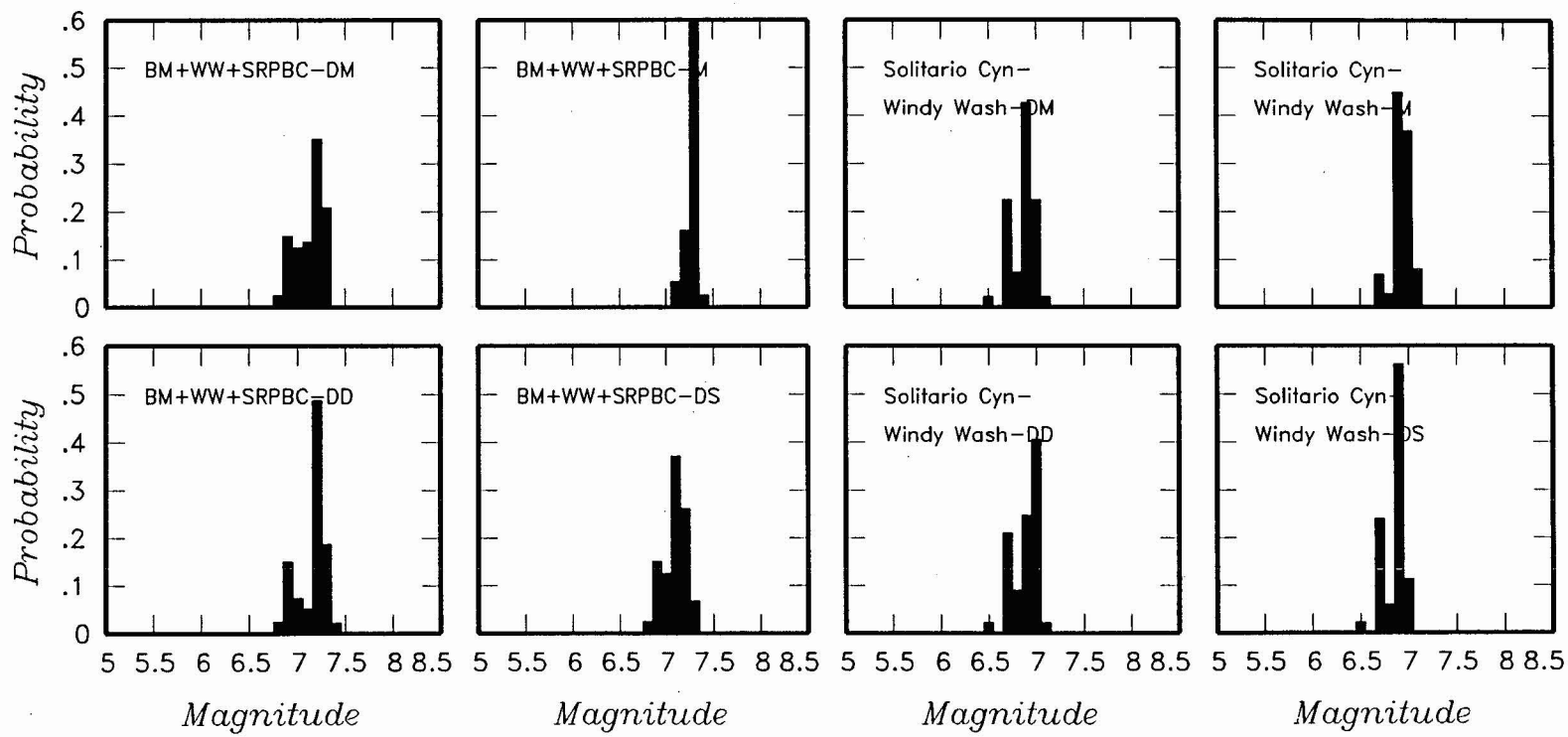

Figure 4-30 (Cont'd.) Maximum magnitude distributions for ASM team's local fault sources

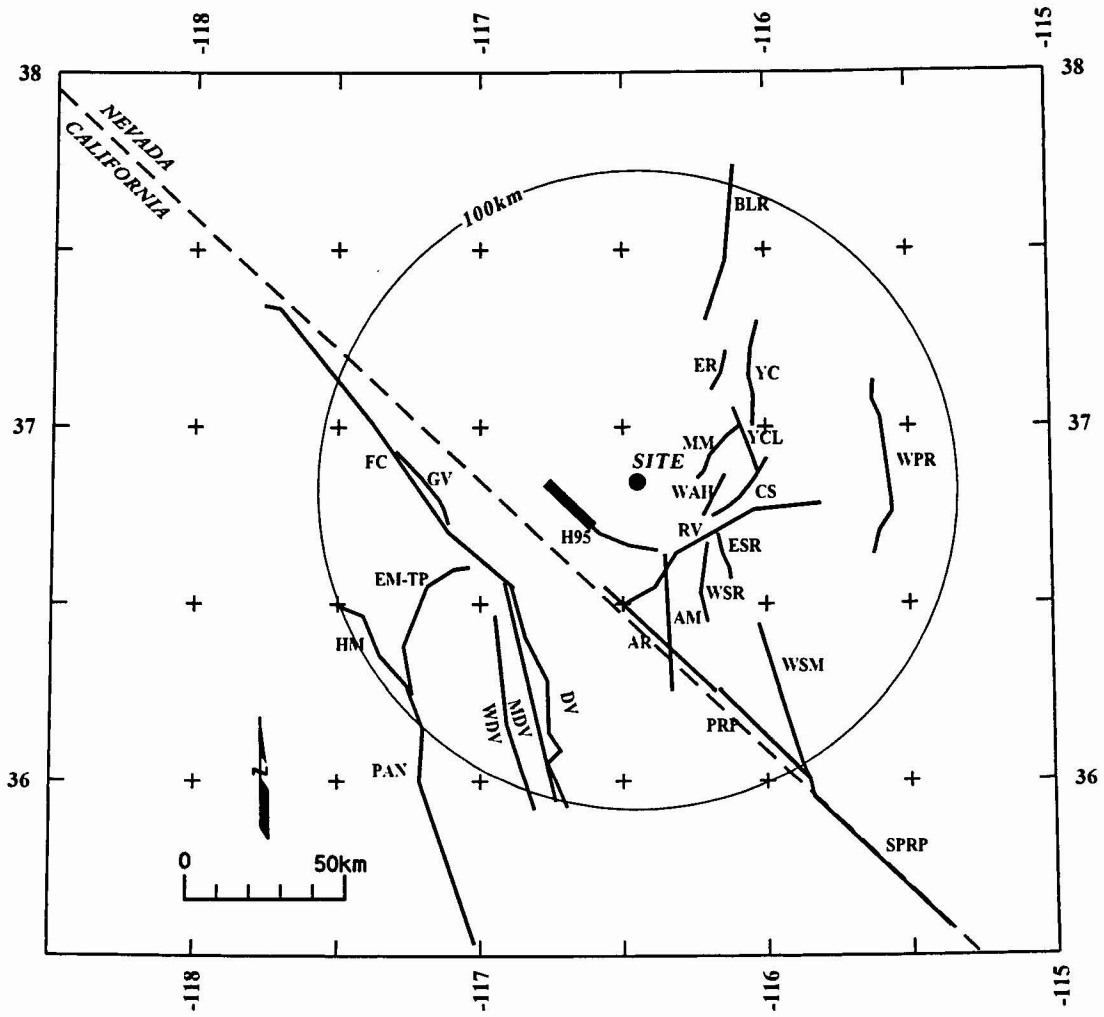

EXPLANATION

NOTE: Fault names are listed in Table 3-2

Fault Lengths:

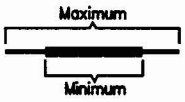

Figure 4-31 Reginal fault sources considered by the ASM team

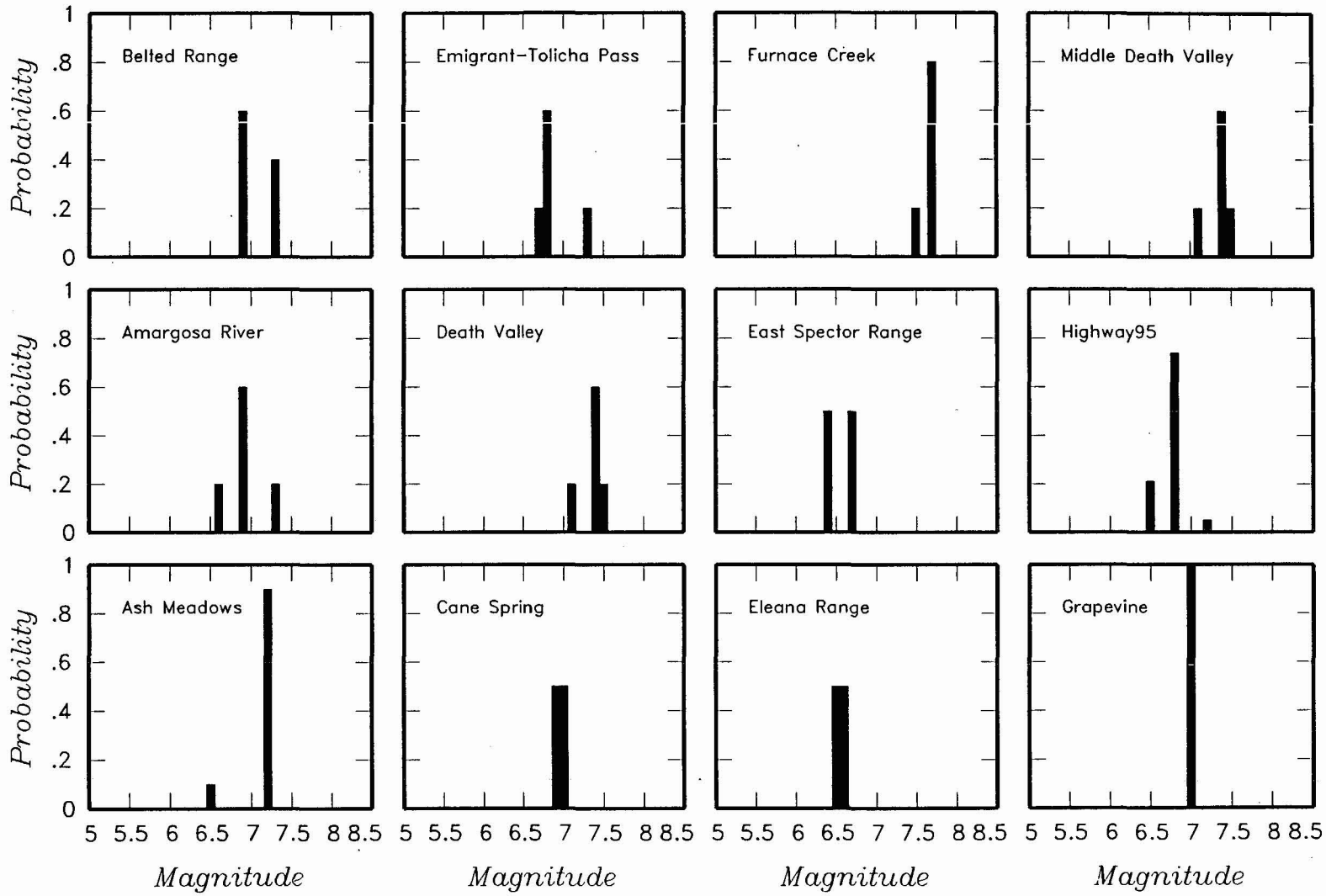

Figure 4-32 Maximum magnitude distributions for ASM team's regional fault sources

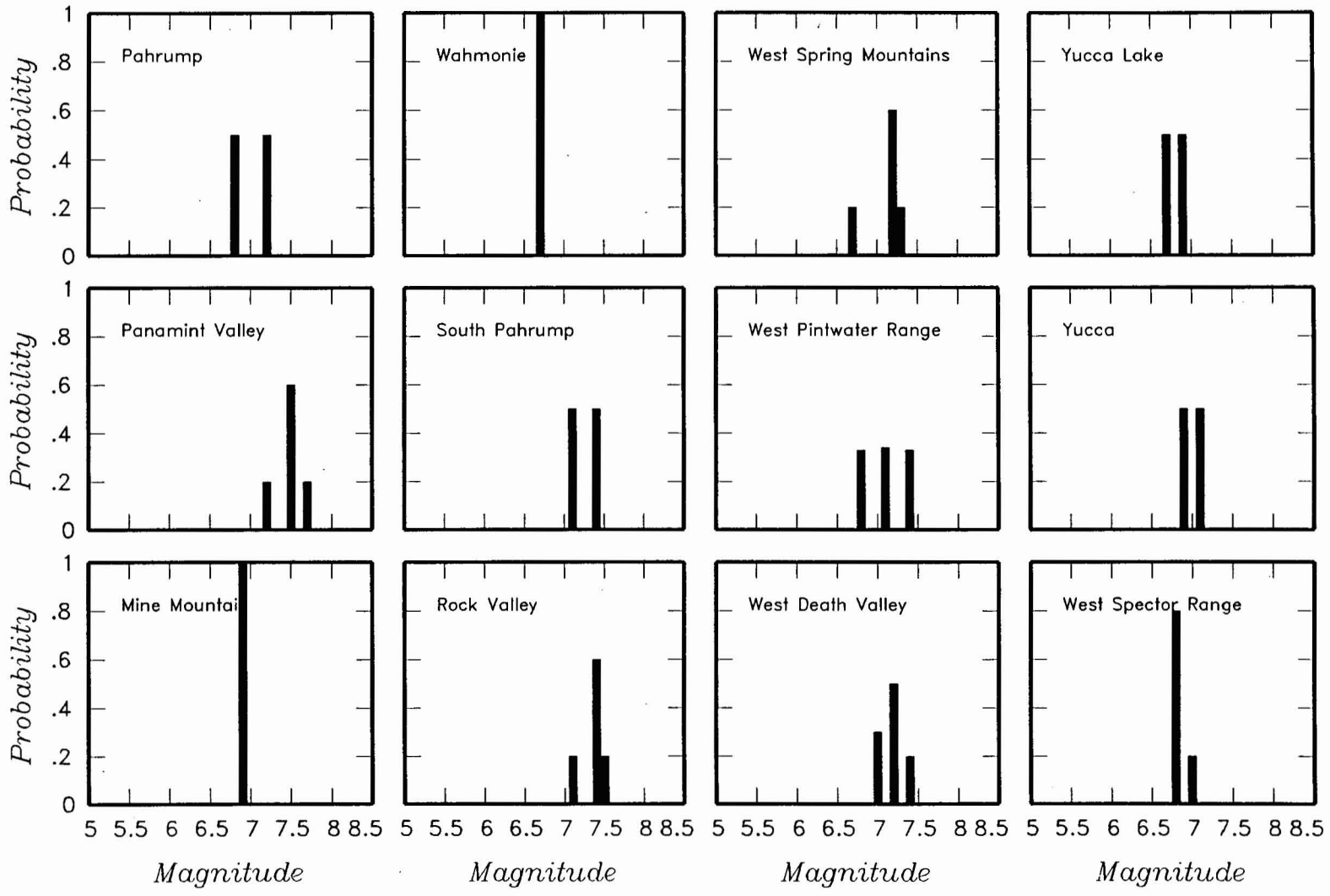

Figure 4-32 (Cont'd.) Maximum magnitude distributions for ASM team's regional fault sources

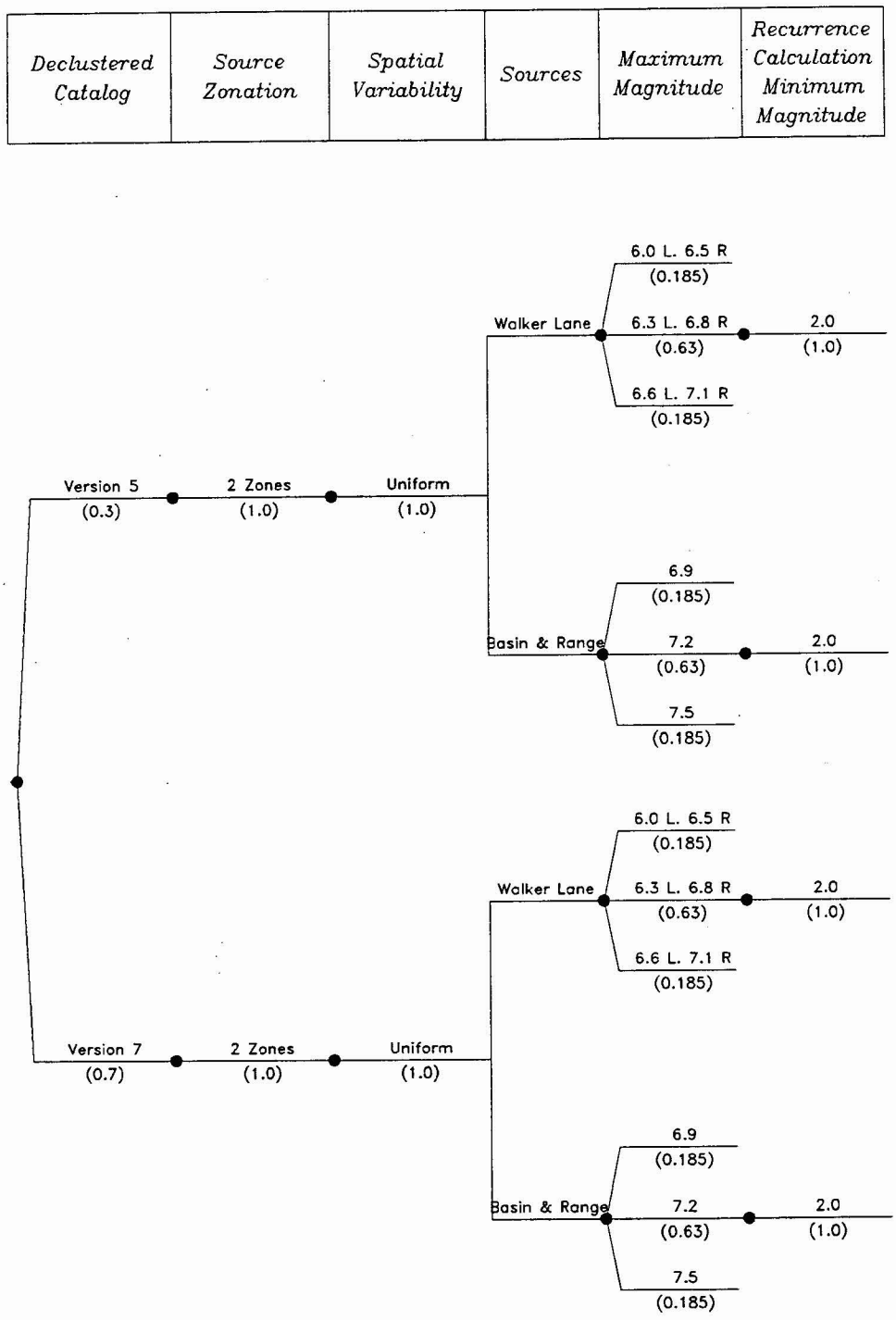

Figure 4-33 Logic tree for regional source zones developed by the ASM team

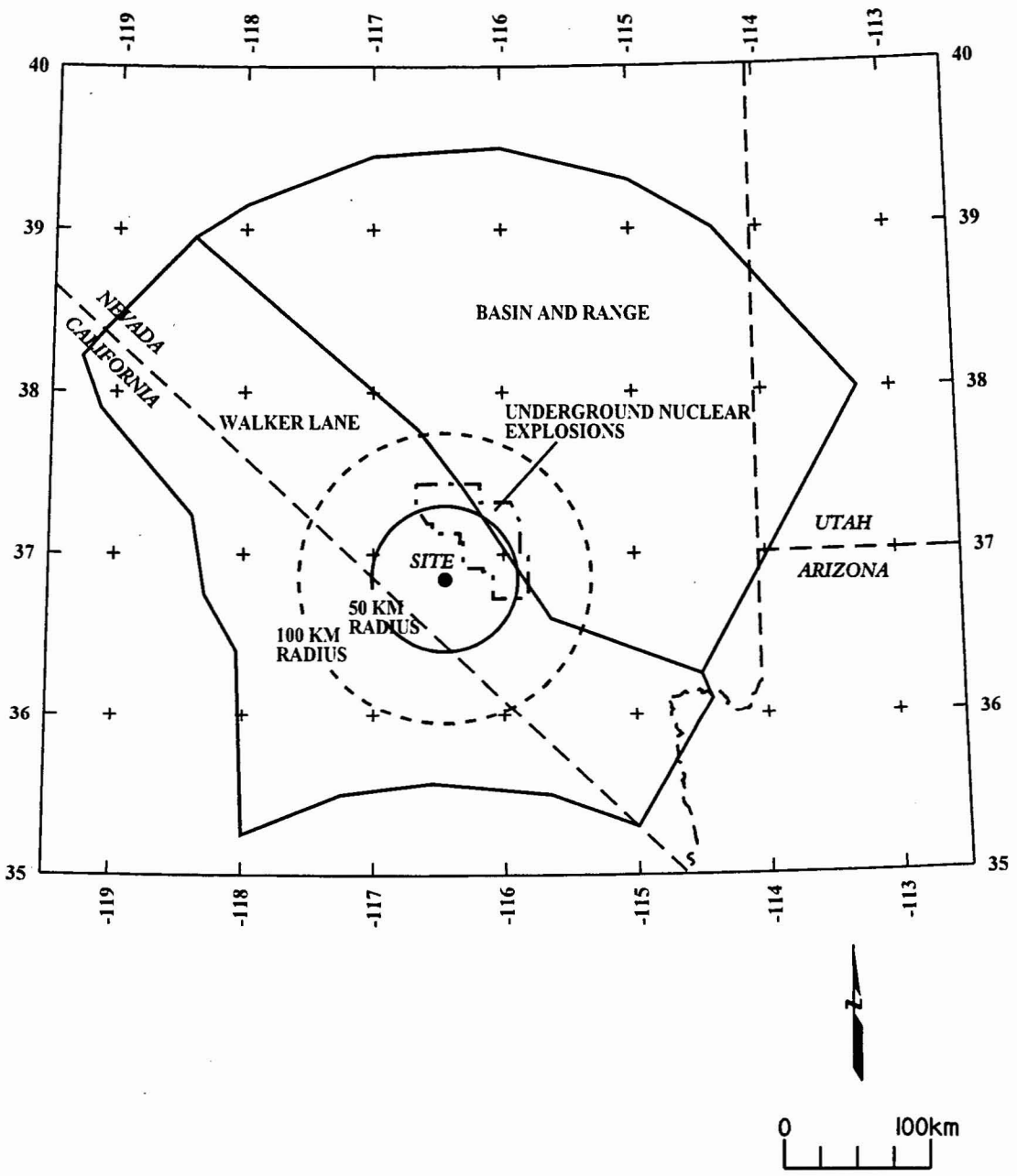

Figure 4-34 Regional source zones considered by the ASM team

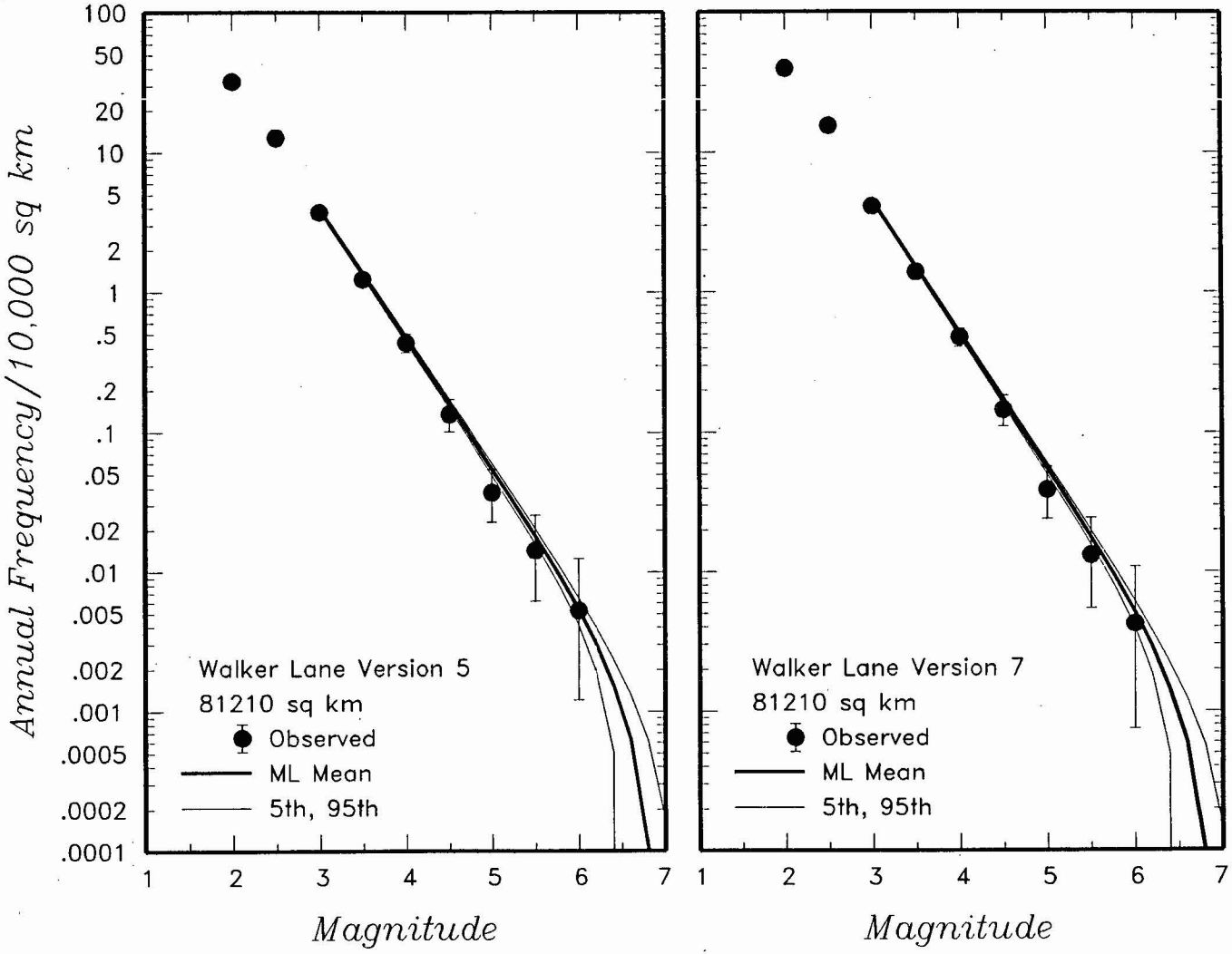

Figure 4-35 Earthquake recurrence relationships for the regional source zones defined by the ASM team. The solid dots with vertical error bars represent the observed data. The thick and thin solid curves are the mean, 5th, and 95th percentiles of the recurrence rates based on the uncertainty in recurrence parameters and maximum magnitude.

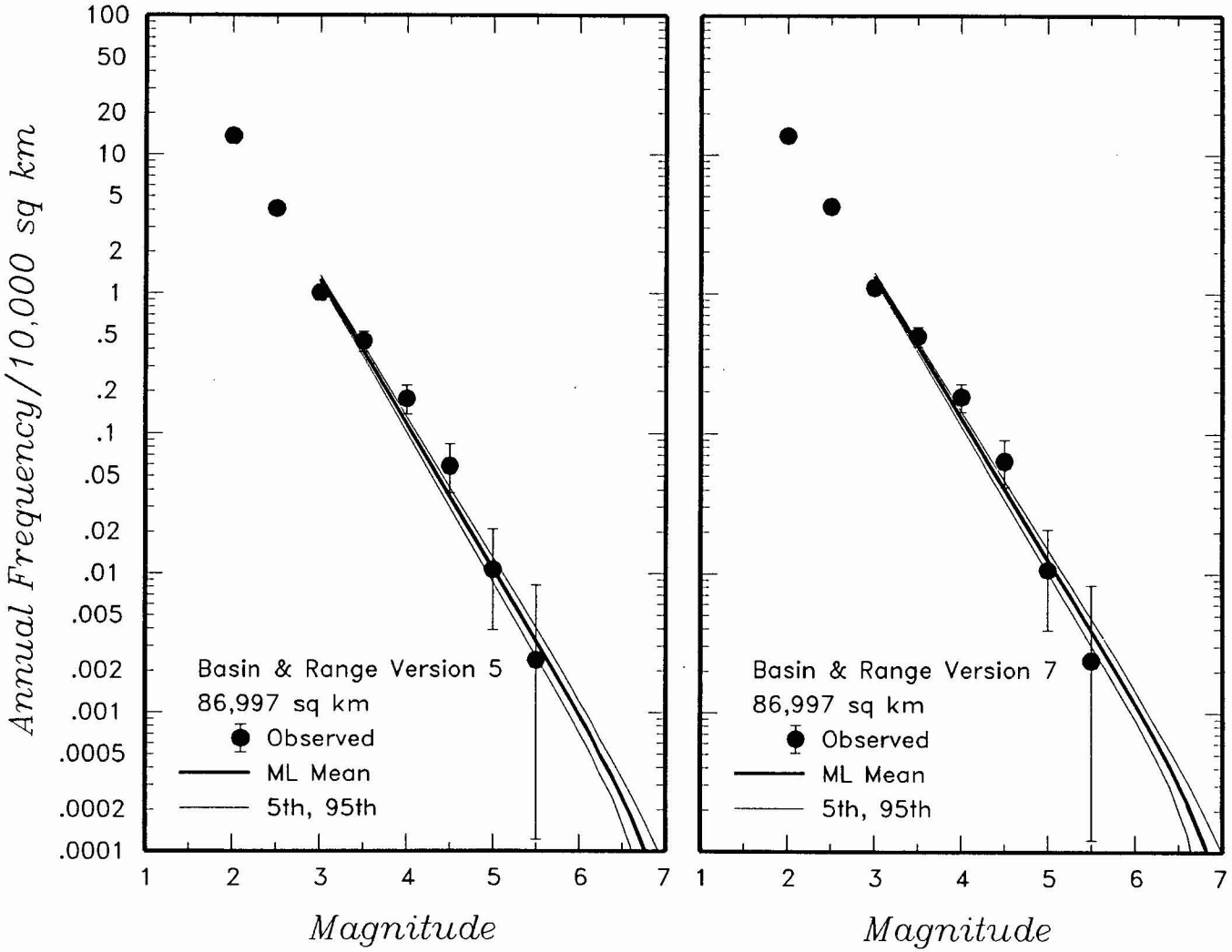

Figure 4-35 (Cont'd.) Earthquake recurrence relationships for the regional source zones defined by the ASM team

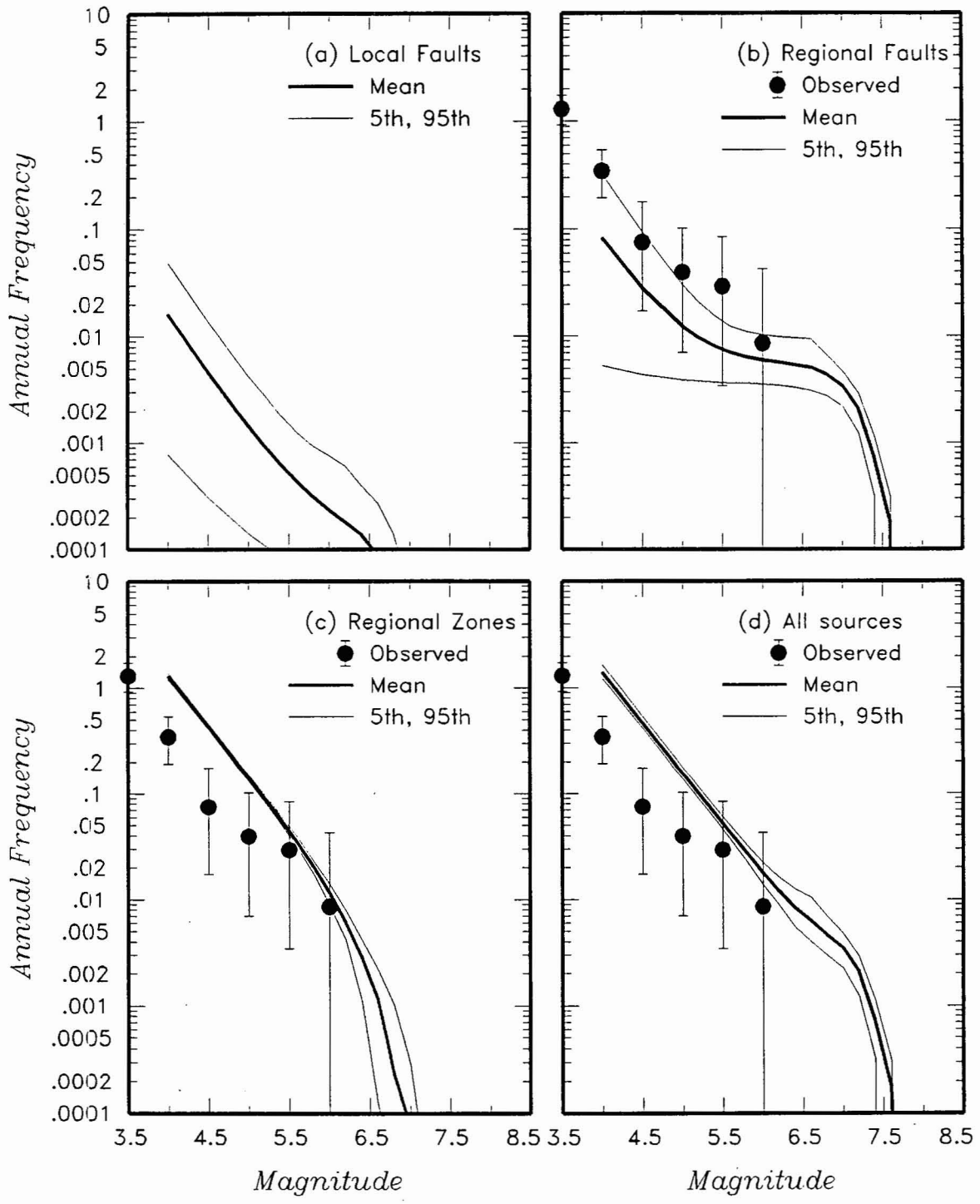

Figure 4-36 Predicted mean, 5th-, and 95th-percentile recurrence rates for (a) local fault sources, (b) regional fault sources, (c) regional source zones, and (d) all sources combined for the ASM team. The solid dots with vertical error bars indicate the observed frequency of earthquakes occurring within 100 km of the Yucca Mountain site.

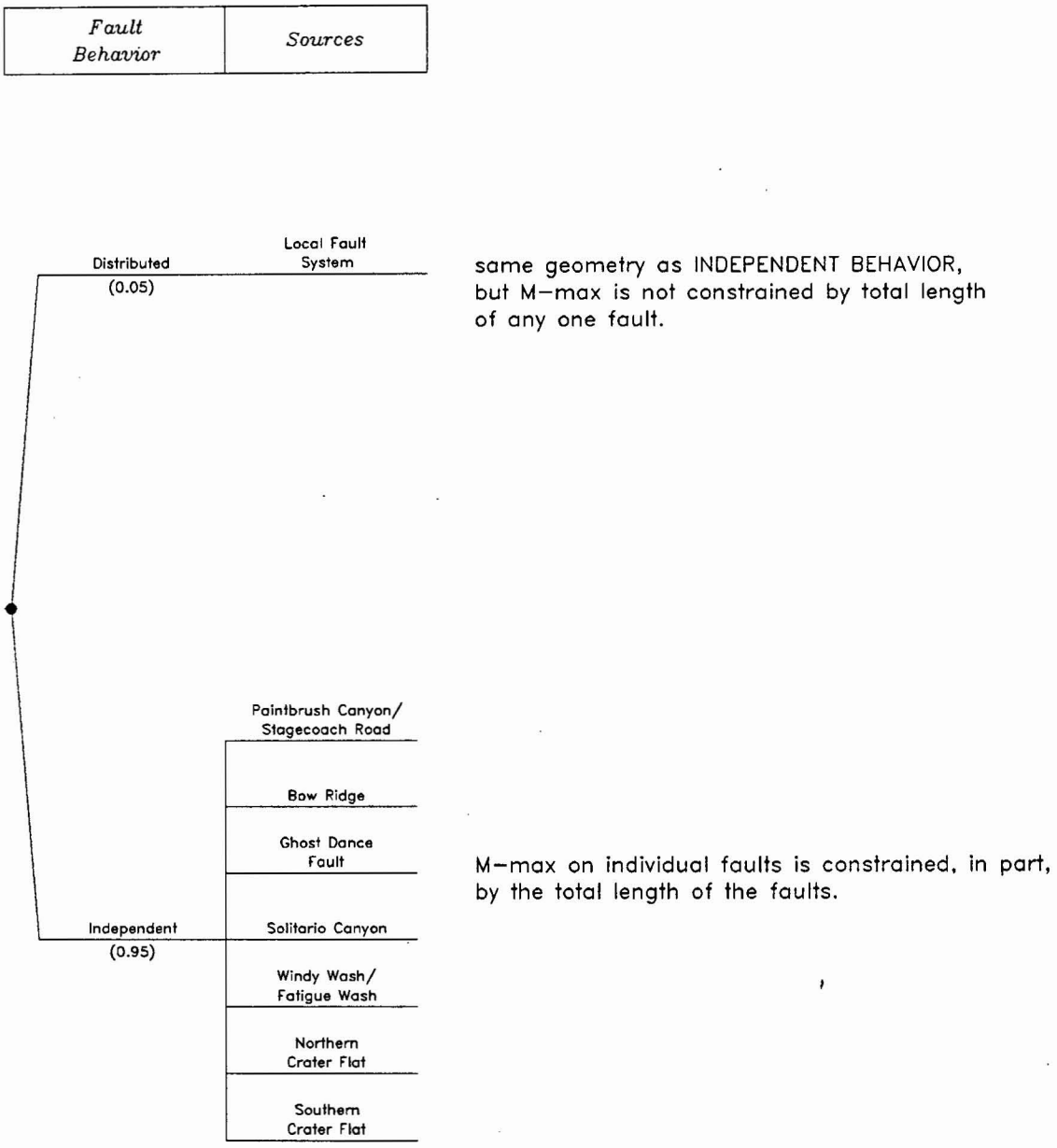

Figure 4-37a Logic tree for local fault sources developed by the DFS team

Seismic Source	*Total Fault Length Scenarios*	*Maximum Rupture Length*	*Structural Model*	*Dip/Width*	*Slip Rate (mm/yr)*	*Maximum Earthquake Method*	*Earthquake Recurrence Model*

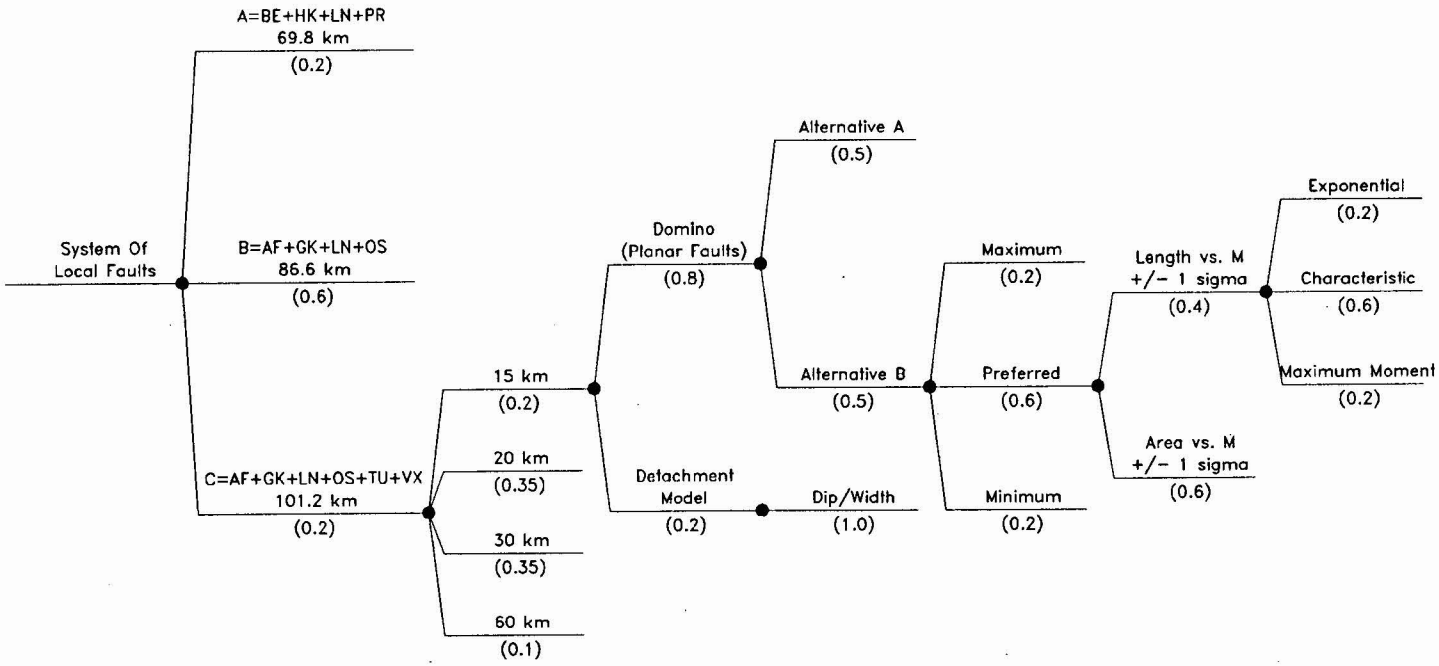

Figure 4-37b Logic tree for local fault source given distributed fault behavior

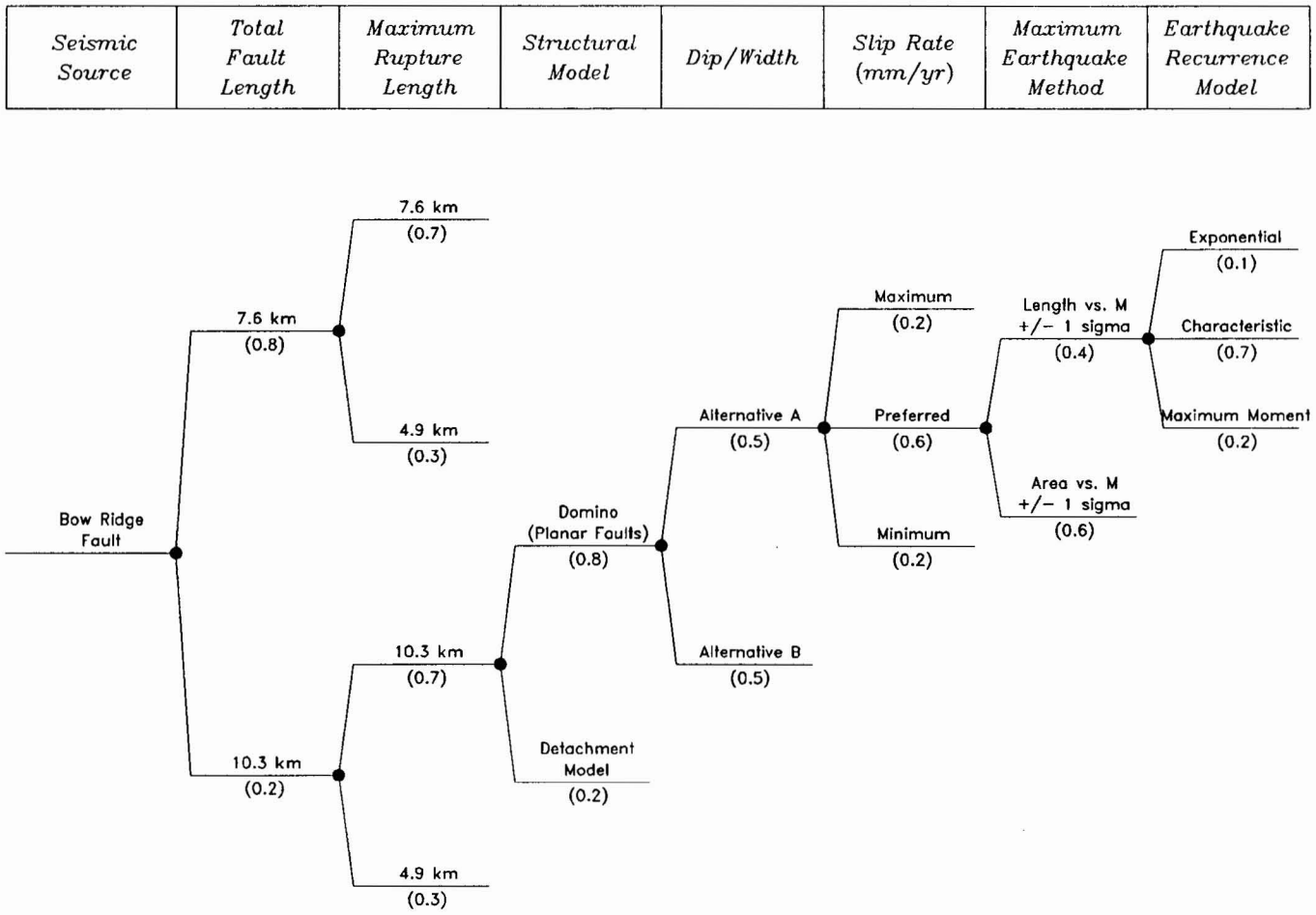

Figure 4-37c Example logic tree for local fault source given independent fault behavior

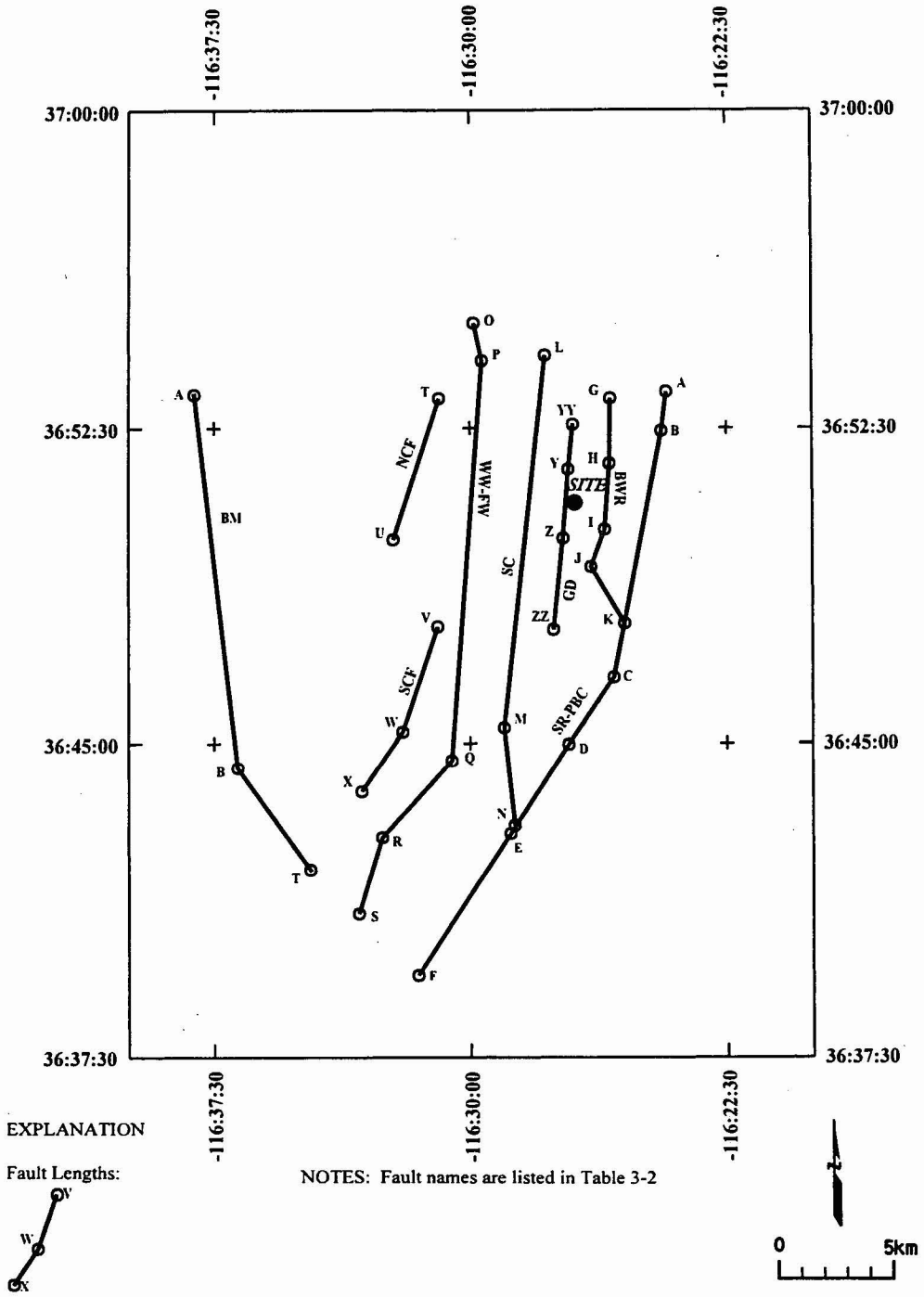

Figure 4-38 Location of local faults considered by the DFS team to be acting as independant sources

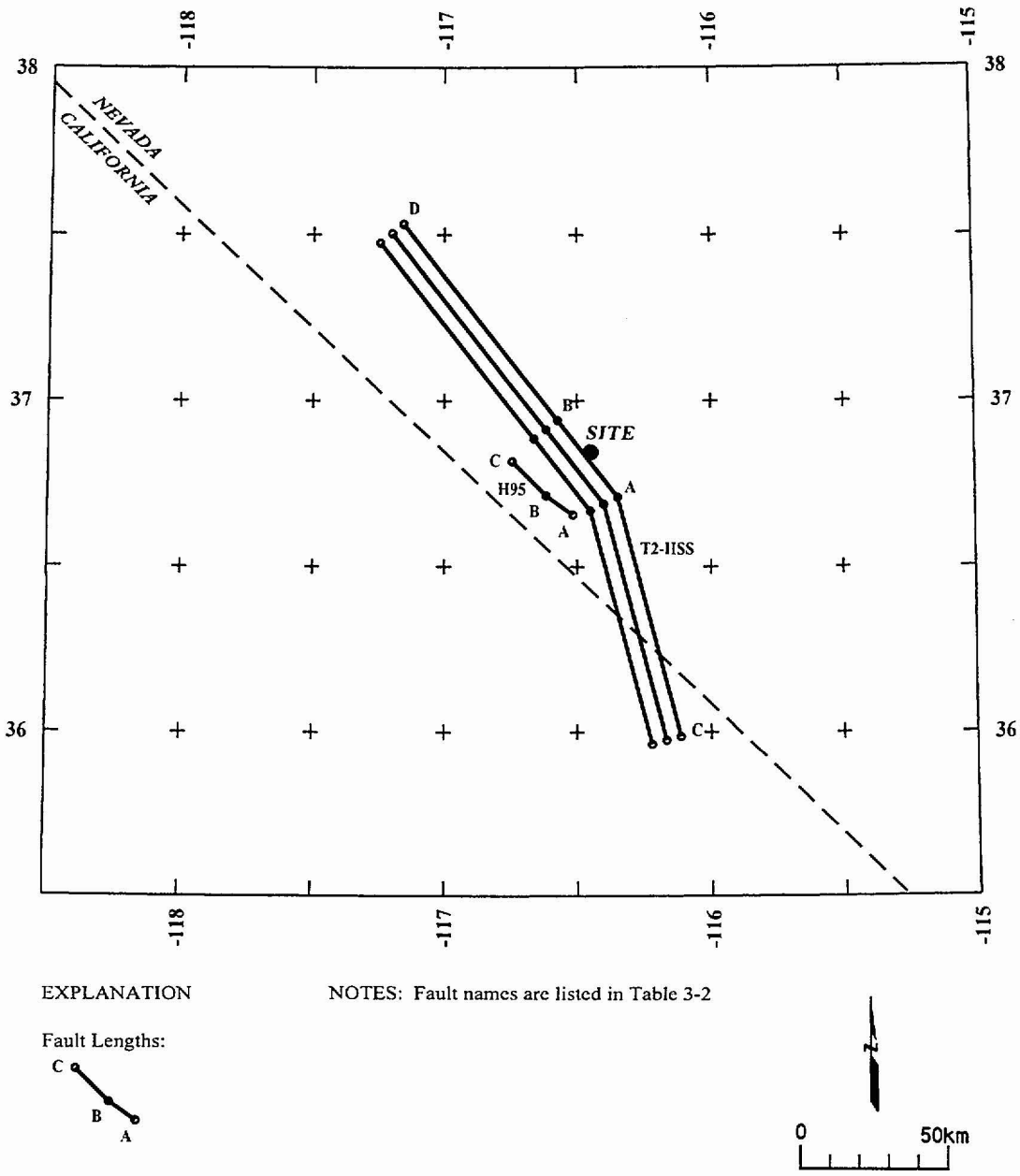

Figure 4-39 Potential locations of DFS team's inferred buried strike-slip sources

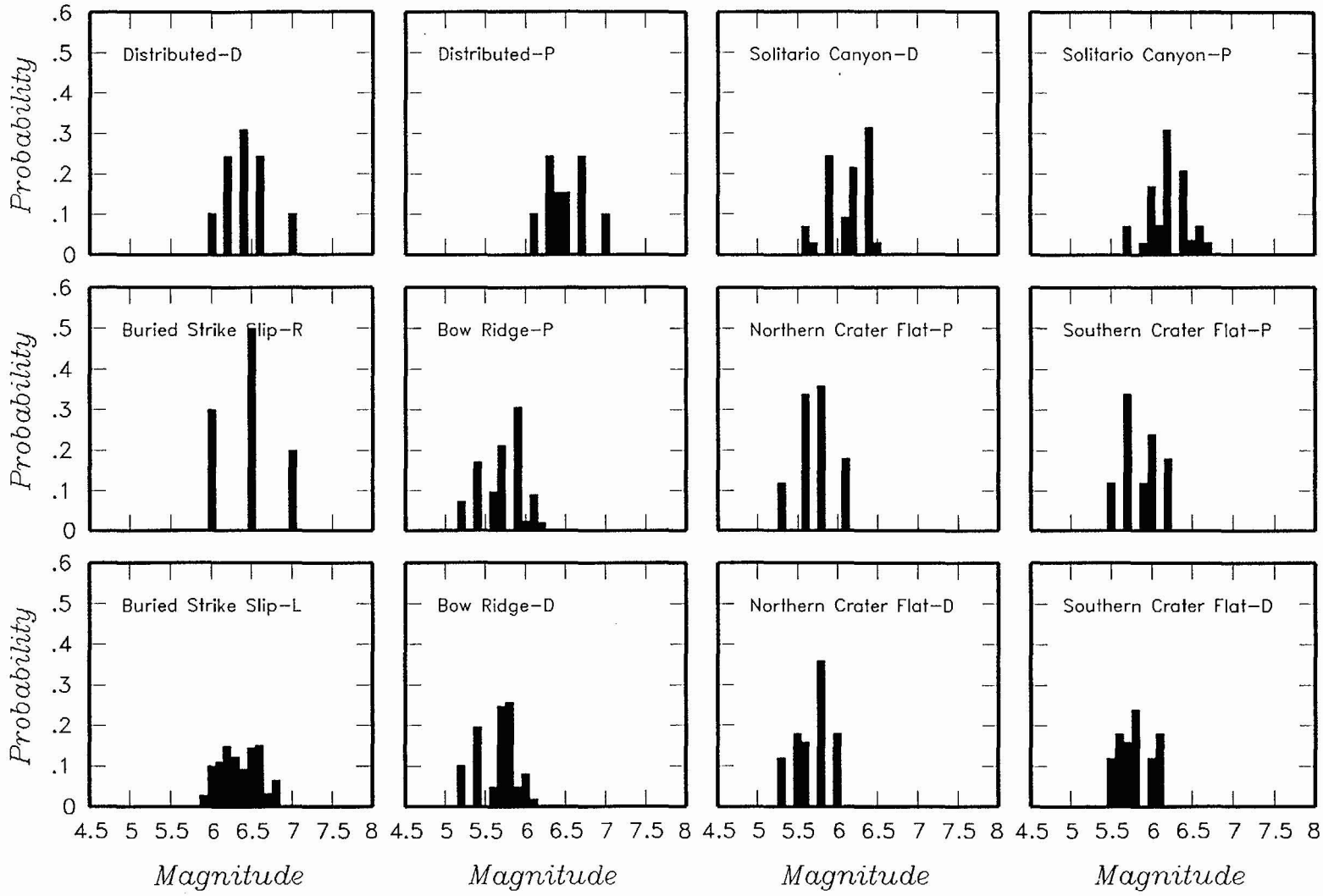

Figure 4-40 Maximum magnitude distributions for DFS team's local fault sources. D–detachment, L–local, R–regional, P–planar.

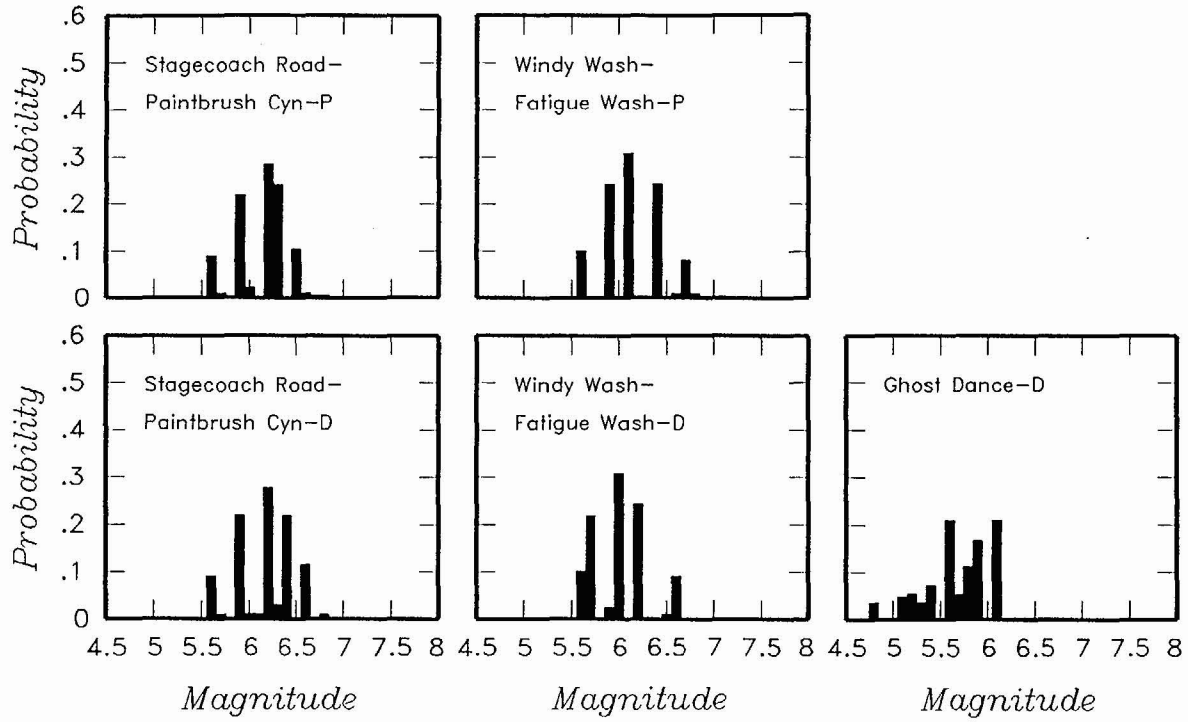

Figure 4-40 (Cont'd.) Maximum magnitude distributions for DFS team's local fault sources

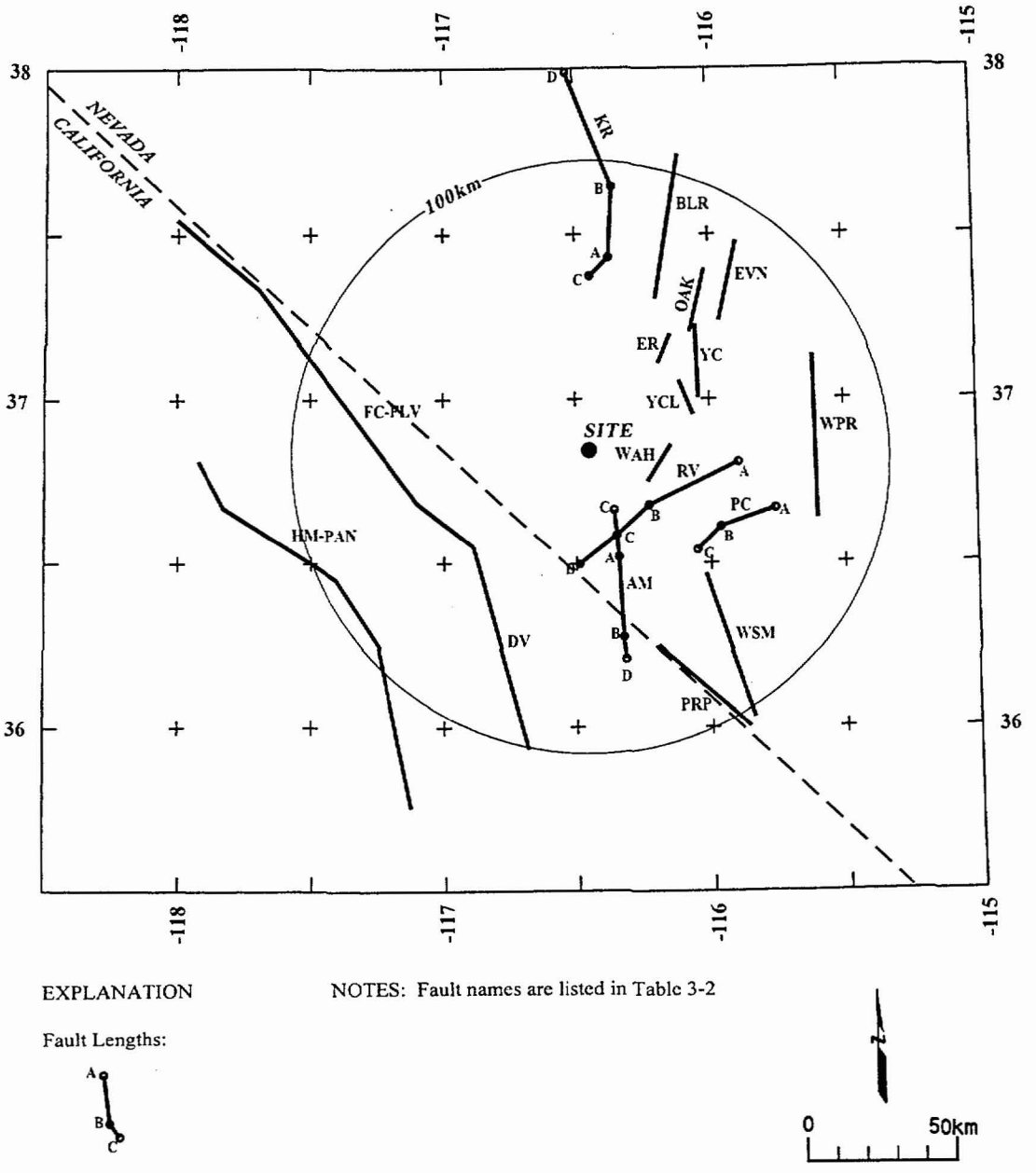

EXPLANATION

Fault Lengths:

A
B
C

NOTES: Fault names are listed in Table 3-2

0 50km

Figure 4-41 Regional fault sources considered by the DFS team